



ISSCC 2021

SESSION 23
THz Circuits and Front-Ends

270-to-300GHz Double-Balanced Parametric Upconverter Using Asymmetric MOS Varactors and a Power-Splitting-Transformer Hybrid in 65nm CMOS

Zhiyu Chen¹, Wooyeol Choi² and Kenneth K. O.¹

¹University of Texas at Dallas, Richardson, TX

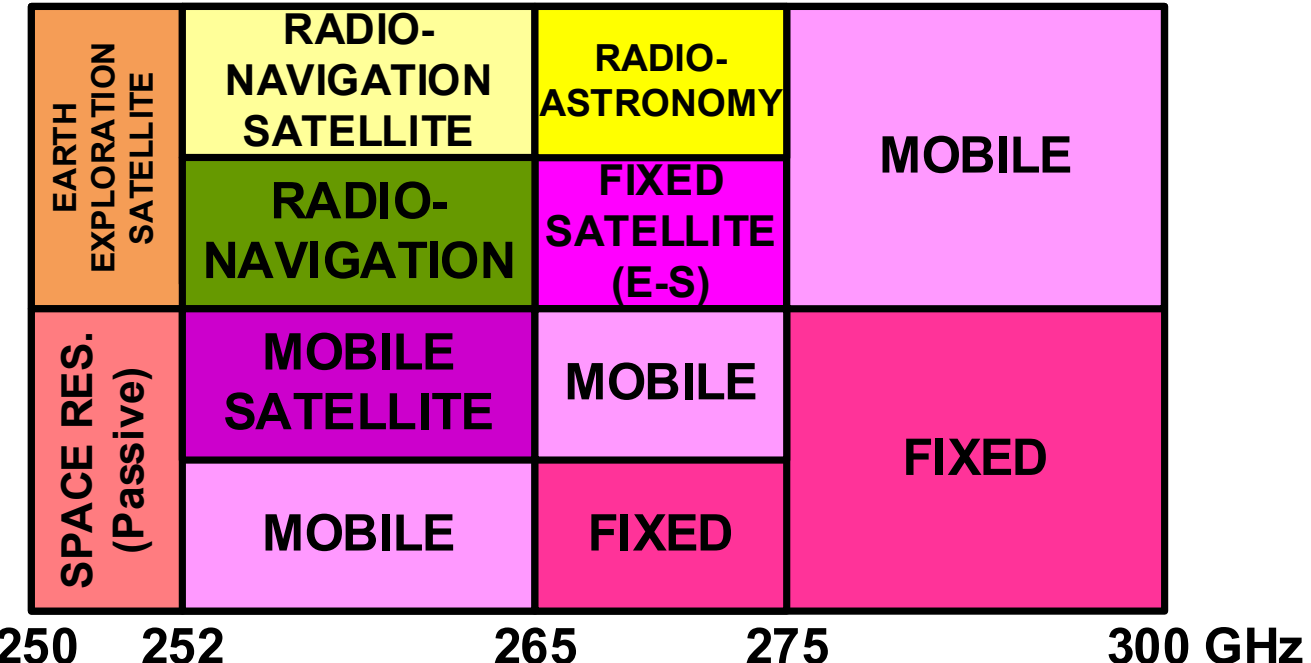
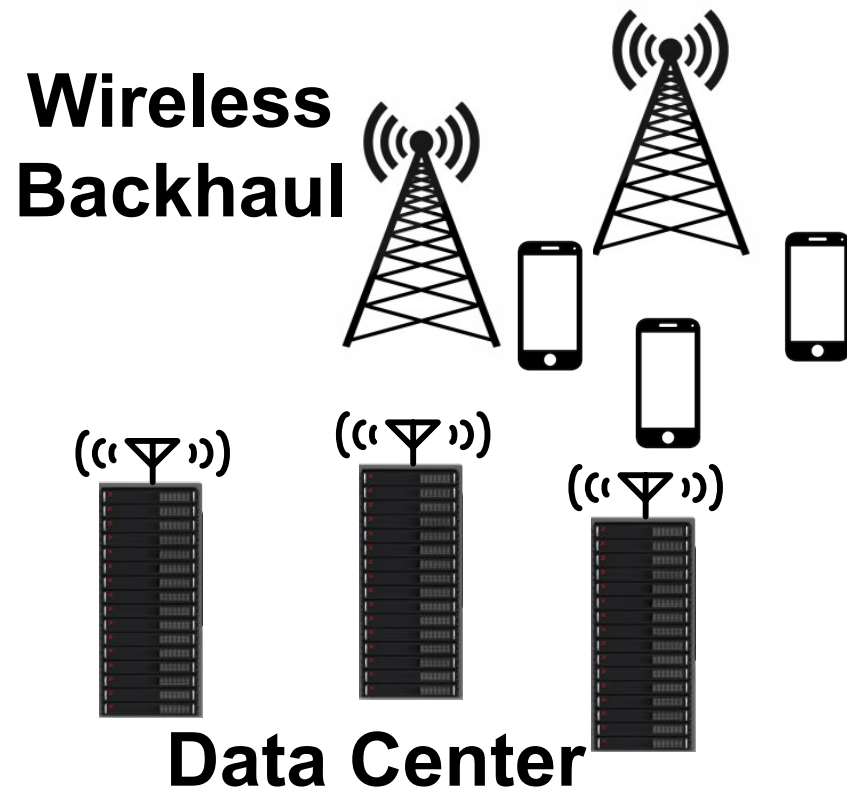
²Oklahoma State University, Stillwater, OK



Outline

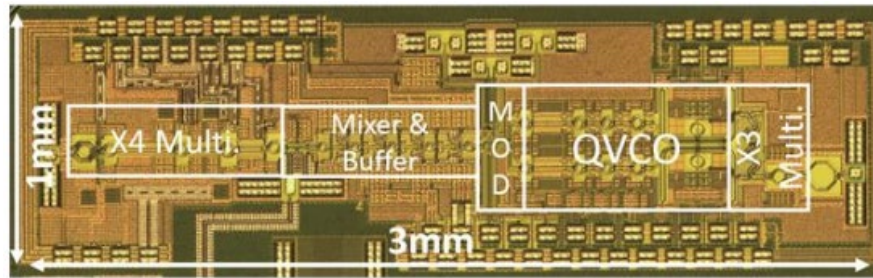
- Introduction
- Manley-Rowe Relation
- Upconverter Implementation
- Measurement Results
- Conclusion

Introduction



- Global data traffic grows exponentially. [fcc.gov]
- Speed of wireless link is proportional to the bandwidth.
- 252-300GHz allocated for wireless communication by FCC.

Prior Arts of 300GHz CMOS TX

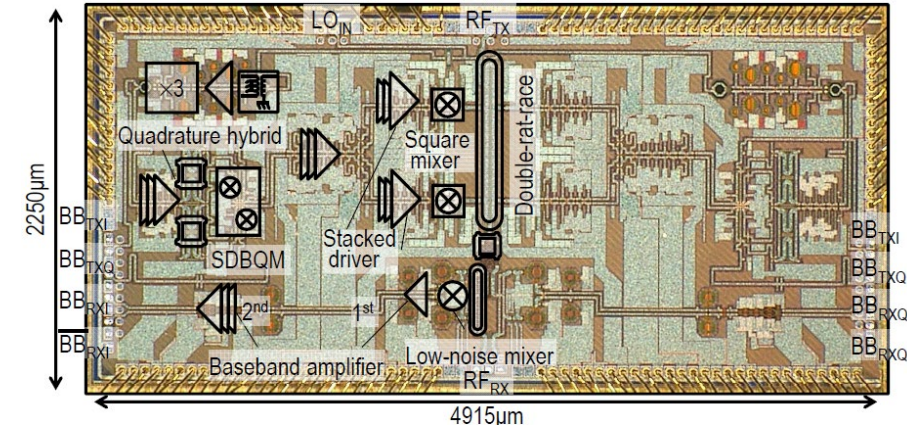


[Q. Zhong, CICC, 2018]

- 30Gbps QPSK with on-chip modulator.
- -6dBm saturated output power.
- Passive double-balanced mixer.

Limited output power.

AWG: Arbitrary Waveform Generator



[S. Lee, ISSCC, 2019]

- 80Gbps 16QAM using AWG.
- -1.6dBm saturated output power.
- Doubler-based “square” mixer.

Power combiner → Complex layout.
 High DC power consumption.

Challenges for upconverter

- Mixer-last topology of transmitters due to limited f_{\max} (~350GHz).
 - High gain (low loss).
 - High output power.
- High data rates system.
 - Broadband operation.
 - High linearity to support high order modulation (e.g. QAM).

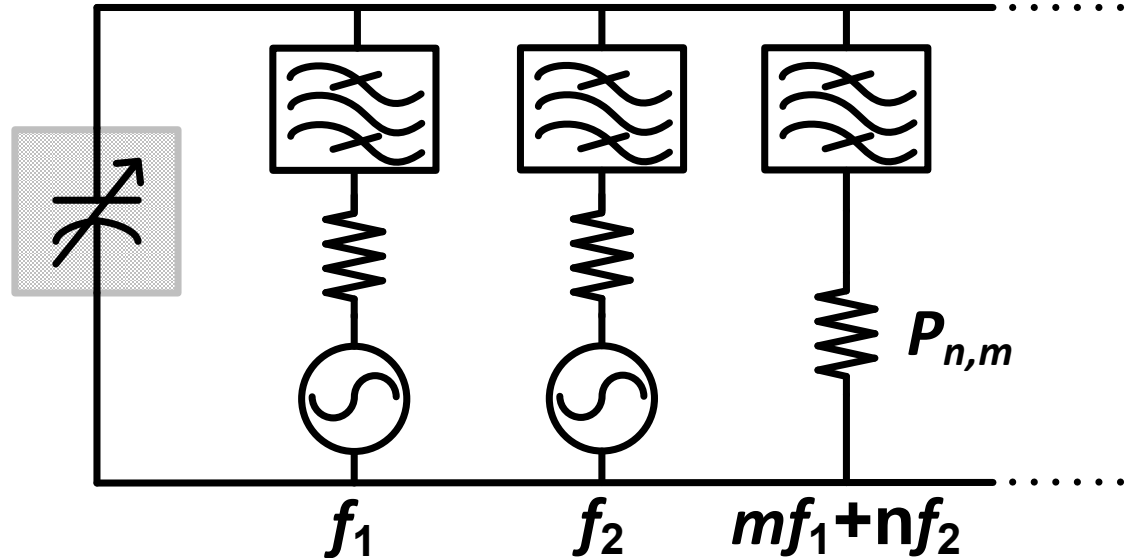
Need high performance upconverter concept!

QAM: Quadrature amplitude modulation

Outline

- Introduction
- Manley-Rowe Relation
- Upconverter Implementation
- Measurement Results
- Conclusion

Manley-Rowe Relation

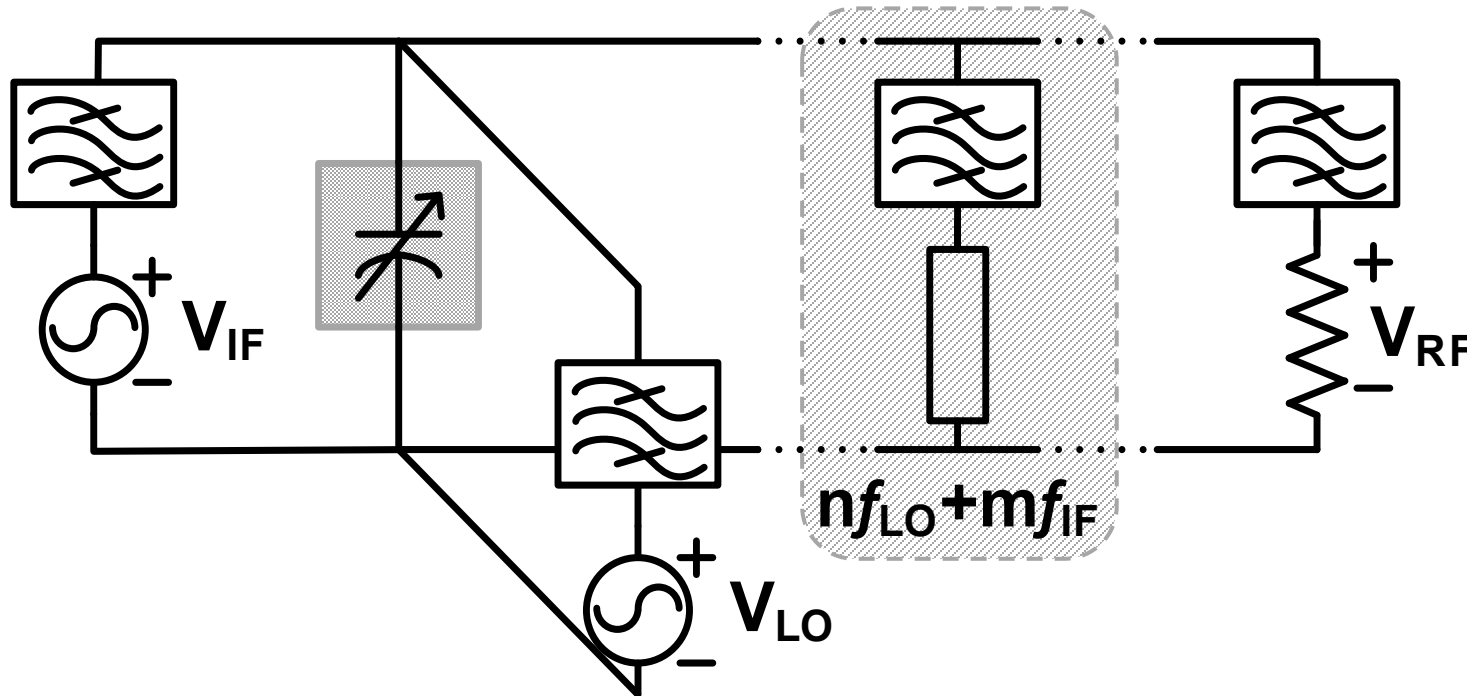


$$\left. \begin{aligned} \sum_{m=0}^{+\infty} \sum_{n=-\infty}^{+\infty} \frac{mP_{n,m}}{mf_1 + nf_2} &= 0 \\ \sum_{n=0}^{+\infty} \sum_{m=-\infty}^{+\infty} \frac{nP_{n,m}}{mf_1 + nf_2} &= 0 \end{aligned} \right\}$$

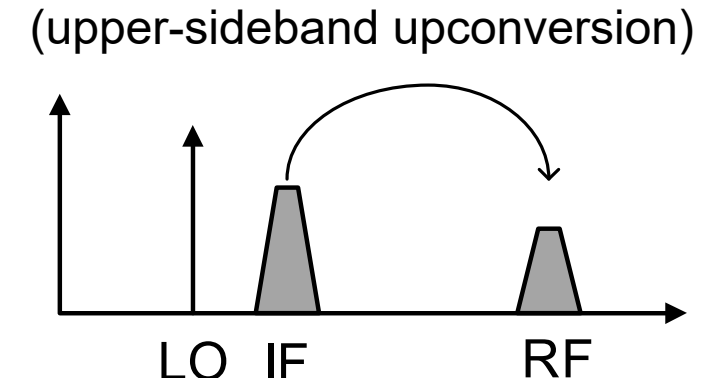
- Lossless nonlinear reactive device.
- Resistive loads with ideal bandpass filters.
- Various applications (e.g. parametric amplifier, up/down converter, multiplier).

[J. Manley and H. Rowe, *Proc. IRE*, 1956]

Parametric Upconverter



$$\frac{P_{RF}}{P_{IF}} = \frac{\omega_{RF}}{\omega_{IF}}$$

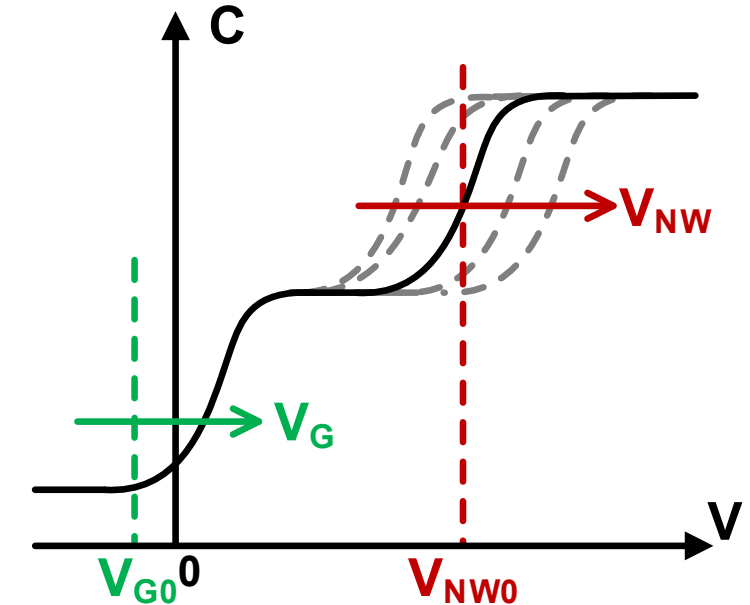
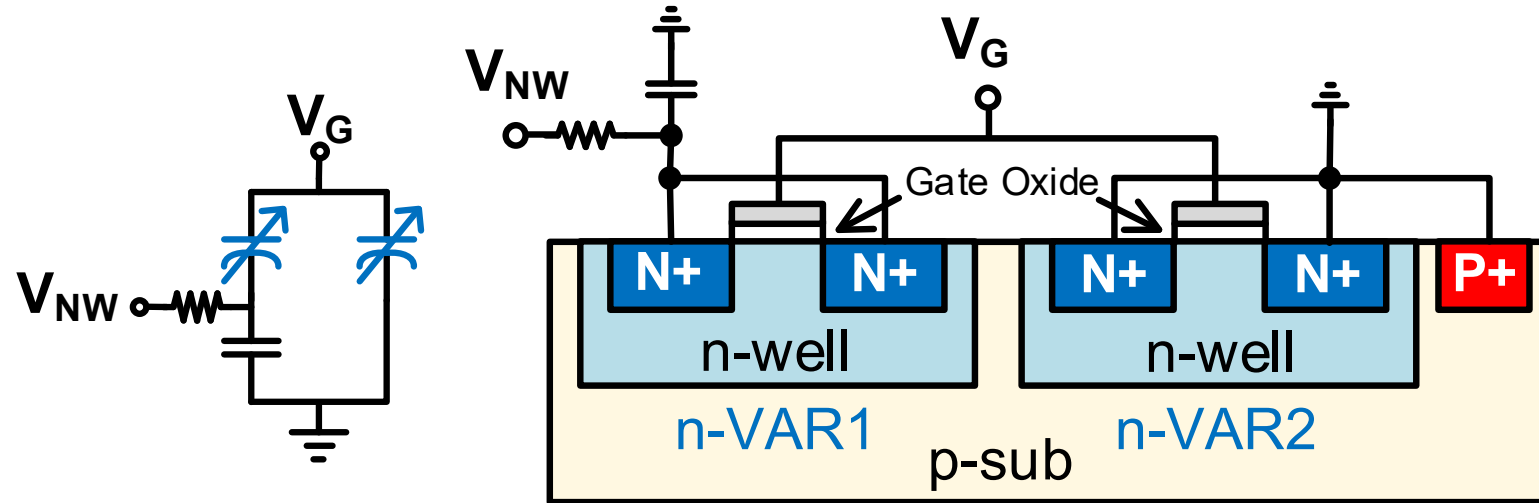


- Conversion gain (CG) is greater than 1 since ω_{RF} is higher than ω_{IF} .
 - 3dB gain when upconverting 150GHz to 300GHz.
- Maximum gain is achieved only when the varactor is lossless, and all other harmonic terms must be properly terminated.

Outline

- Introduction
- Manley-Rowe Relation
- Upconverter Implementation
- Measurement Results
- Conclusion

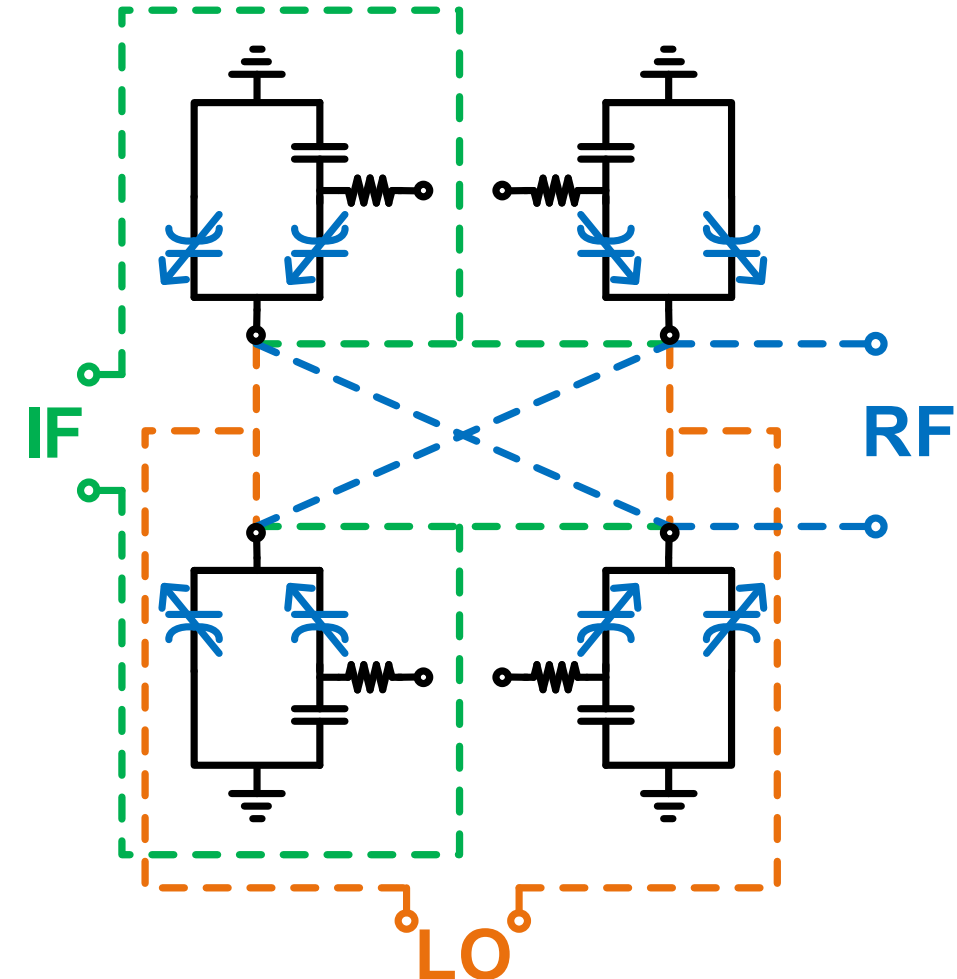
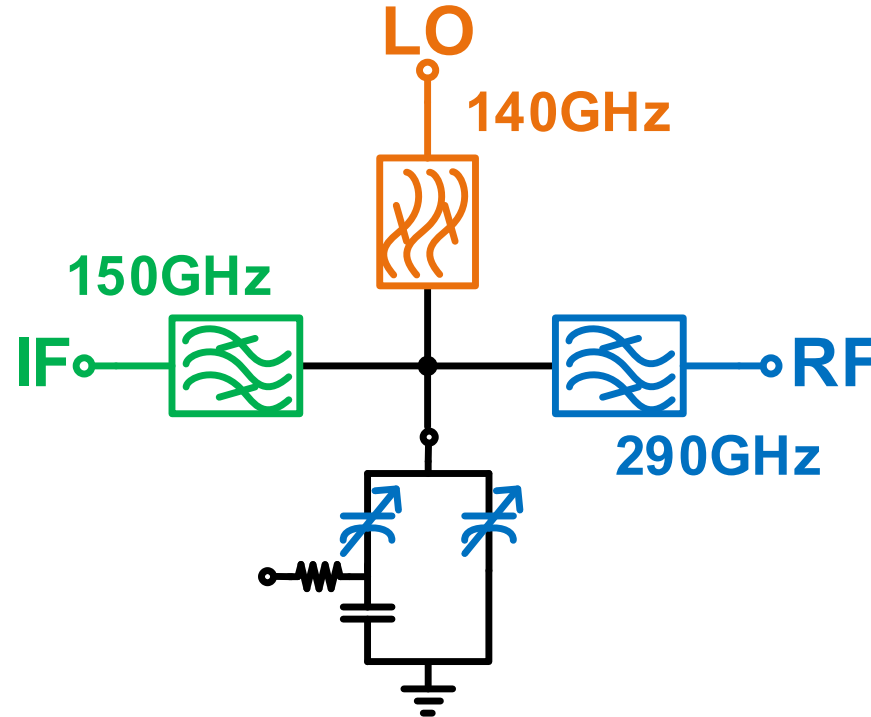
Asymmetric MOS Varactors (ASVAR)



- Odd-order harmonic cancellation.
- Even-order harmonic generation.
- High dynamic cut-off frequency ($f_{cd} = \left(\frac{1}{C_{min}} - \frac{1}{C_{max}} \right) / 2\pi R_s \right)$.

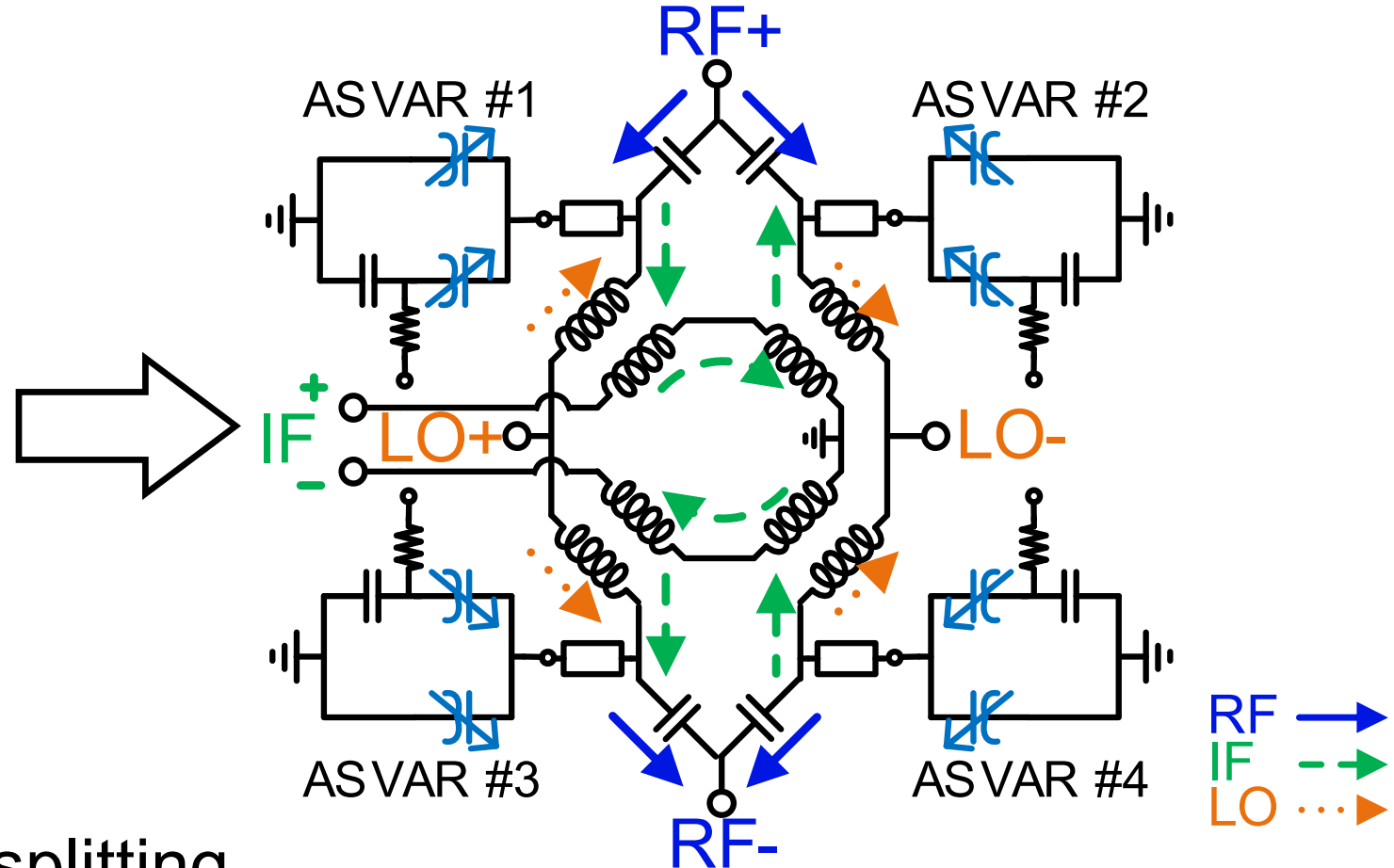
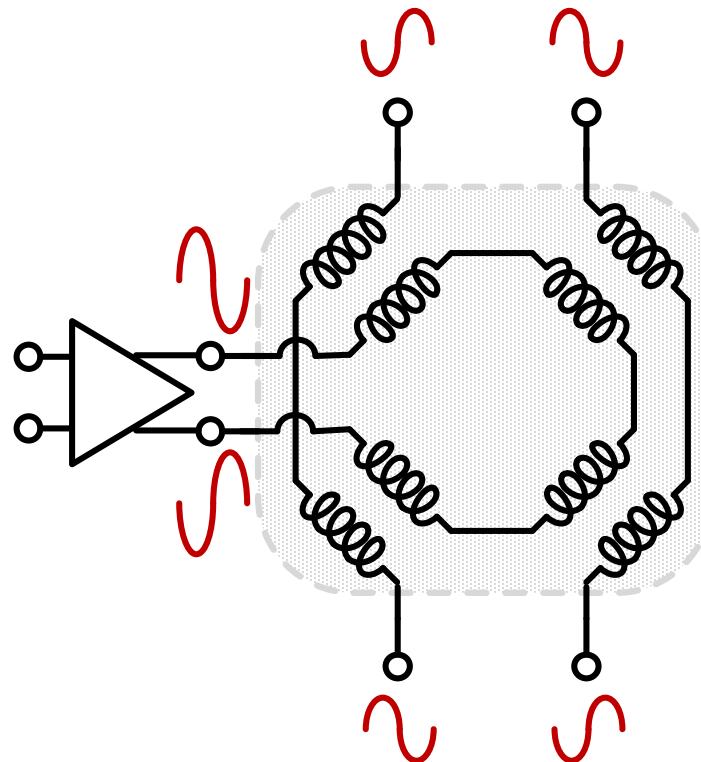
[Z. Ahmad, ISSCC, 2016]

Port Isolation



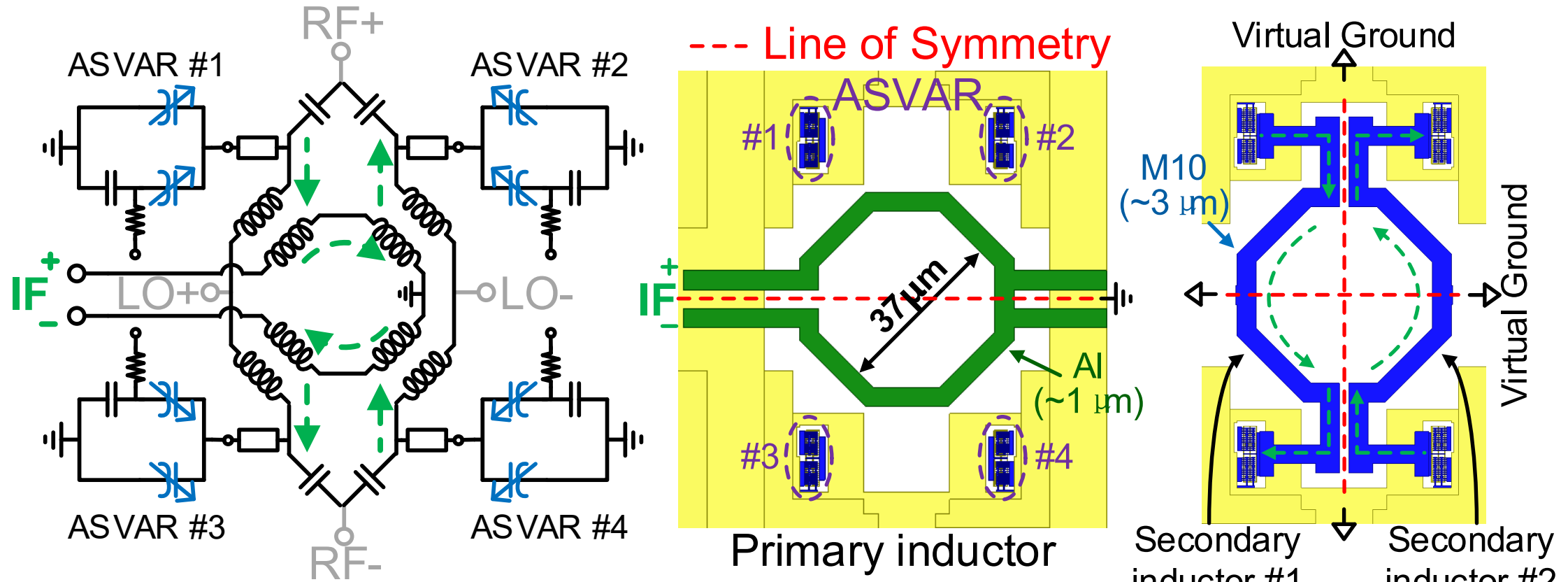
- One port device.
- How to separate IF/LO/RF path in a differential structure?

Power-Splitting-Transformer Hybrid



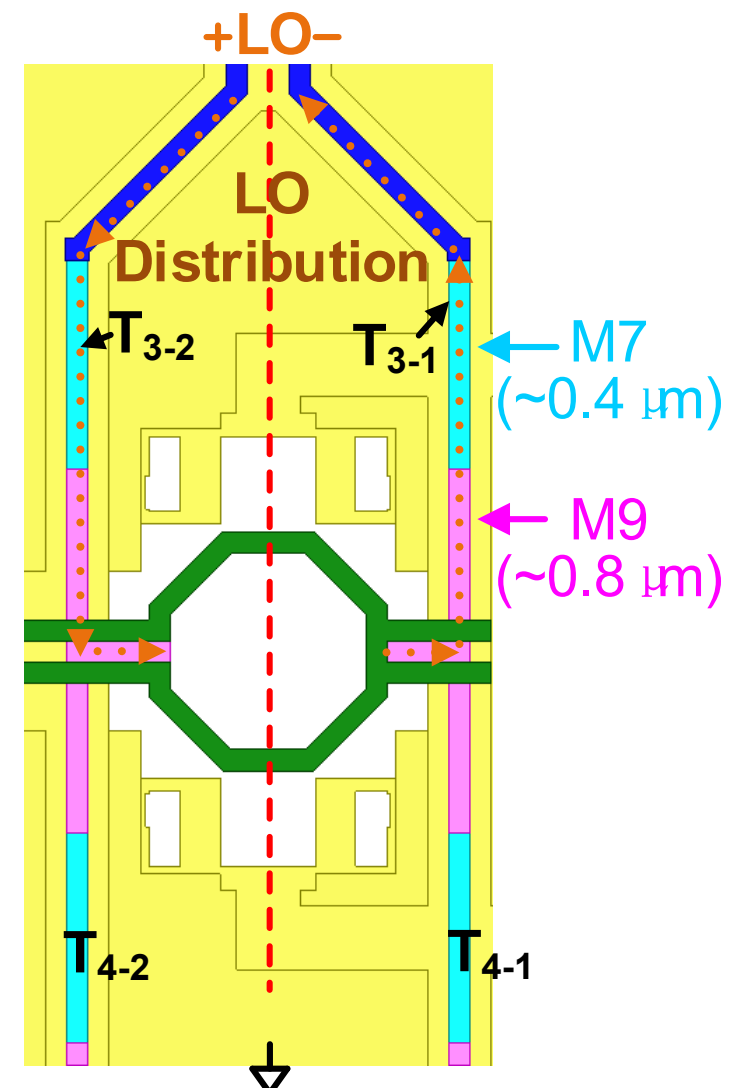
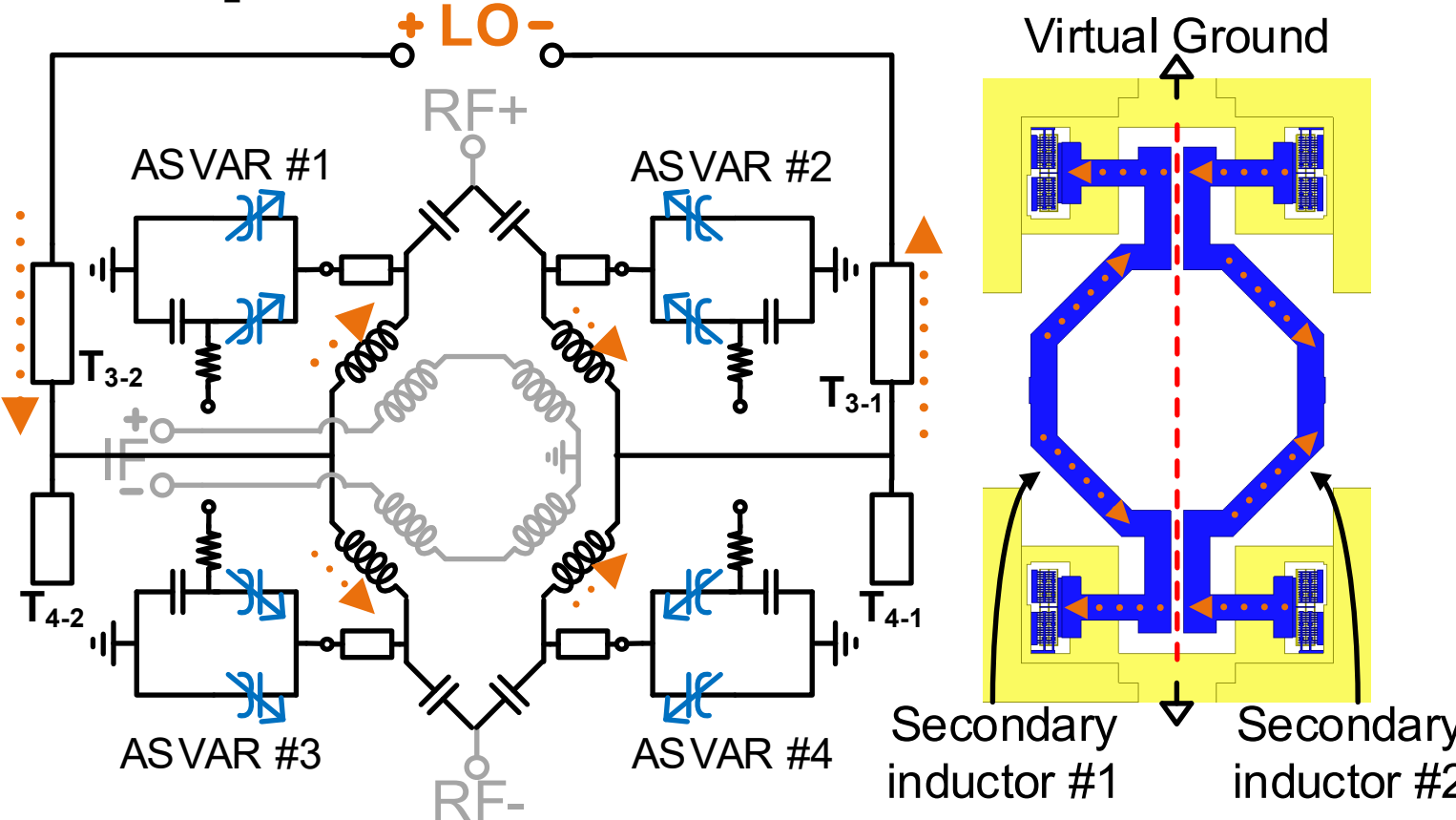
- Transformer for power splitting.
- Differential signal isolation.

IF Equivalent Circuit



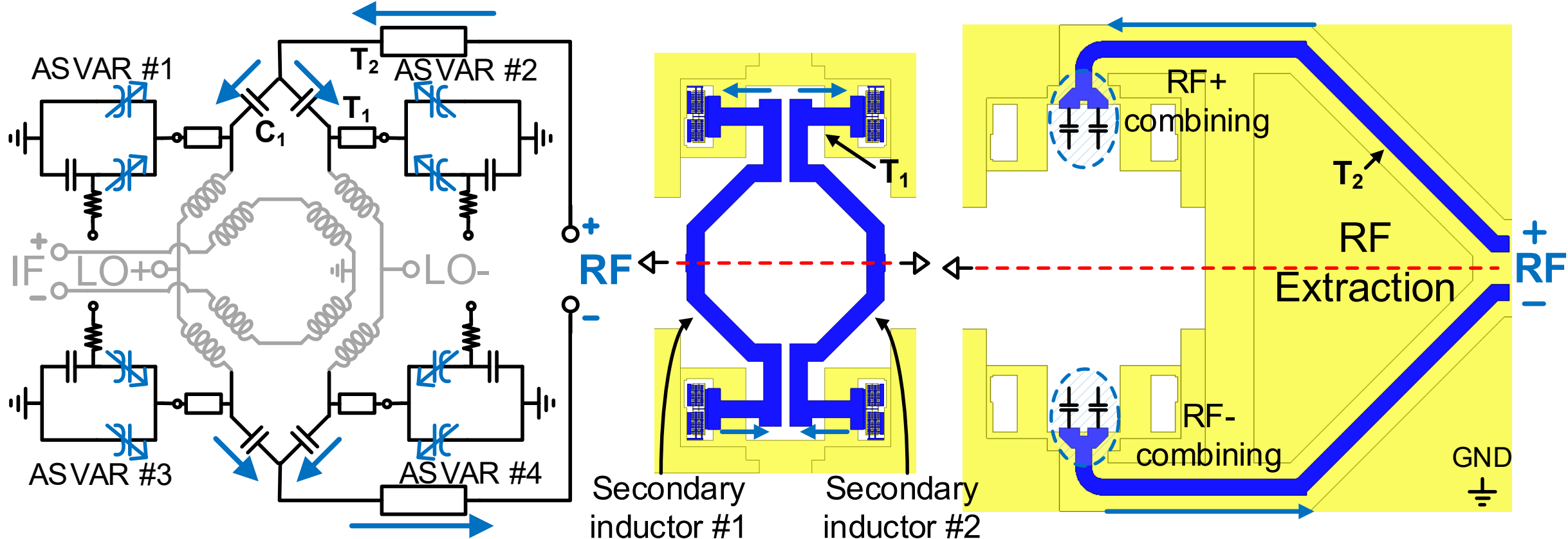
- Differential IF input at primary inductor.
- LO and RF ports as virtual ground for IF.

LO Equivalent Circuit



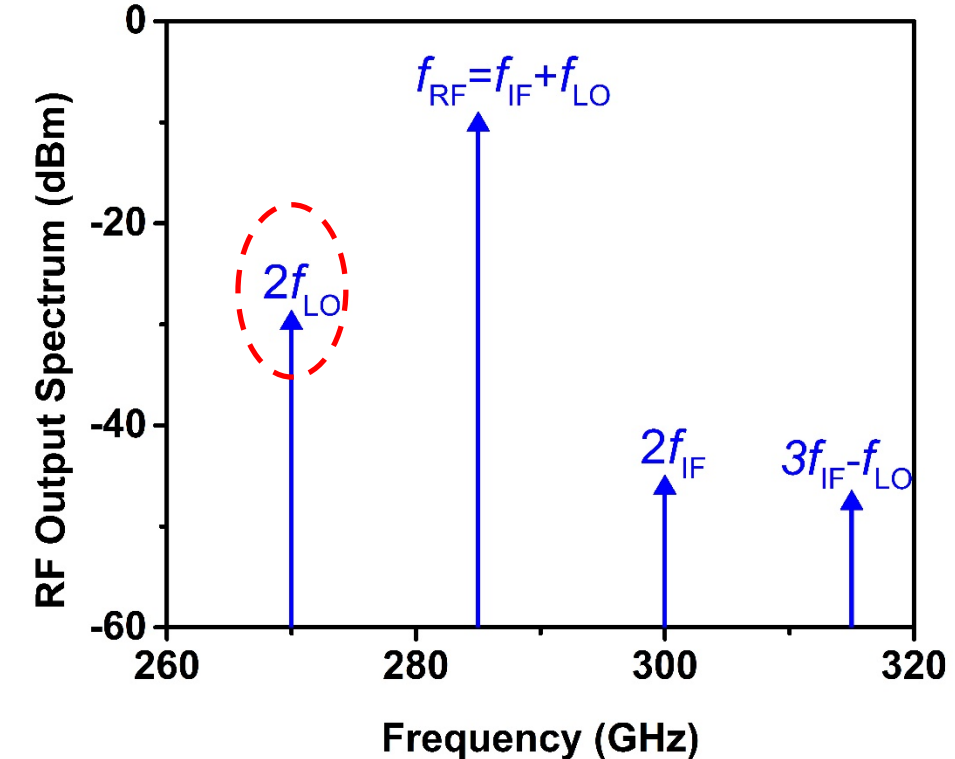
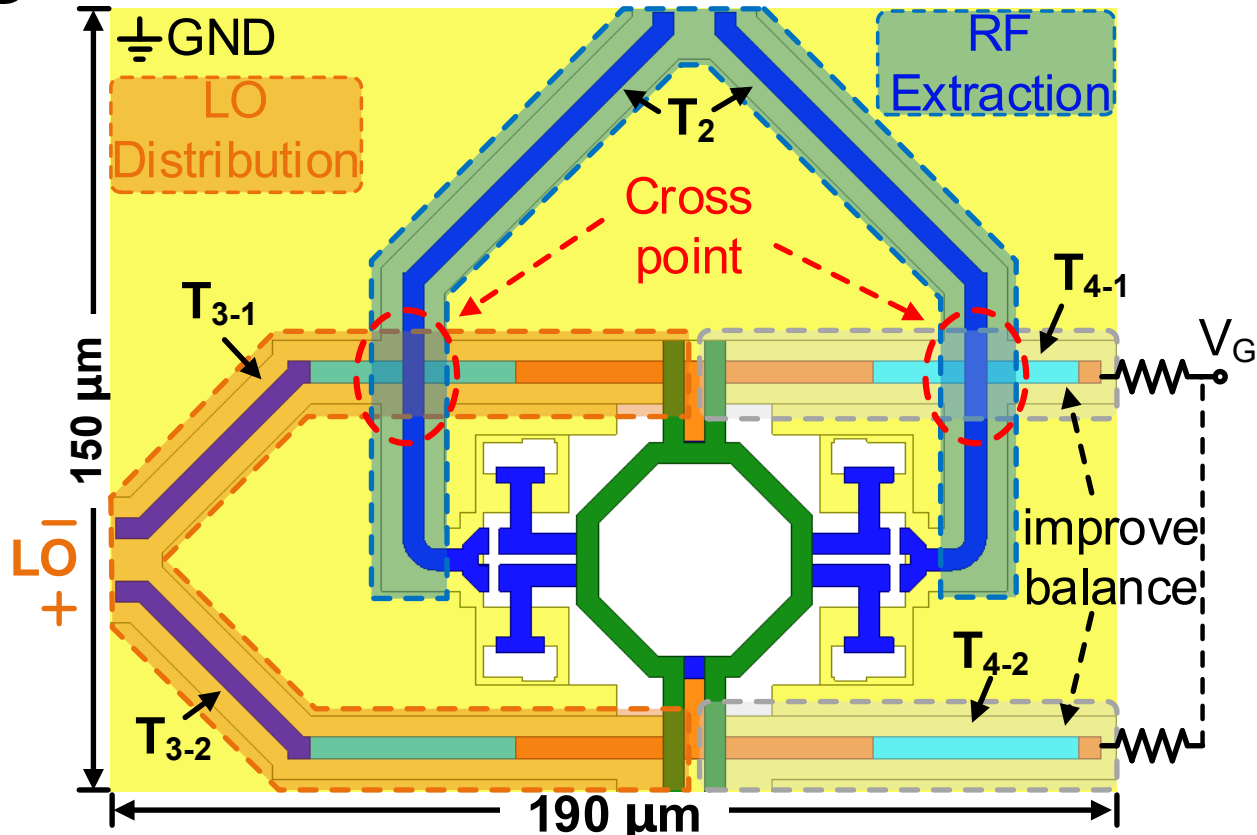
- Differential LO input at center of two secondary inductors.
- IF and RF ports as virtual ground for LO.
- Additional GCPW for LO distribution.

RF Equivalent Circuit



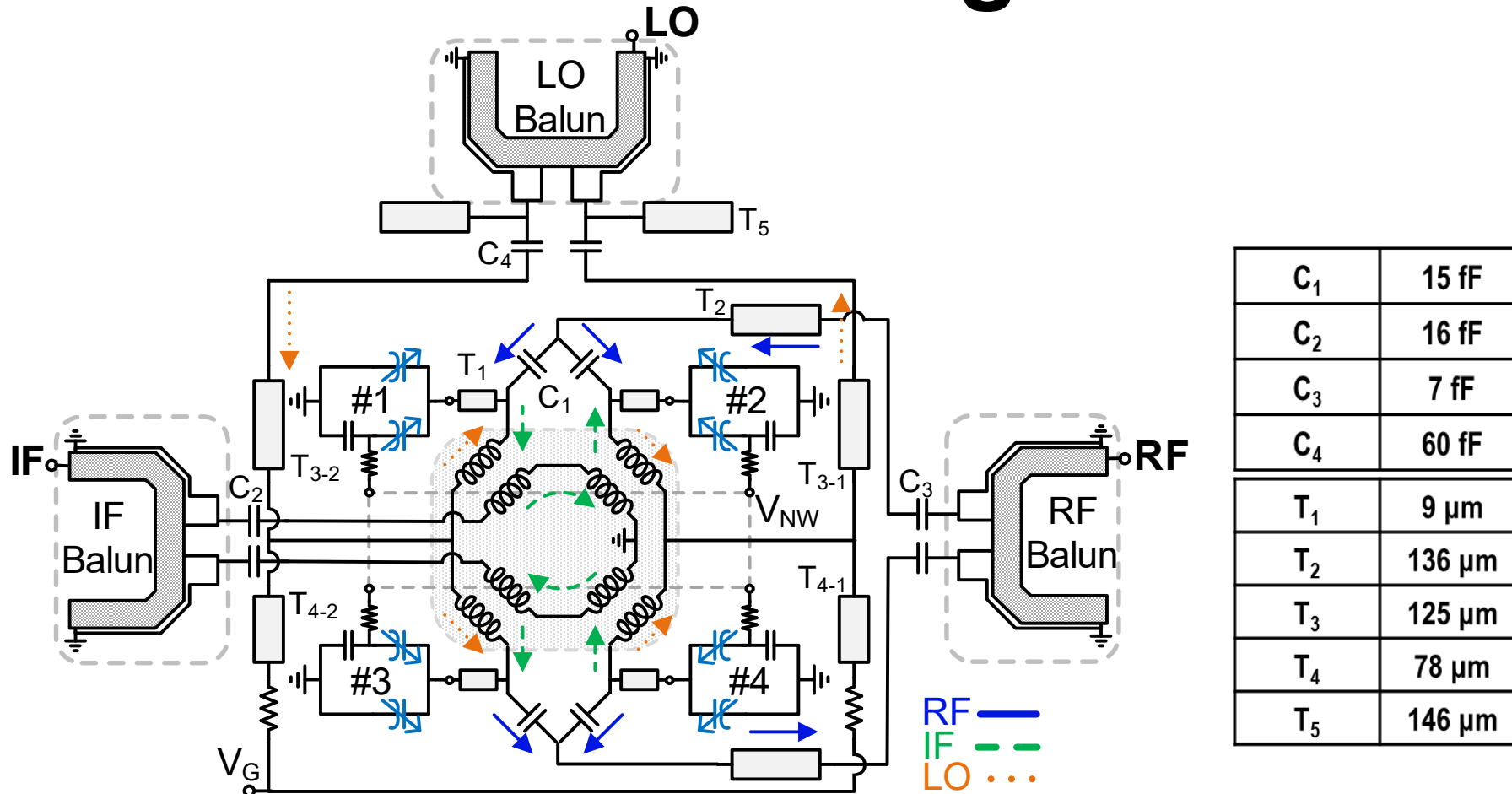
- Differential RF output from ASVAR #1,2 and #3,4.
- IF and LO ports as virtual ground for RF.
- Additional GCPW for RF extraction.

Hybrid Imbalance



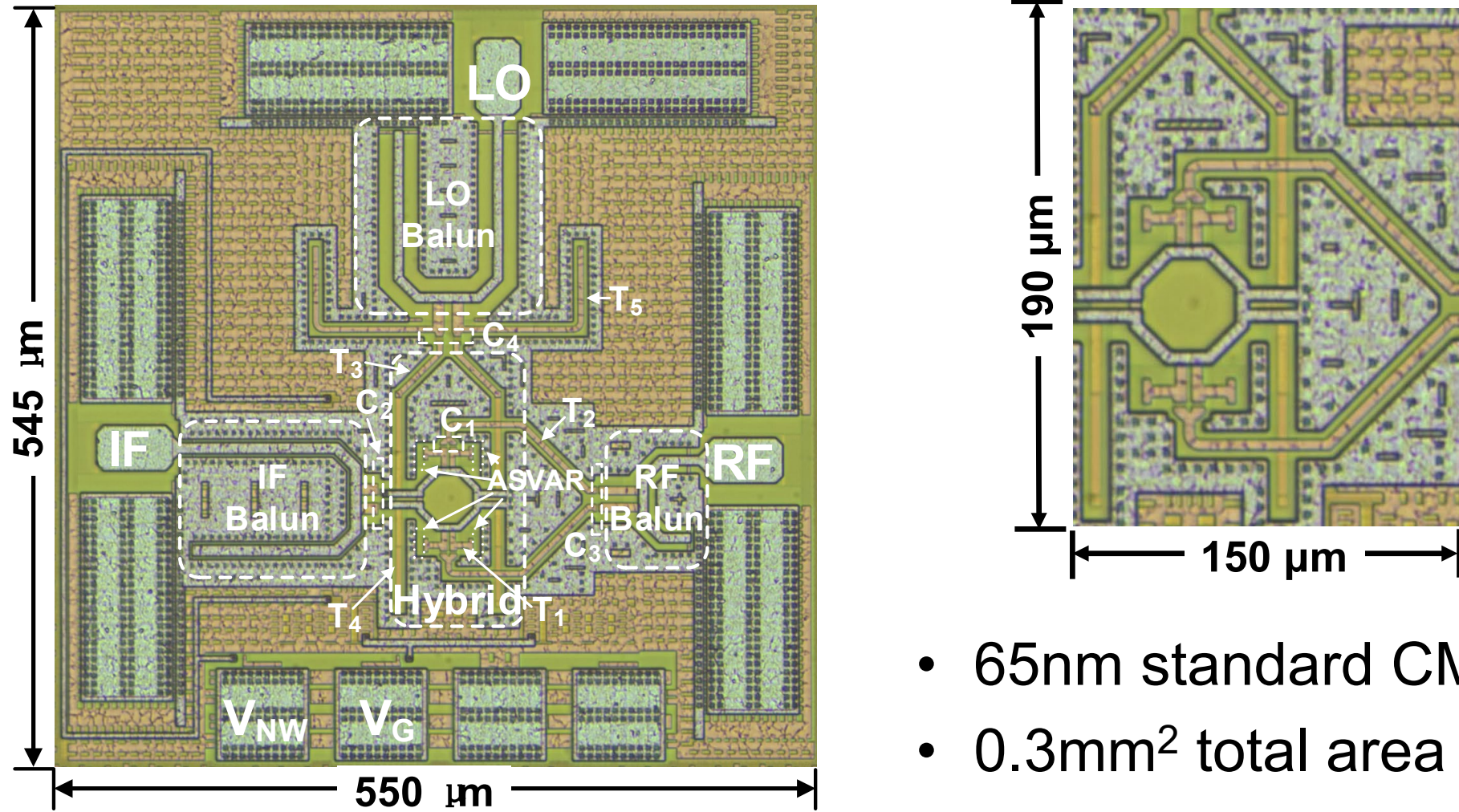
- Asymmetry due to LO distribution and RF extraction.
- Additional $T_{4-1,2}$ to improve balance.
- Resulting in a $2f_{LO}$ leakage.

Upconverter Circuit Diagram



- Double-balanced fundamental upconverter using ASVAR.
- Three baluns for measurement.

Chip Micrograph

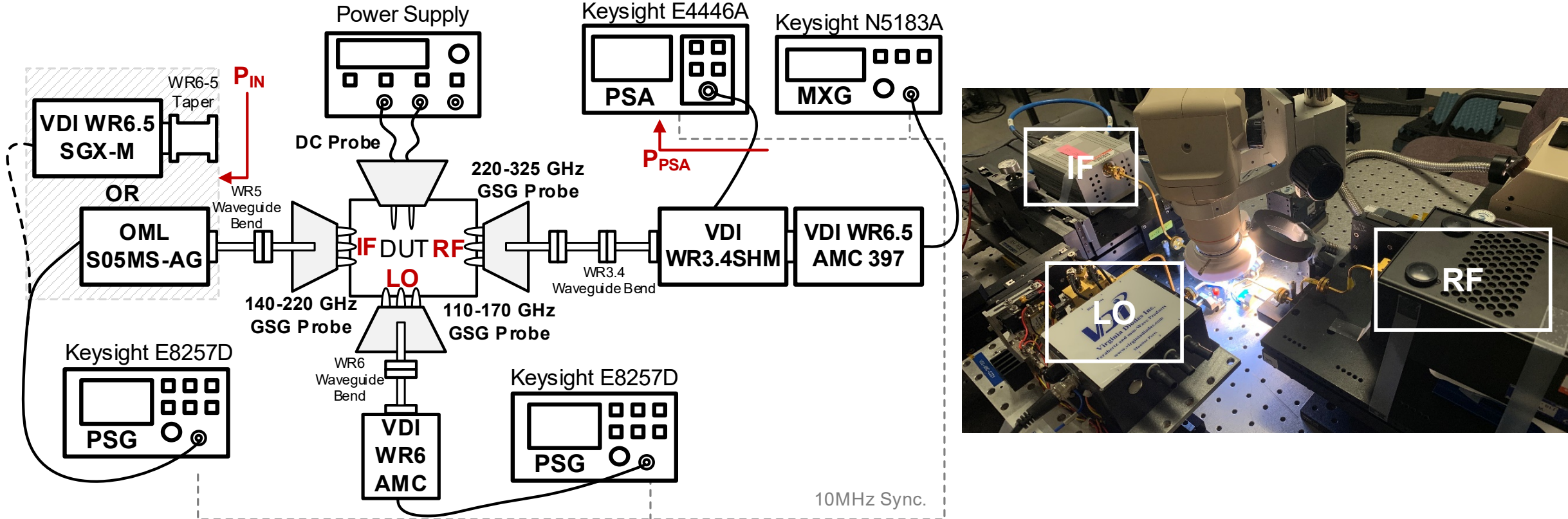


23.1: 270-to-300GHz Double-Balanced Parametric Upconverter Using Asymmetric MOS Varactors and a Power-Splitting-Transformer
Hybrid in 65nm CMOS

Outline

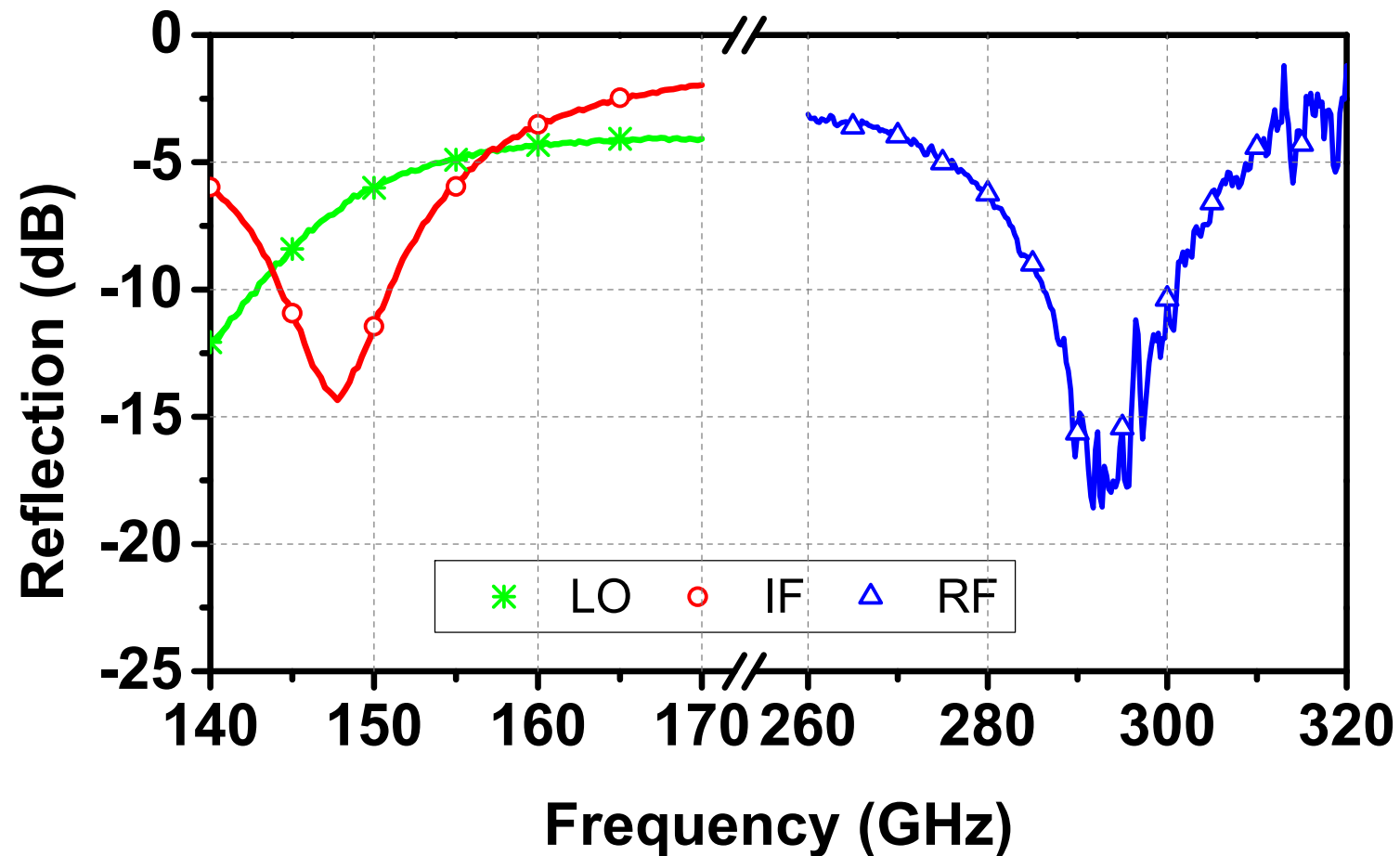
- Introduction
- Manley-Rowe Relation
- Upconverter Implementation
- Measurement Results
- Conclusion

Measurement Setup

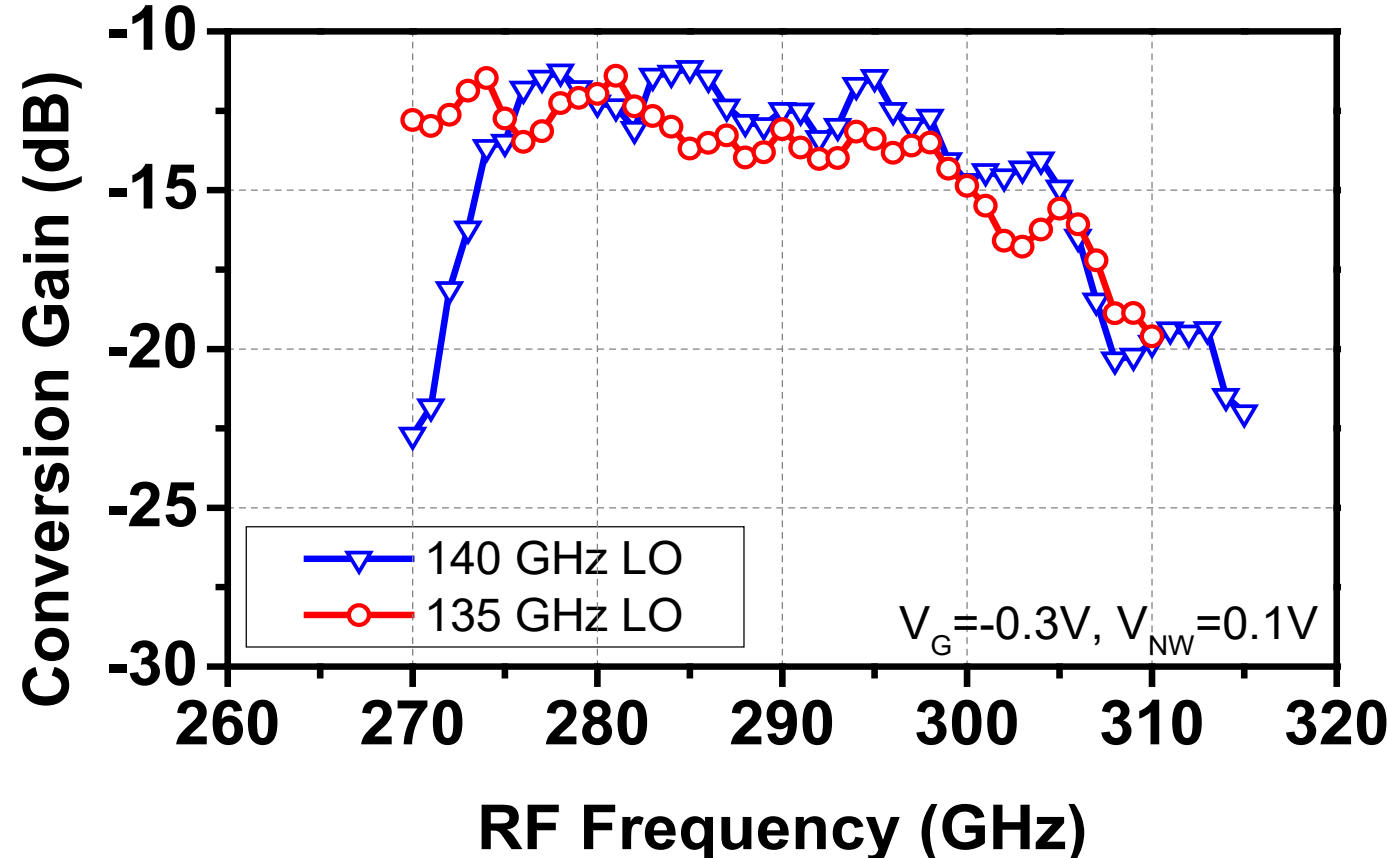


- RF output power (dBm) $P_{RF} = P_{PSA} - CG_{SHM} + L_{325\text{Probe}} + L_{WR3.4\text{Bend}}$
- Conversion Gain (dB) $CG = P_{RF} - P_{IN} + L_{220\text{Probe}} + L_{WR5\text{Bend}}$

Measurement Results

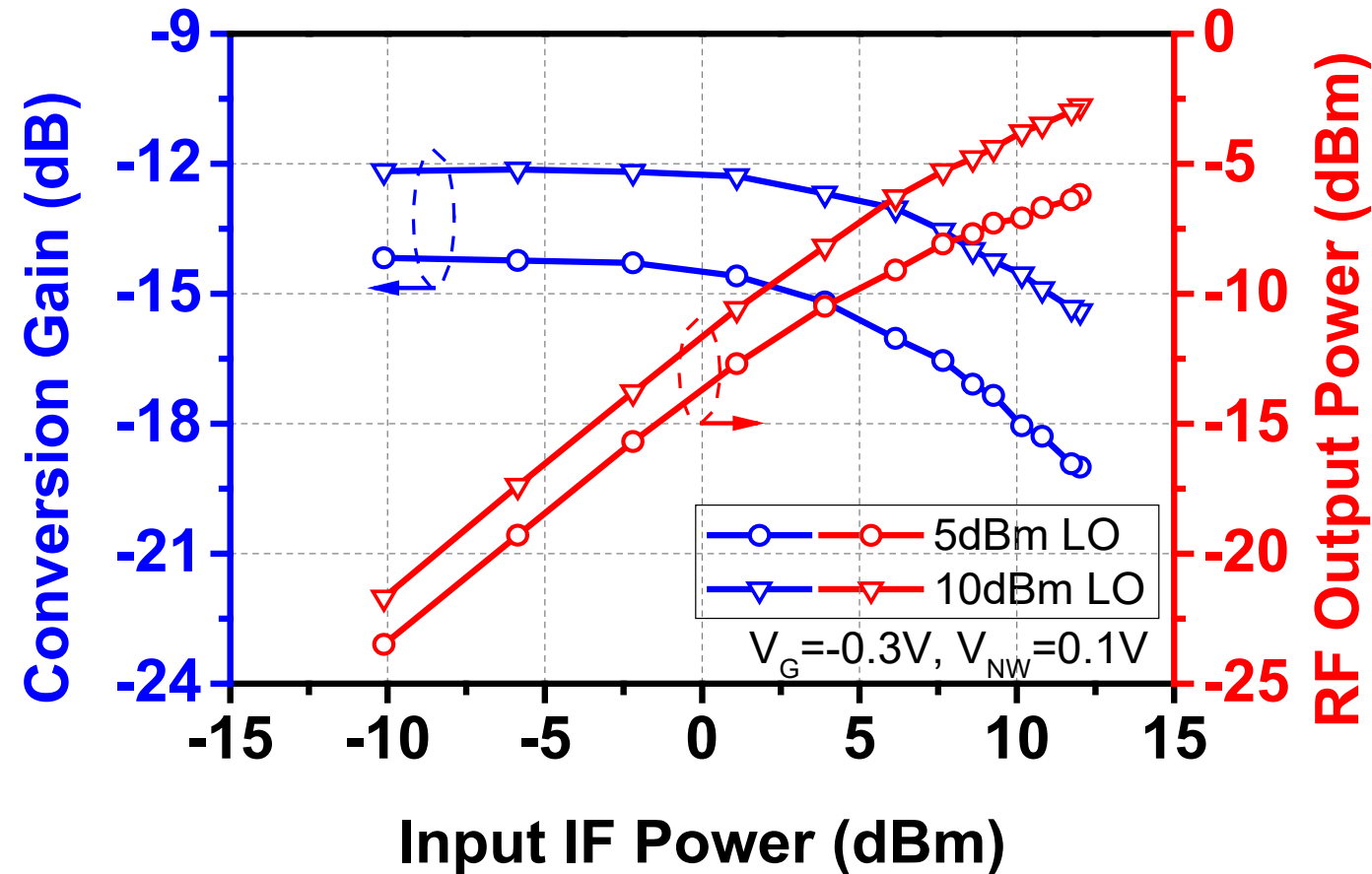


Measurement Results



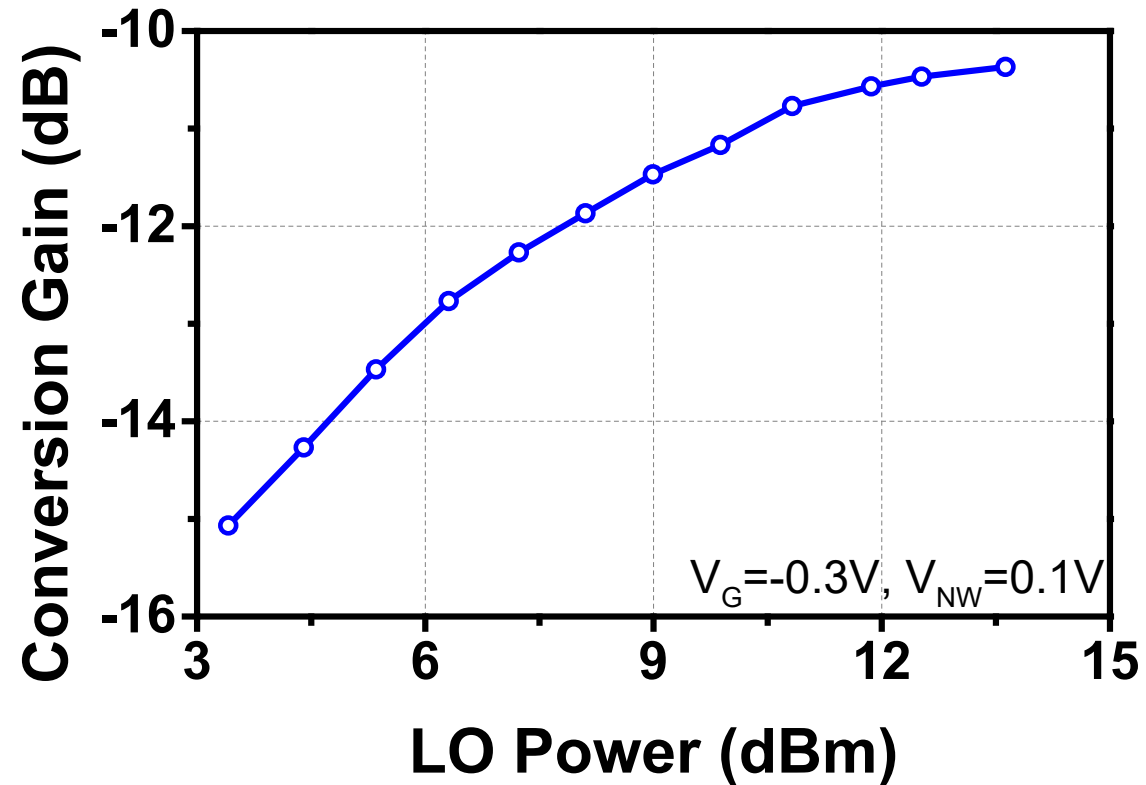
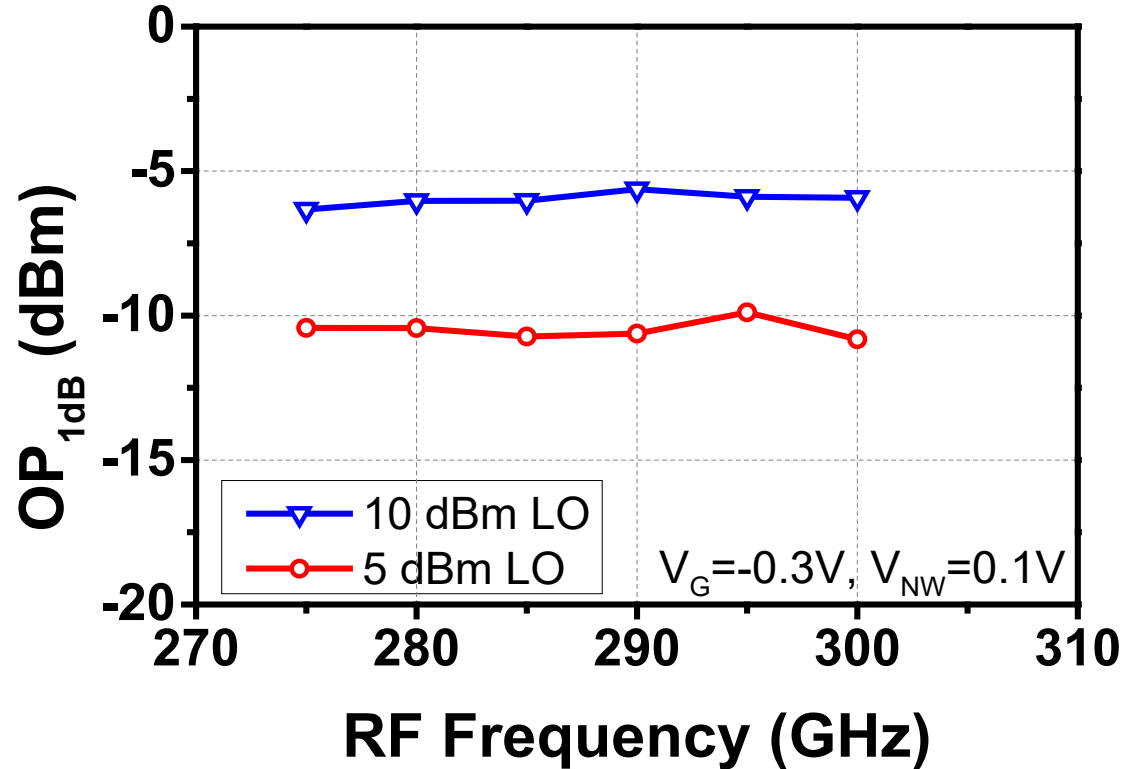
- Measured maximum CG is -11.2dB and -11.4dB with a 10-dBm LO at 140 and 135 GHz.

Measurement Results



- Measured OP_{1dB} is -6.4dBm and -10.5dBm with LO power of 10 and 5 dBm at 140 GHz.

Measurement Results



- OP_{1dB} varies within 0.5dB over bandwidth.
- CG saturated at -10.4dB with an LO power of 13 dBm.

Comparison Table

Reference	H. Hamada JSSC 2020	H. Song TMTT 2014	Q. Zhong CICC 2018	K. Takano ISSCC 2017	S. Lee ISSCC 2019	This Work	
Topology	Single-ended Resistive	Single-balanced Half-Gilbert	Double- balanced Passive-Gilbert	Single-balanced Square ^(b)		Double-balanced Reactive	
RF (GHz)	270-302	280-320	285-315	289-311	252-275	270-299	275-300
IF (GHz)	0-32	0-20	110-140	144-166	120-143	135-164	140-160
LO (GHz)	270	300	175	145	132	135	140
P _{LO} (dBm)	6.5	-5	--	--	--	10	
Max CG ^(a) (dB)	-15	-15	--	--	--	-11.4	-11.2
OP _{1dB} ^(a) (dBm)	-16.5	--	--	--	--	-7.5	-6.2
P _{sat} ^(a) (dBm)	--	--	-6	-14.5 ^(c)	-7.6 ^(c)	>-3 ^(d)	
P _{DC} ^(a) (mW)	0	22	0	19.95 ^(c)		0	
Area ^(a) (mm ²)	1	--	0.02 ^(e)	0.05 ^{(c)(e)}		0.3	
Technology	80nm InP	250nm InP	65nm CMOS	40nm CMOS	40nm CMOS	65nm CMOS	

(a) Mixer only. (b) Doubler-based. (c) Per channel. (d) Limited by instrument. (e) Estimated from die photo.

Outline

- Introduction
- Manley-Rowe Relation
- Upconverter Implementation
- Measurement Results
- Conclusion

Conclusion

- Reactive mixer using varactors in CMOS can have better performance.
- A double-balanced parametric upconverter using asymmetric MOS varactors is demonstrated in 65nm CMOS.
- A power-splitting-transformer hybrid is proposed for improved port isolation.
- Highest CG and OP_{1dB} are achieved among all CMOS upconversion mixers with RF of ~300 GHz.

Acknowledgment

- This work was supported in part by SRC JUMP and DARPA, and in part by the Regents of the University of California.
- We would like to thank members from ComSenTer for discussions.
- We would like to thank Prof. R. Henderson from UT Dallas for measurement support.

A 436-to-467GHz Lens-Integrated Reconfigurable Radiating Source with Continuous 2D Steering and Multi-Beam Operations in 65nm CMOS

Hossein Jalili, Omeed Momeni

High-Speed Integrated Electronic Systems Lab (HISIES)
University of California, Davis



About The Speaker



Hossein Jalili

- [currently] Postdoctoral fellow, Georgia Institute of Technology
- Postdoctoral scholar, University of California Davis
- PhD, electrical engineering , University of California Davis
- M.Sc., electrical engineering, Sharif University of Technology
- B.S., electrical engineering, Sharif University of Technology

- IEEE SSCS 2018-2019 predoctoral achievement award
- IEEE MTT-S 2018 graduate fellowship award
- UC Davis Allen G. Marr 2020 distinguished dissertation award
- UC Davis ECE Anil Jain best PhD thesis prize
- UC Davis ECE Richard and Joy Dorf graduate student award

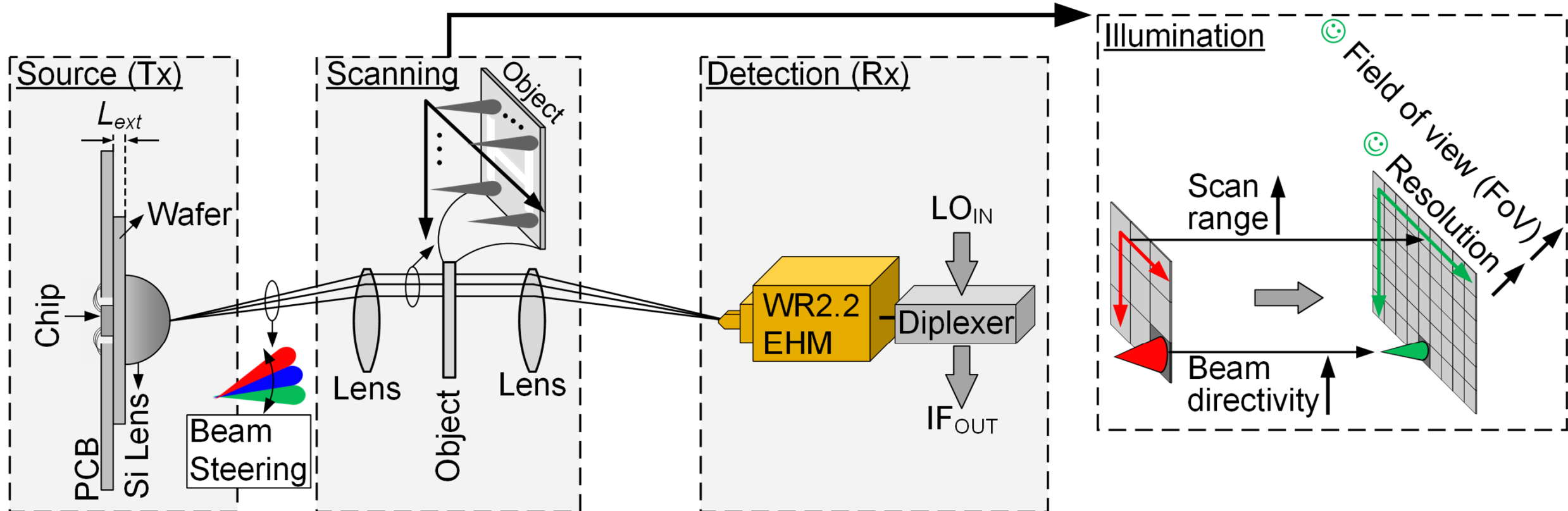
Outline

- Introduction
- Lens-integrated beam steering
- Reconfigurable array architecture
 - Array's unit cell: core oscillator + on-chip antenna
 - Reconfigurable coupling
- Experimental Results
- Conclusion

Outline

- Introduction
- Lens-integrated beam steering
- Reconfigurable array architecture
 - Array's unit cell: core oscillator + on-chip antenna
 - Reconfigurable coupling
- Experimental Results
- Conclusion

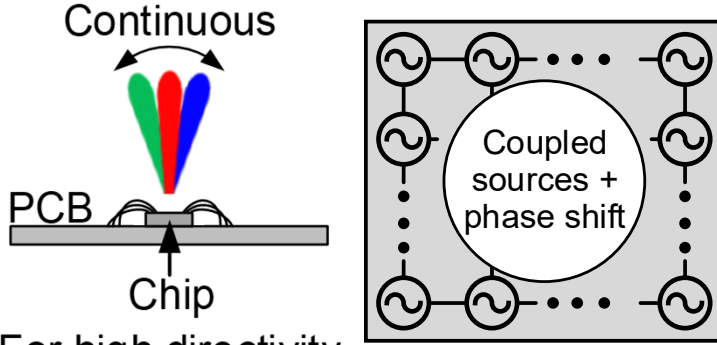
THz Imaging/Sensing



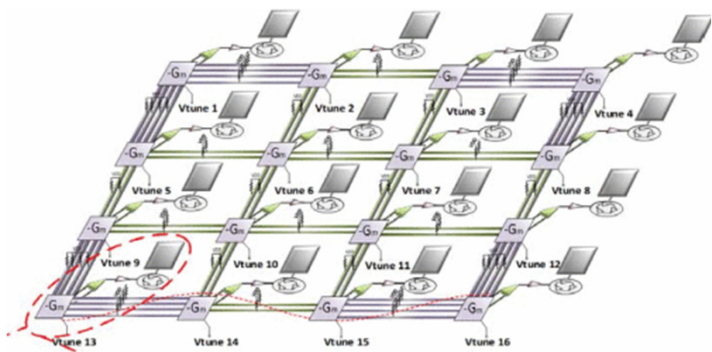
- THz imaging/sensing applications:
 - Wide-angle scalable electronic scanning → fast + large field of view (FoV)
 - Continuous uninterrupted high-directivity scan → high-resolution

THz beam-steering/scanning

Phased Array

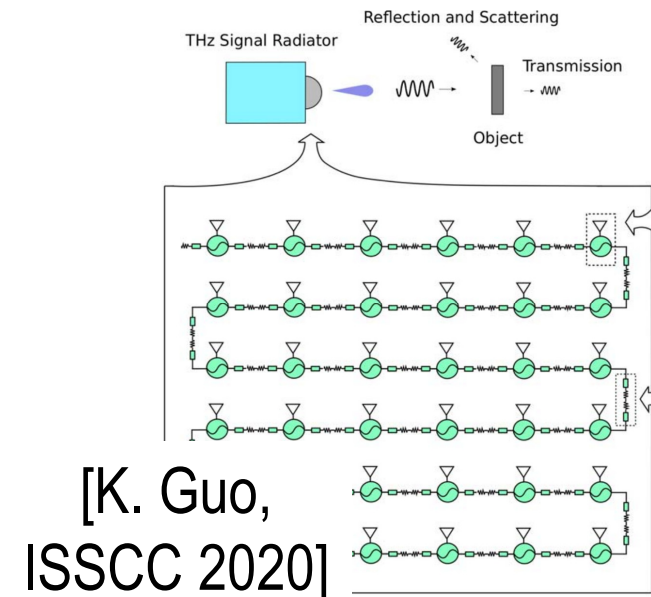
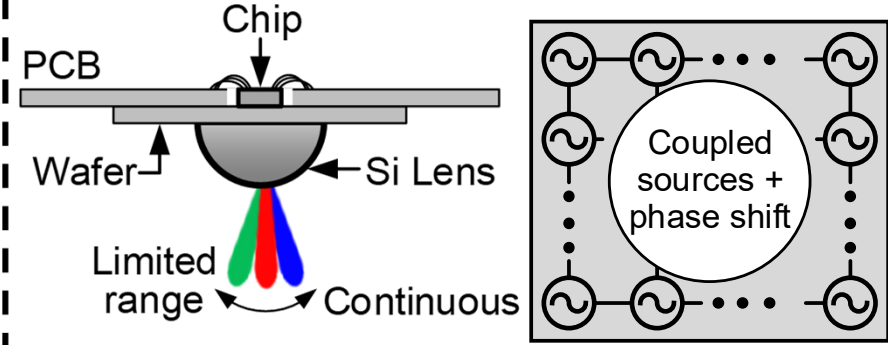


For high directivity
→ large array size
→ large DC power



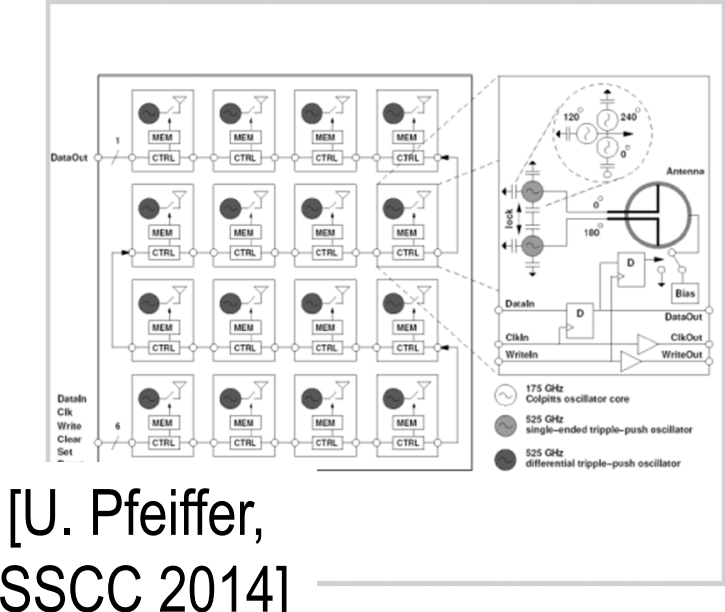
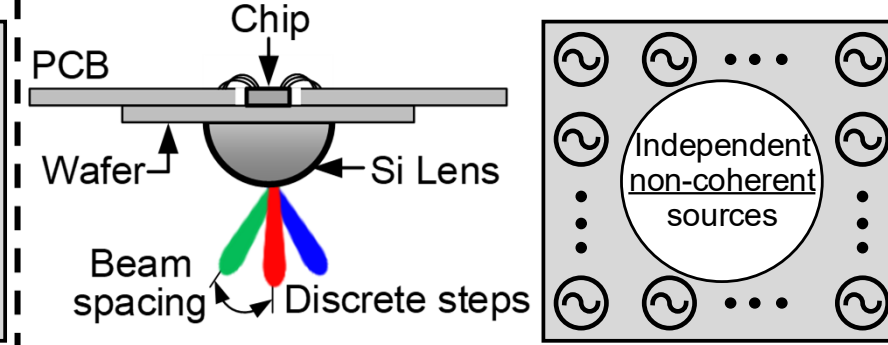
[H. Saeidi, ISSCC 2020]

Phased Array + lens



[K. Guo,
ISSCC 2020]

Non-coherent array



[U. Pfeiffer,
ISSCC 2014]

Electronic Scanning Methods: Comparison

Phased Array (w/o lens)

- 😊 Continuous scanning
- 😊 Limited non-scalable scan range
- 😊 Large power consumption cost for high directivity

Phased Array (w/ lens)

- 😊 Continuous scanning
- 😊 Scan range: further limited, and non-scalable
- 😊 Inefficient directivity/power consumption

Non-coherent Array

- 😊 Discrete-steps scanning
→ low-resolution + blind spots
- 😊 Scalable scan range
- 😊 Efficient directivity/power consumption

Reconfigurable Array

- 😊 Continuous uninterrupted high-directivity scanning
- 😊 Extended & scalable scan range
- 😊 Efficient directivity/power consumption

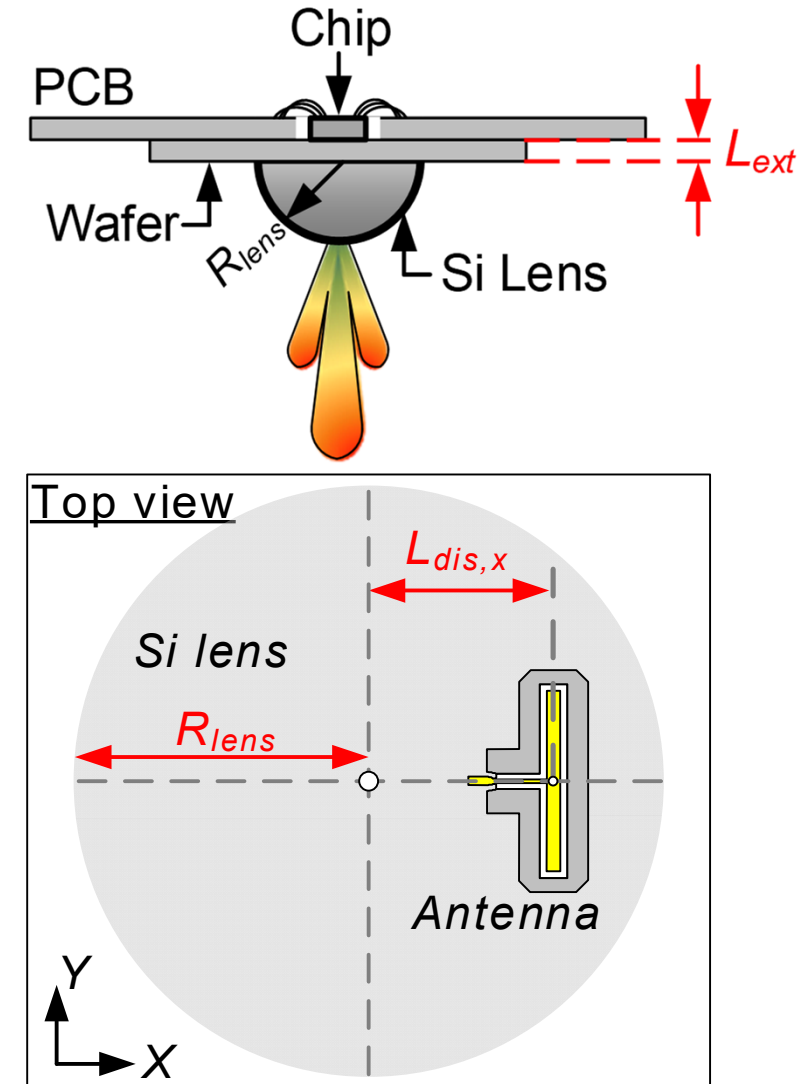
Outline

- Introduction
- **Lens-integrated beam steering**
- Reconfigurable array architecture
 - Array's unit cell: core oscillator + on-chip antenna
 - Reconfigurable coupling
- Experimental Results
- Conclusion

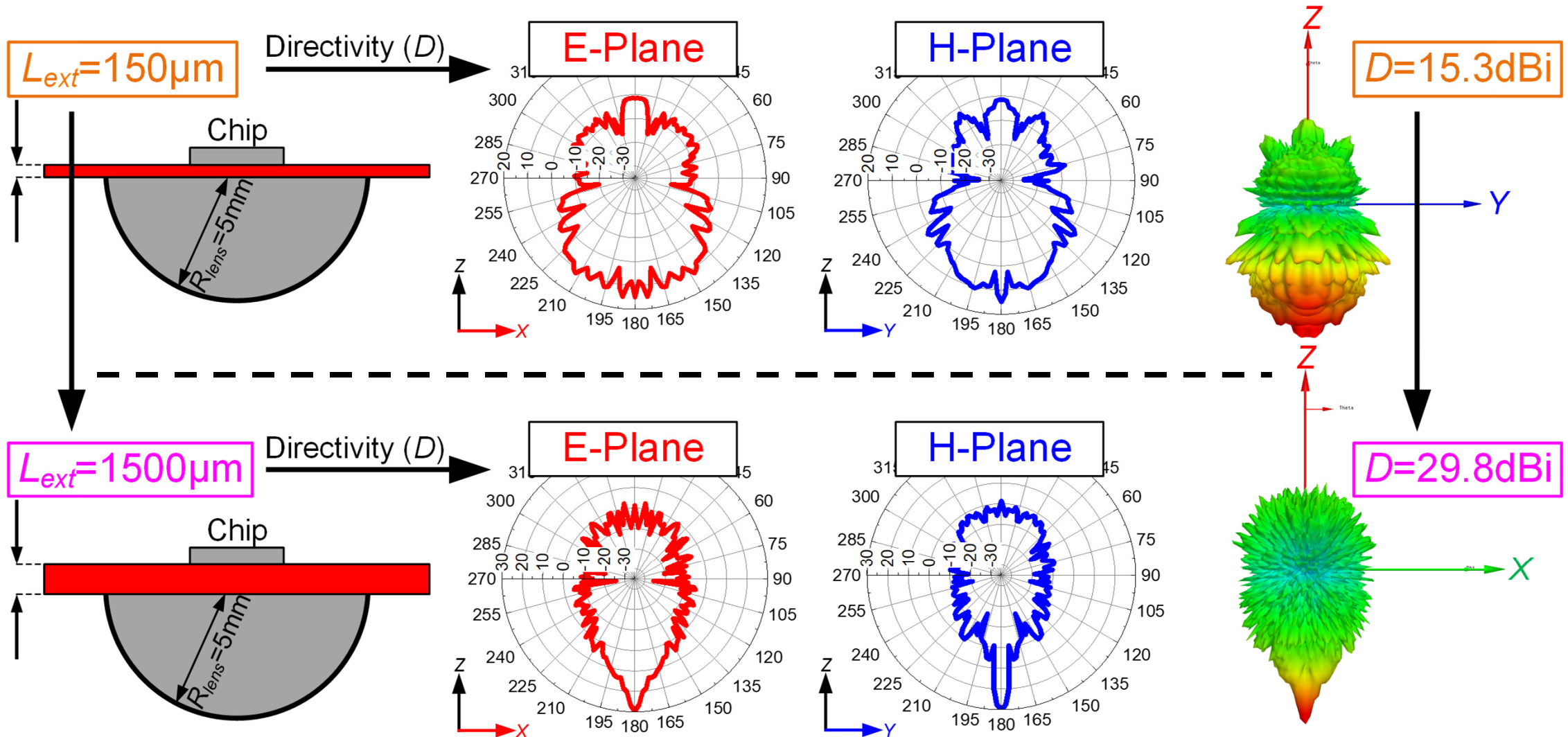
Lens-Coupled Radiation

- Radiation through substrate and Si lens
→ higher directivity & radiation efficiency

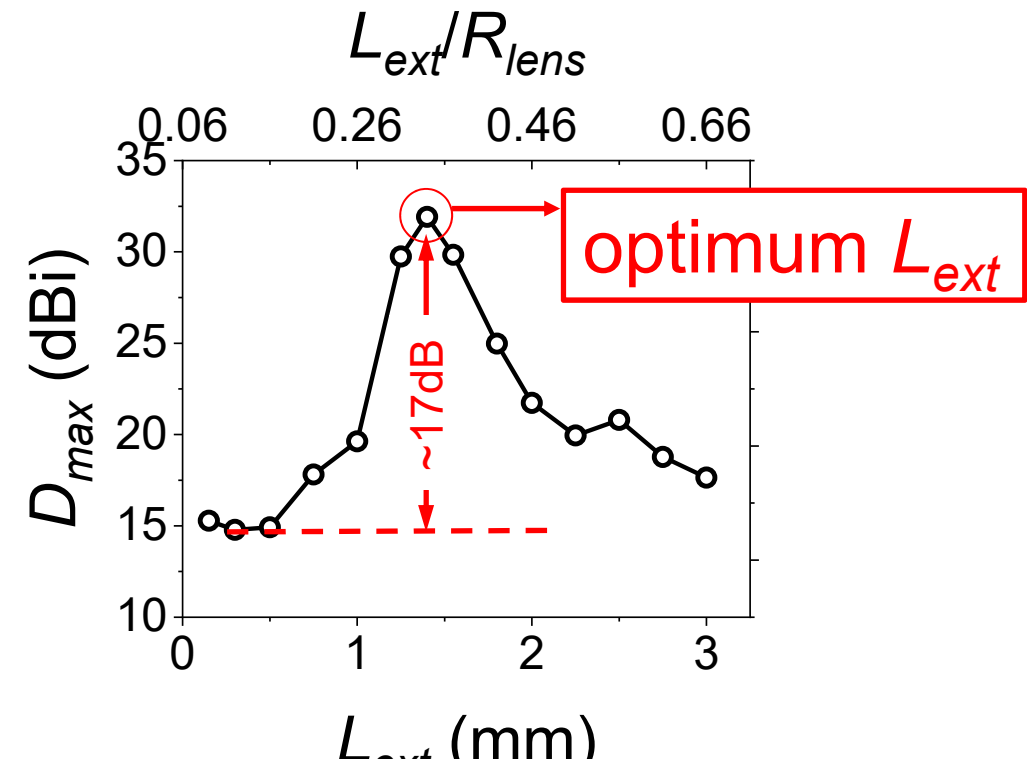
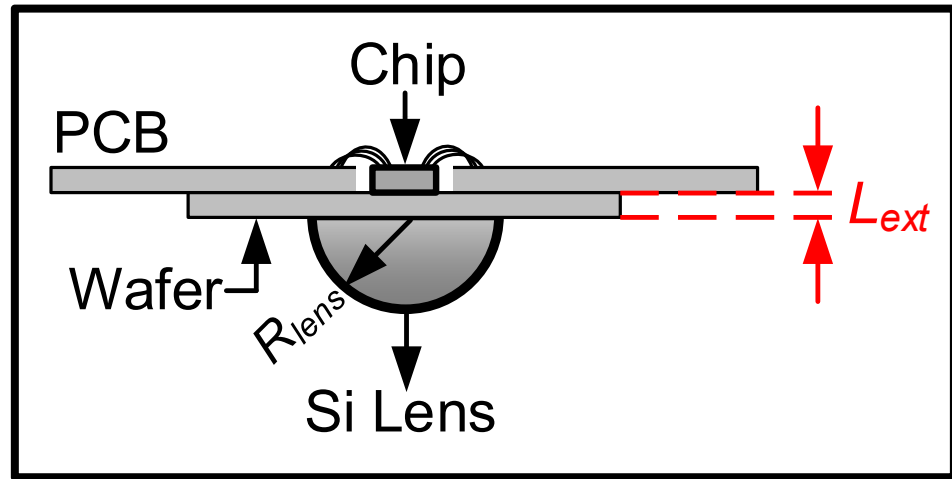
- Radiation patterns determined by:
 1. On-chip antenna
 2. Lens size (R_{lens})
 3. Extension length (L_{ext})
 4. Alignment (L_{dis})



Si Lens Radiation: L_{ext} (Extension Length)



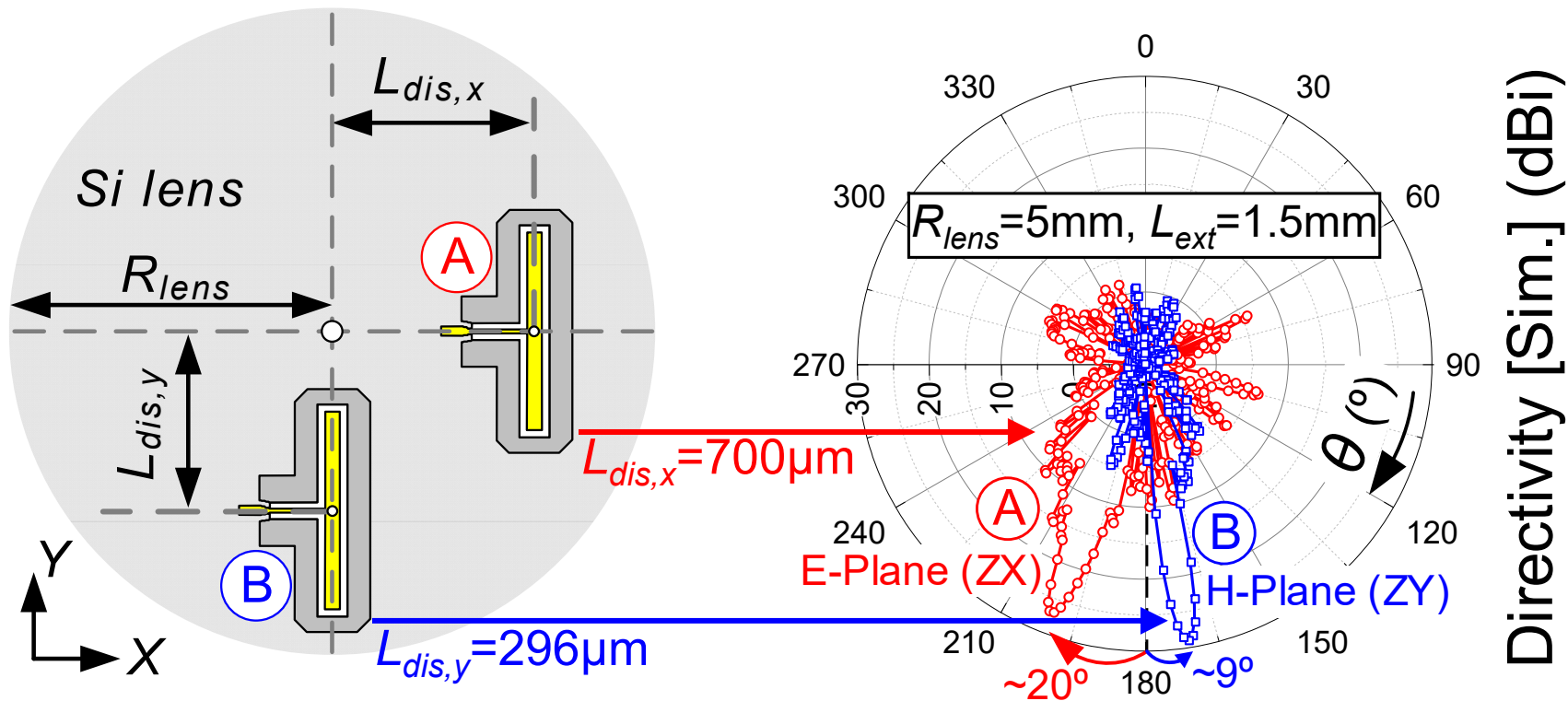
Si Lens Radiation: L_{ext} (Extension Length)



[H. Jalili, JSSC 2020]

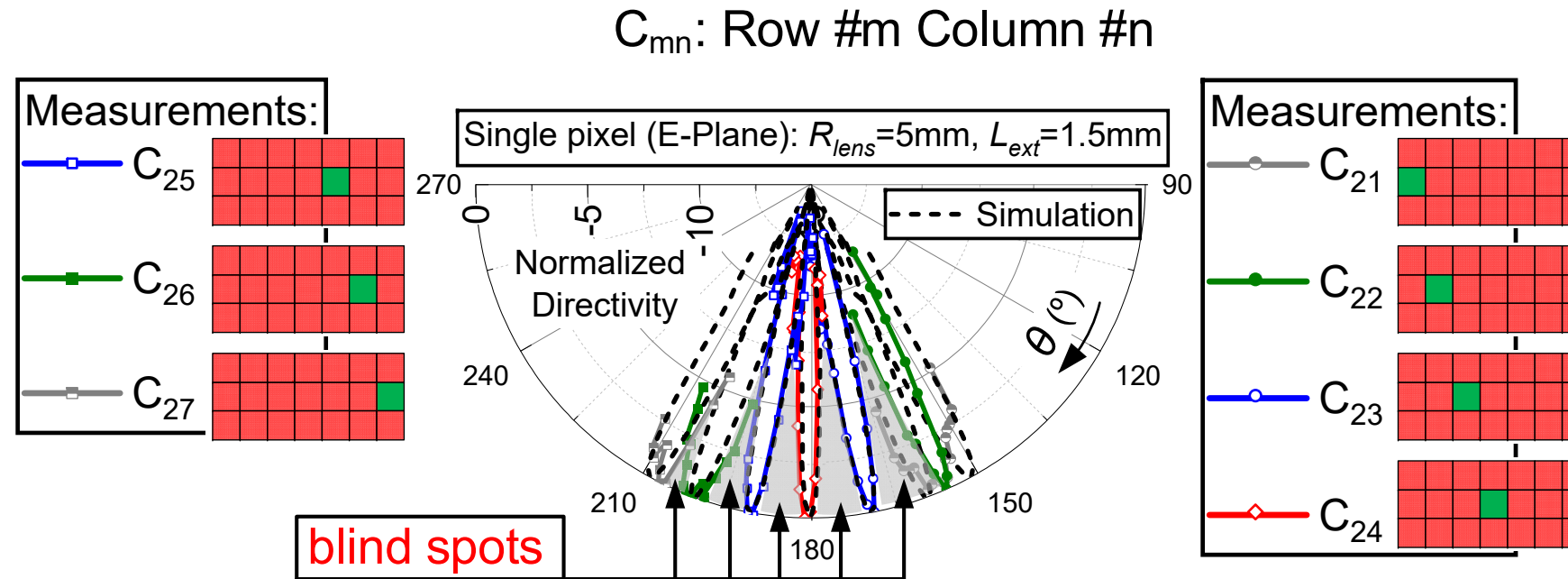
- L_{ext} has a significant impact on the directivity [D. Filipovic, TMTT 1993]
- Single antenna directivity (D_{max}) maximized at $L_{ext}/R_{lens} \sim 0.36$

Si Lens Radiation: L_{dis} (Displacement Offset)



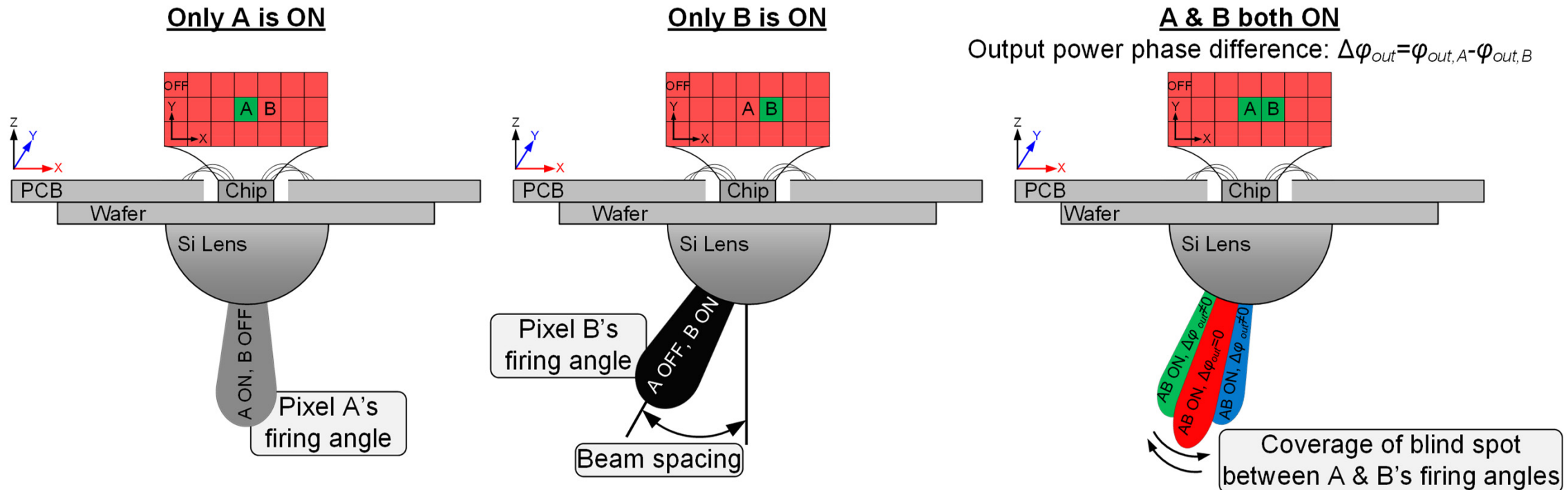
- ❑ Beam steering due to “displacement offset (L_{dis})” [H. Jalili, JSSC 2020]
- ❑ Steering angle $\propto L_{dis}/R_{lens}$ [D. Filipovic, Trans. Ant. Prop. 1997]

Blind Spots



- Displacement offsets of pixels → Discrete beam steering angles
→ “Blind spots” between individual beams uncovered by scanning
→ Reduction of resolution

Blind Spot Coverage



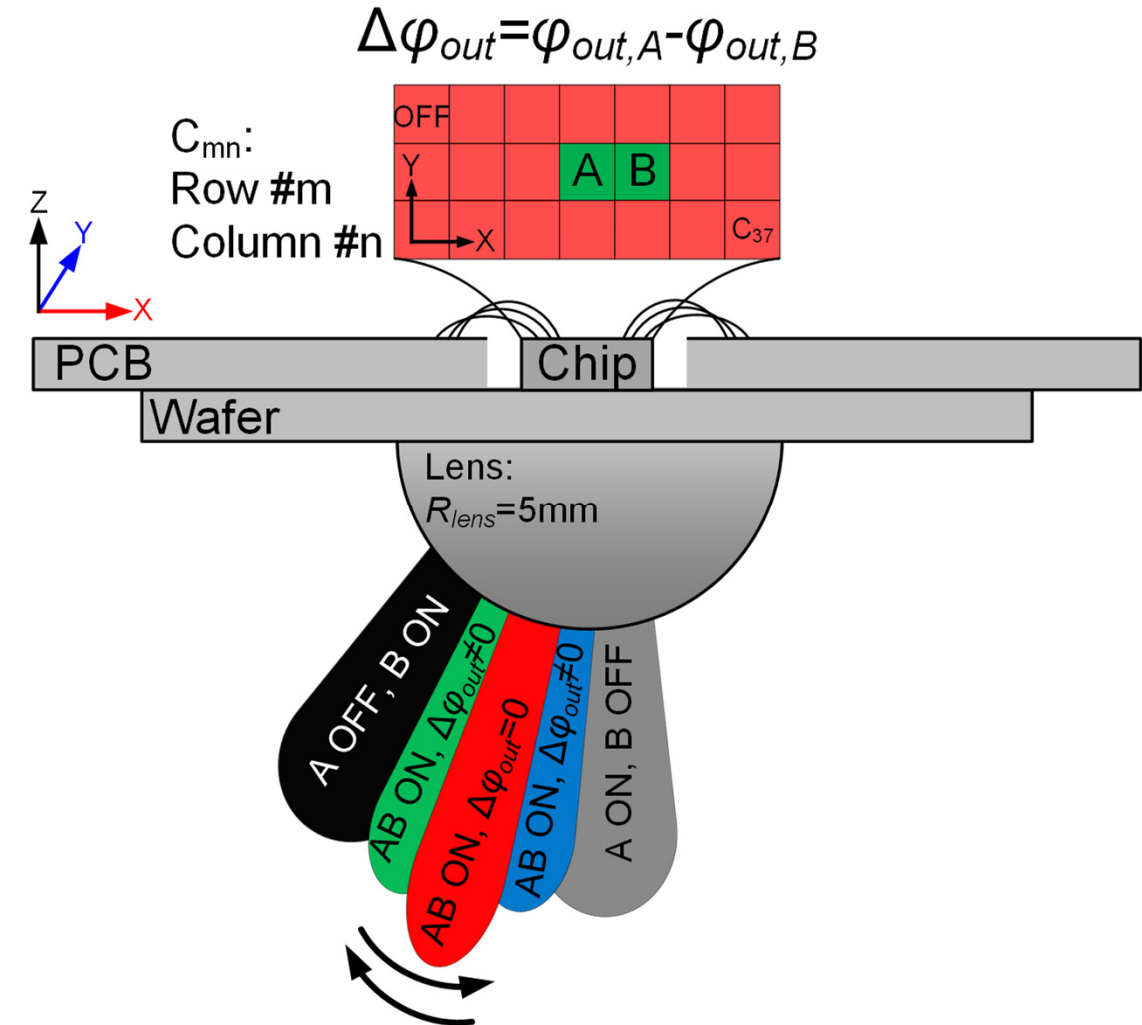
- Create phase shift ($\Delta\varphi$) between adjacent activated cells
 - Coverage of blind spots between their individual beams
 - Continuous uninterrupted beam steering

Advantages

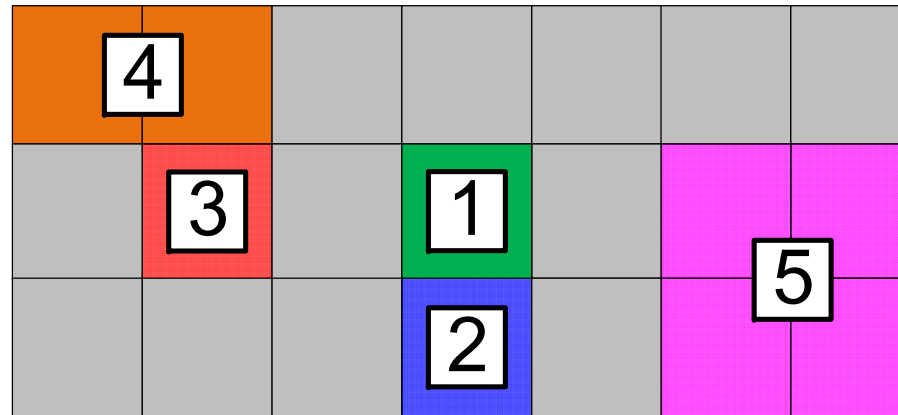
□ Combining 2 steering methods:

1. Antenna displacement
2. Phase shifting

- 😊 High-resolution continuous scanning
- 😊 High directivity
- 😊 Low power consumption
- 😊 Scalable



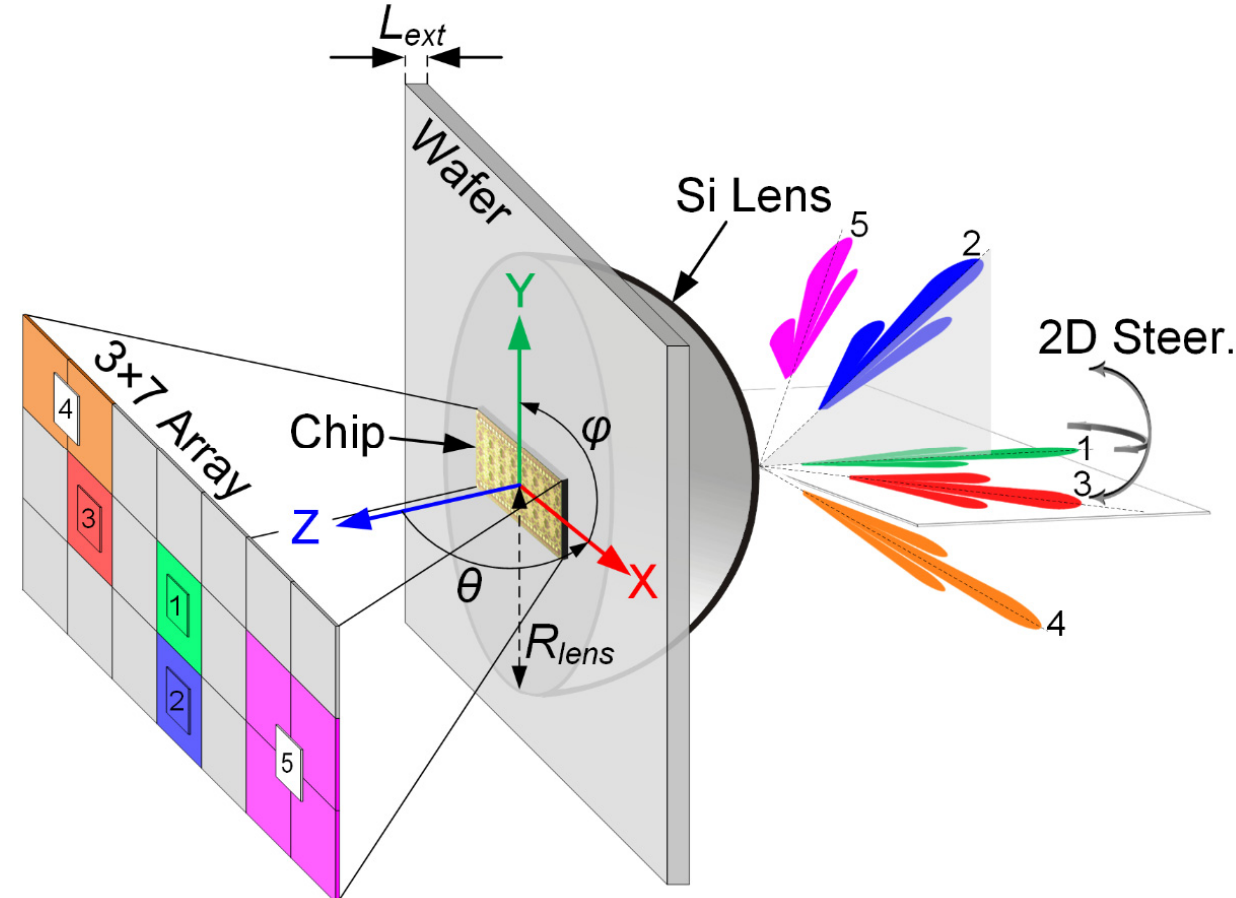
Reconfigurable Array



- Automatic phase/frequency coupling between adjacent ON cells
- Unwanted loading from OFF cells suppressed
→ ~ Unchanged operation (frequency & output power)
- Any desired sub-array can be turned ON
- Multiple non-intersecting sub-arrays can be ON at the same time

Reconfigurable Array + Lens

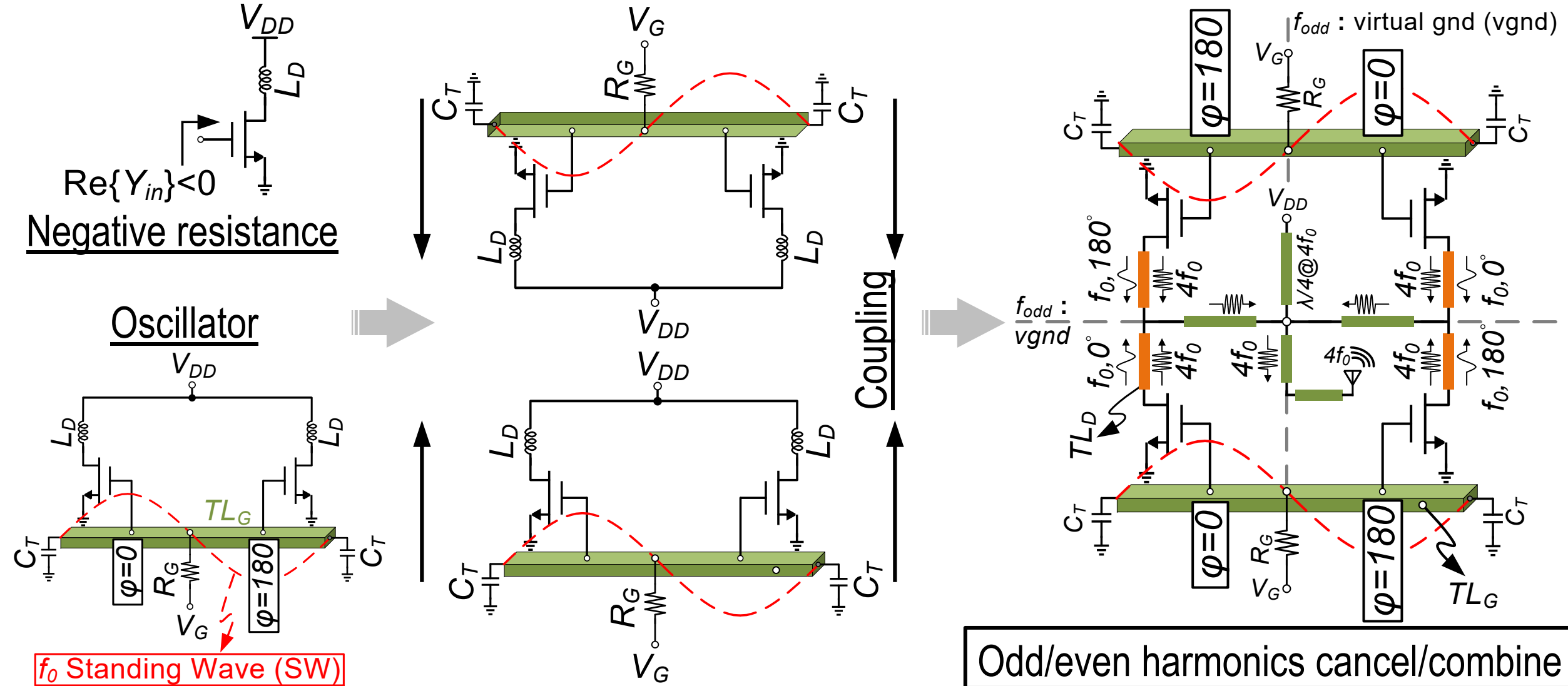
- Activated sub-array position
→ beam steering (2D)
- Simultaneous Multi-beam/-freq.
operation
- Sub-array activation + phase shift
→ *continuous* fine coverage of
blind spots between sub-array's
individual pixels



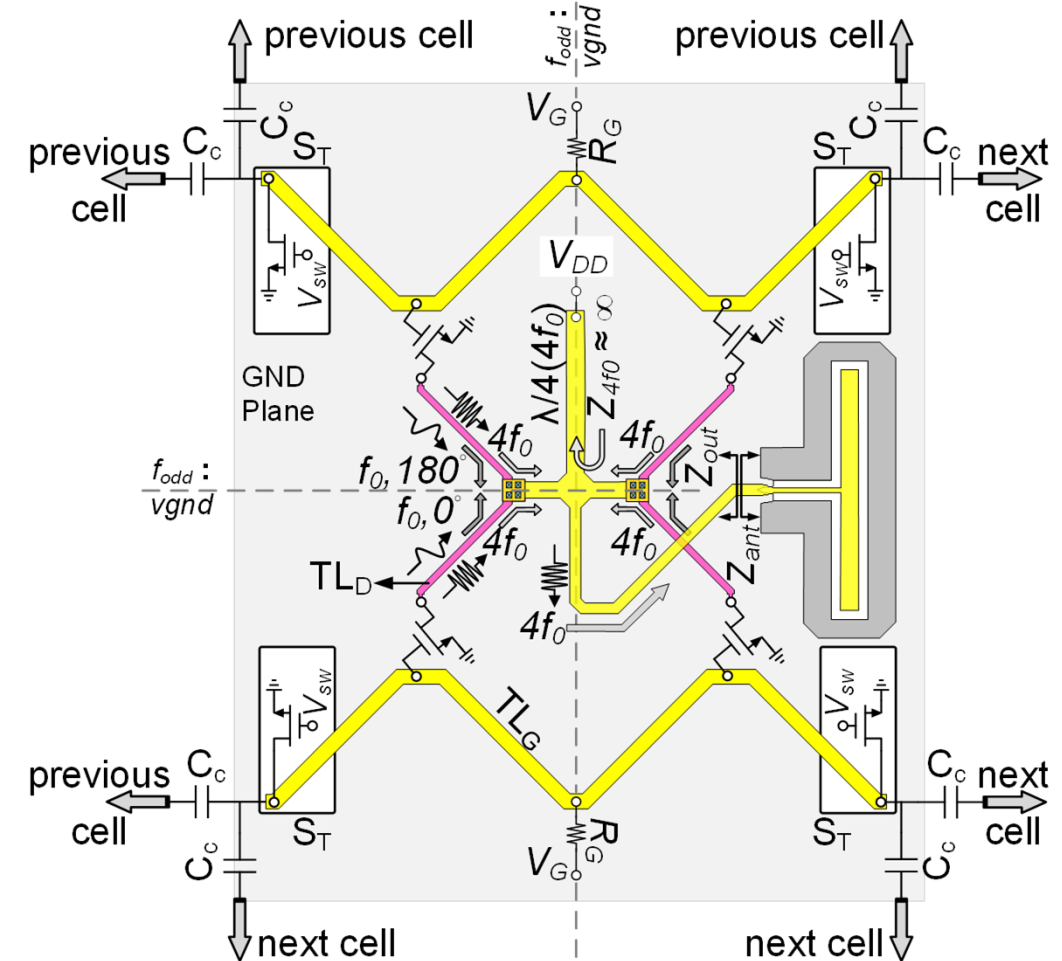
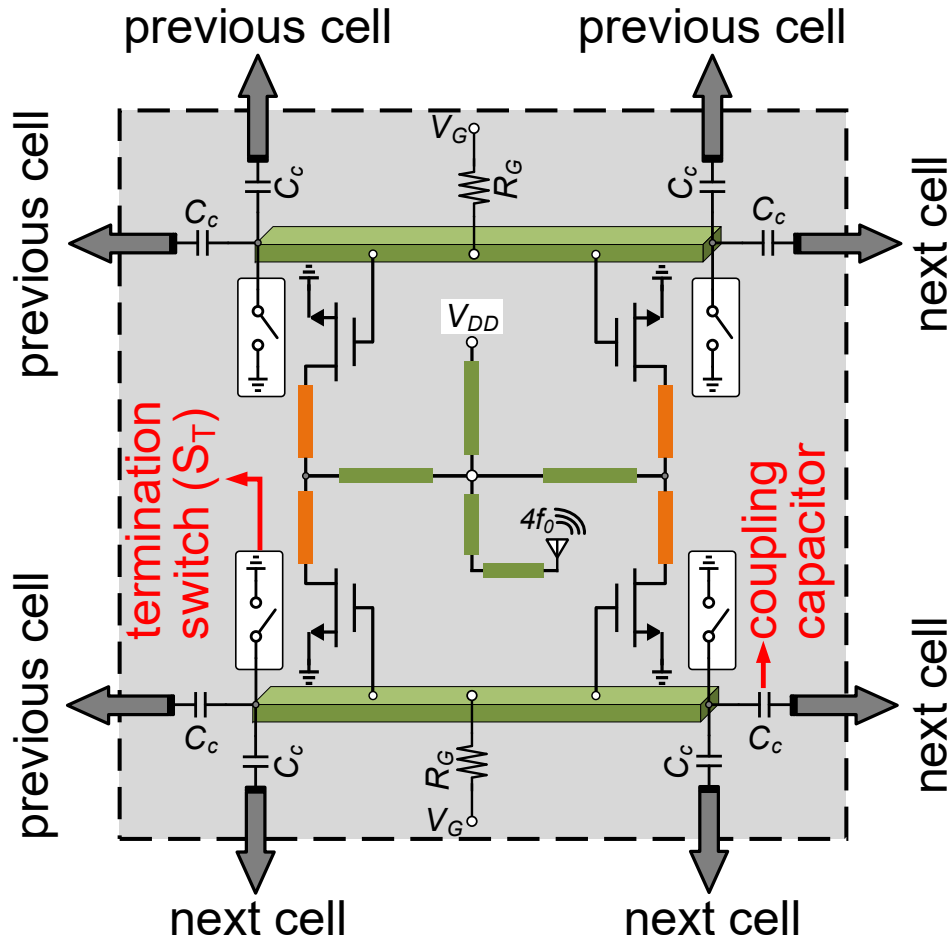
Outline

- Introduction
- Lens-integrated beam steering
- **Reconfigurable array architecture**
 - Array's unit cell: core oscillator + on-chip antenna
 - Reconfigurable coupling
- Experimental Results
- Conclusion

Unit Cell: Standing Wave Oscillator (SWO)

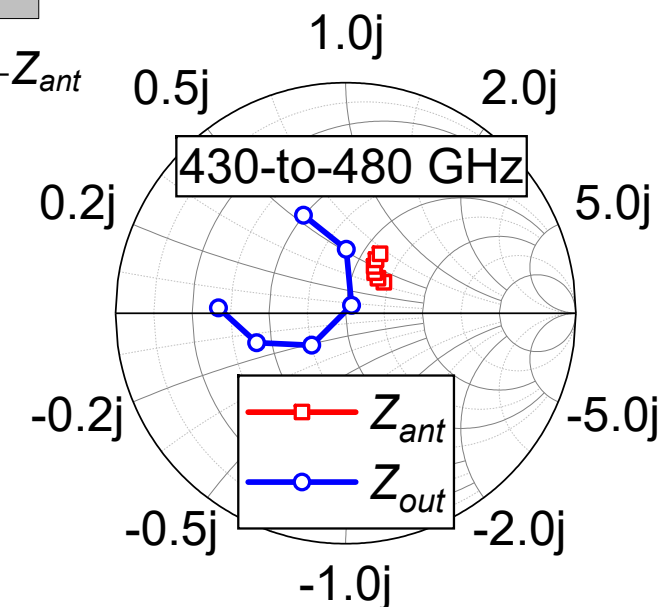
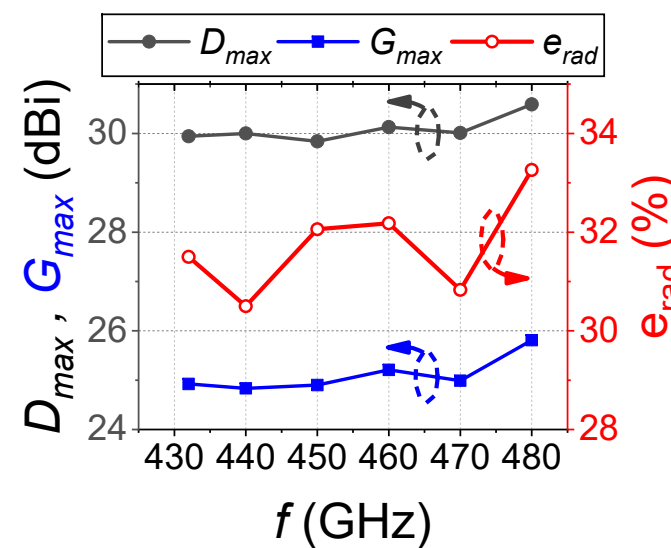
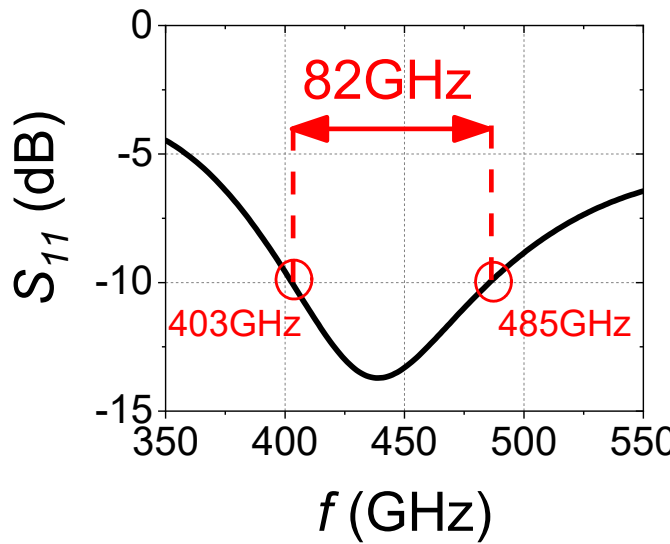
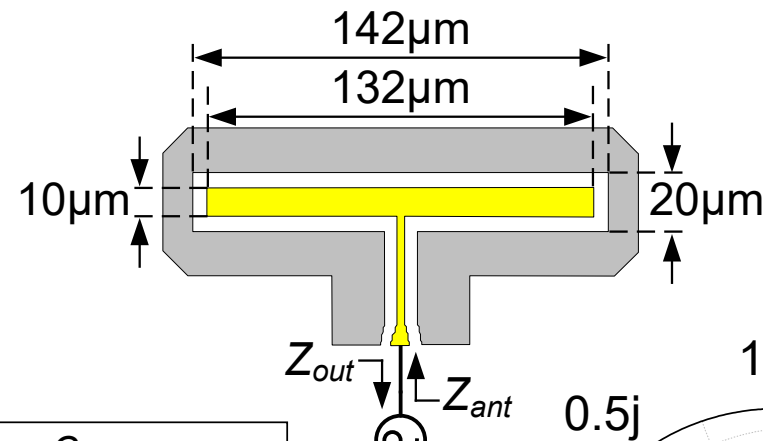
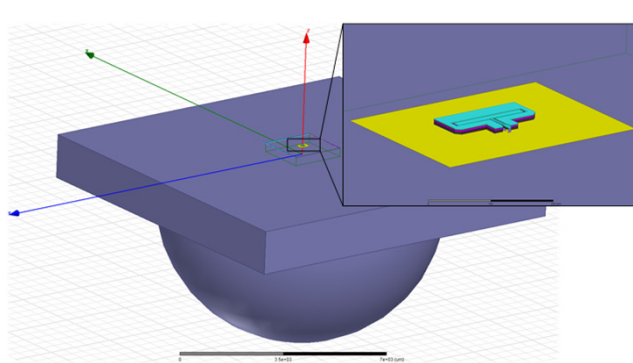


Unit SWO & Implementation



Coupling capacitor (C_c) + termination switch (S_T) → coupling reconfigurability

On-Chip Folded Slot Antenna



😊 + Si lens: high directivity

😊 Wideband

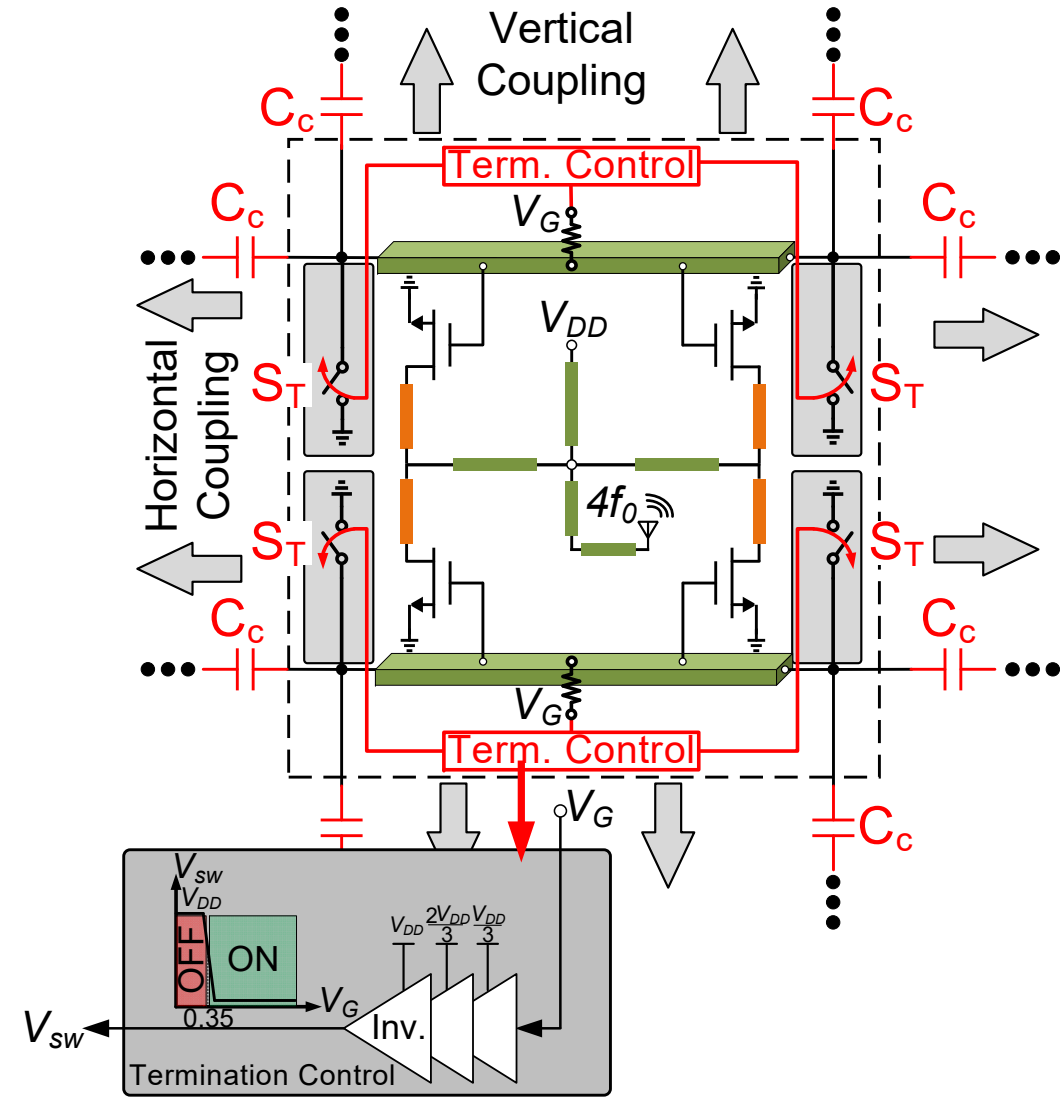
😊 High-efficiency

Outline

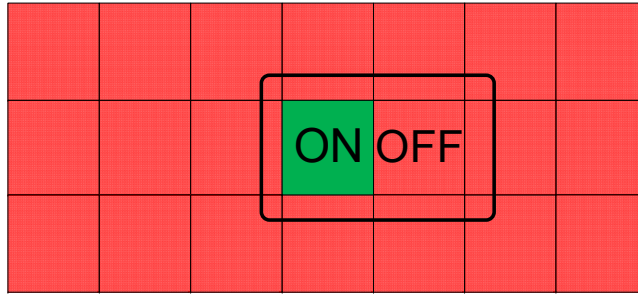
- Introduction
- Lens-integrated beam steering
- **Reconfigurable array architecture**
 - Array's unit cell: core oscillator + on-chip antenna
 - Reconfigurable coupling
- Experimental Results
- Conclusion

Turning Cells ON/OFF

- Cells coupled through C_c coupling capacitors
- Simple “**Termination Control**” block automatically adjusts termination in ON/OFF modes by controlling **termination switches (S_T)**
- Coupling capacitor (C_c) switched between injection/termination in ON/OFF modes

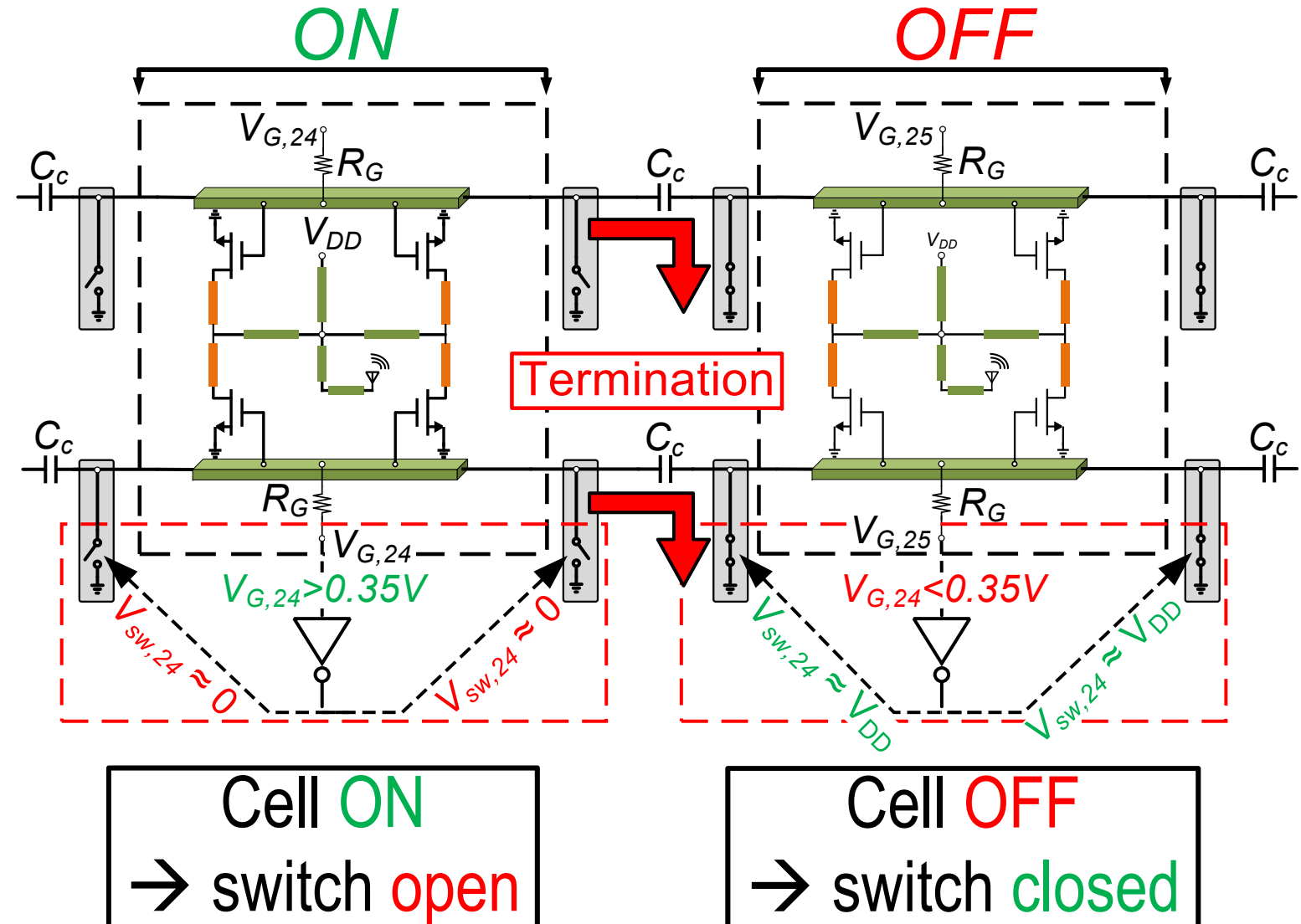


Injection/Termination in ON/OFF Modes

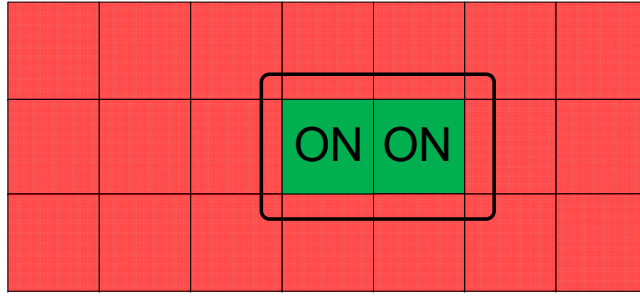


C_c : Termination

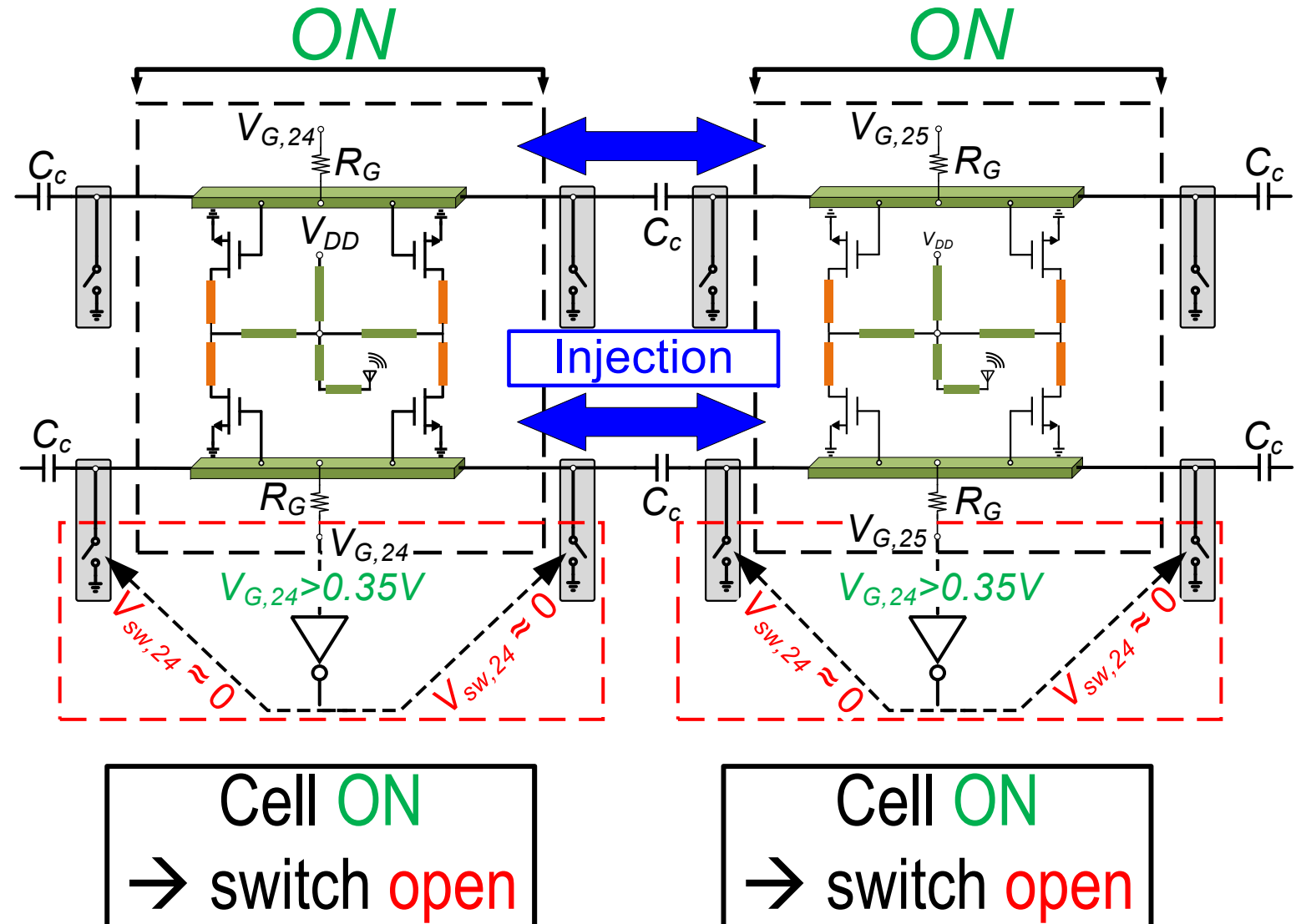
- At edges of activated segment
- Suppresses loading from OFF cells
- Maintains operation (frequency & power)



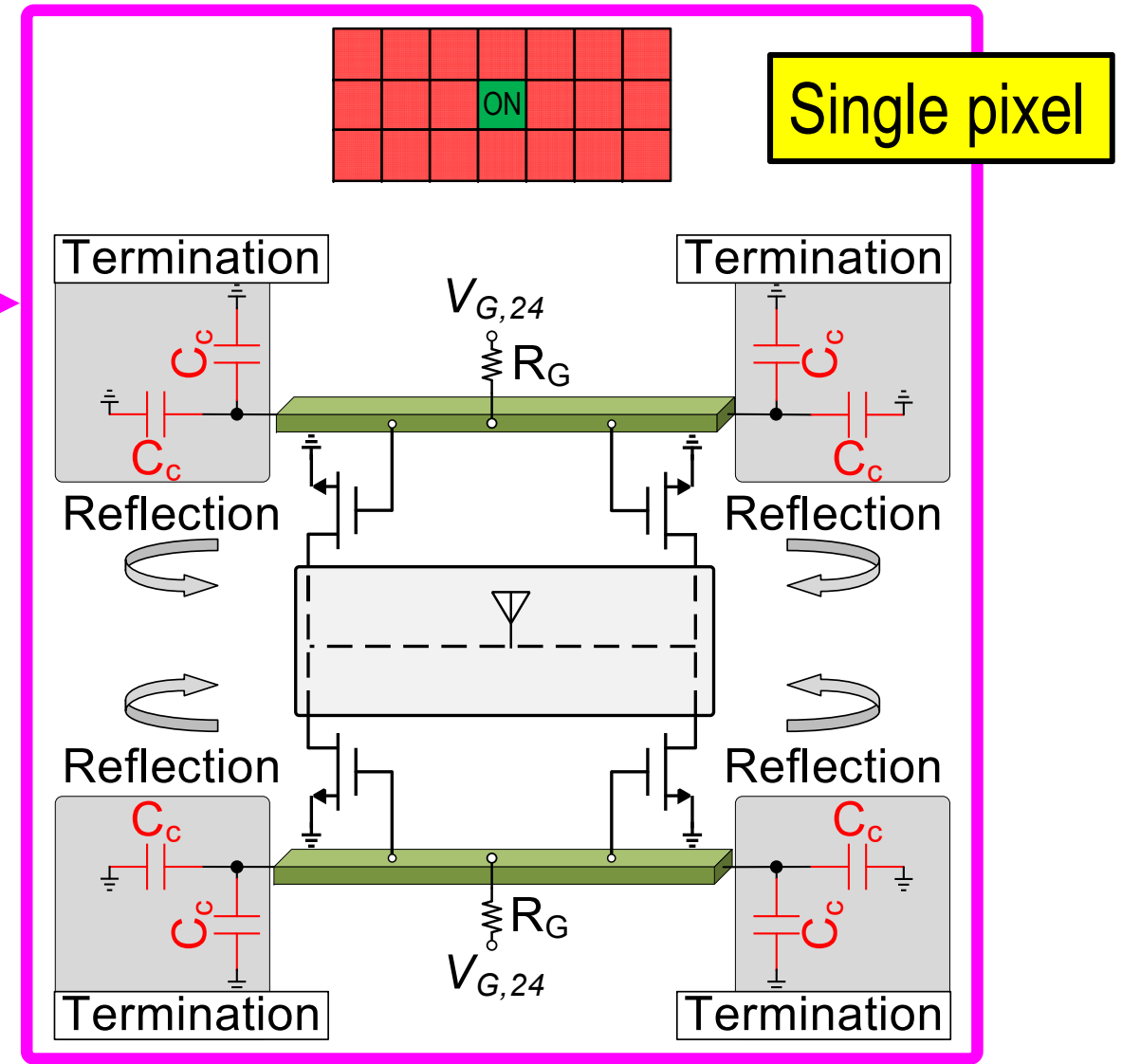
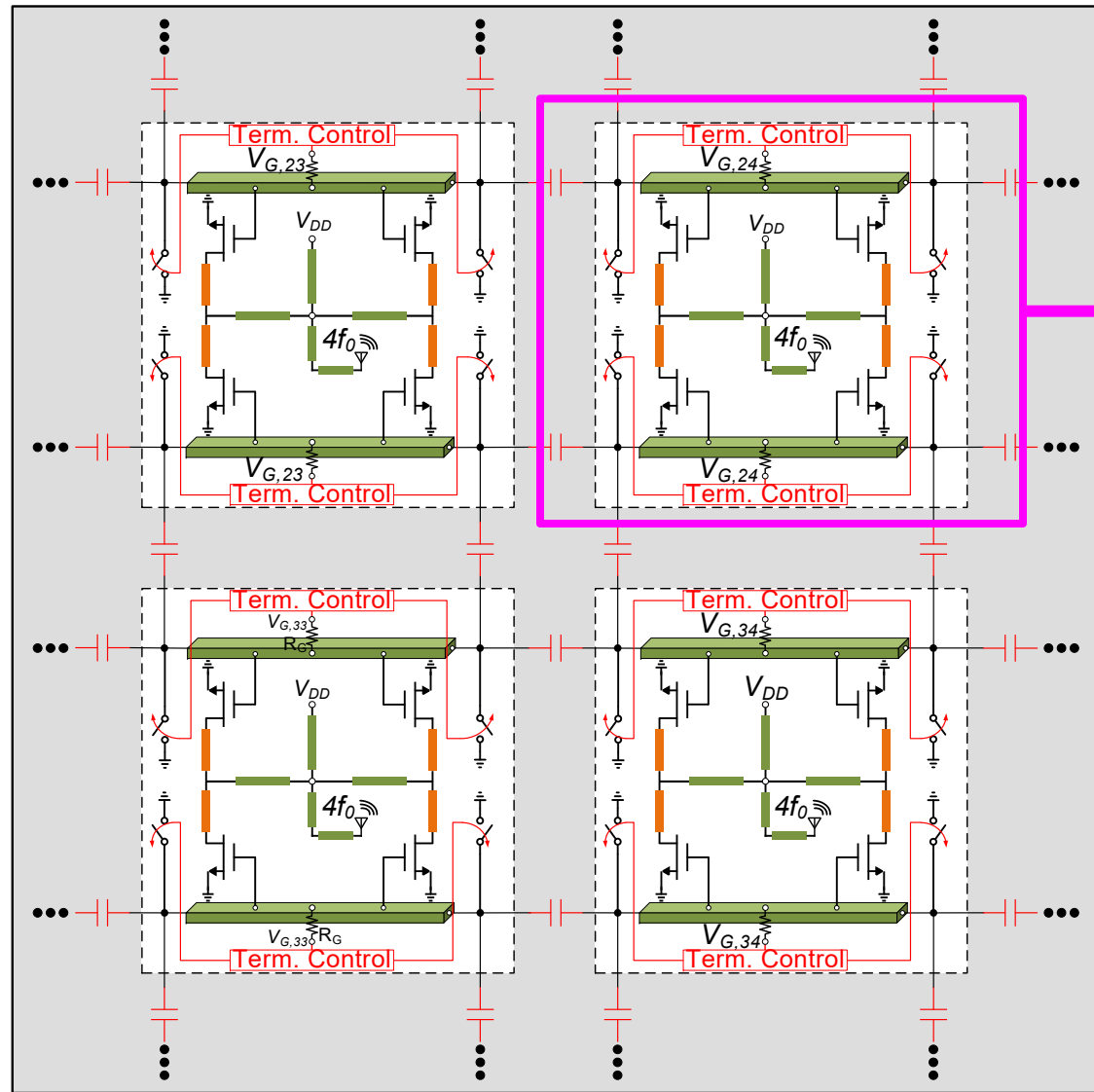
Injection/Termination in ON/OFF Modes



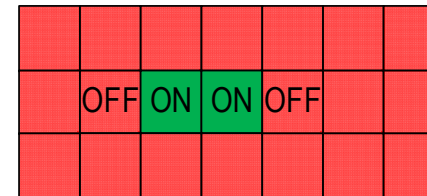
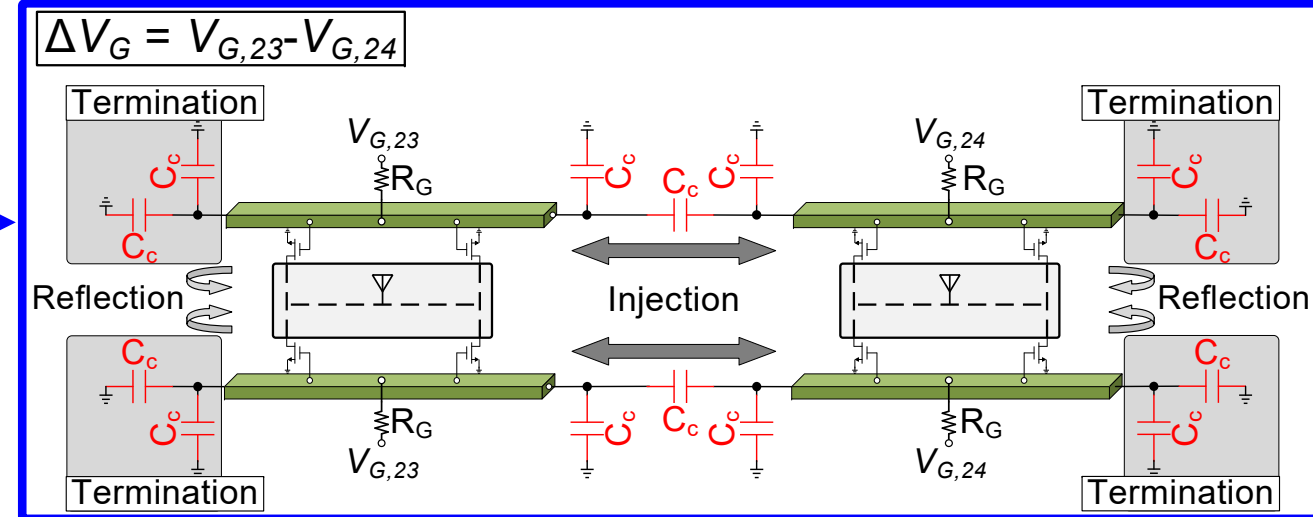
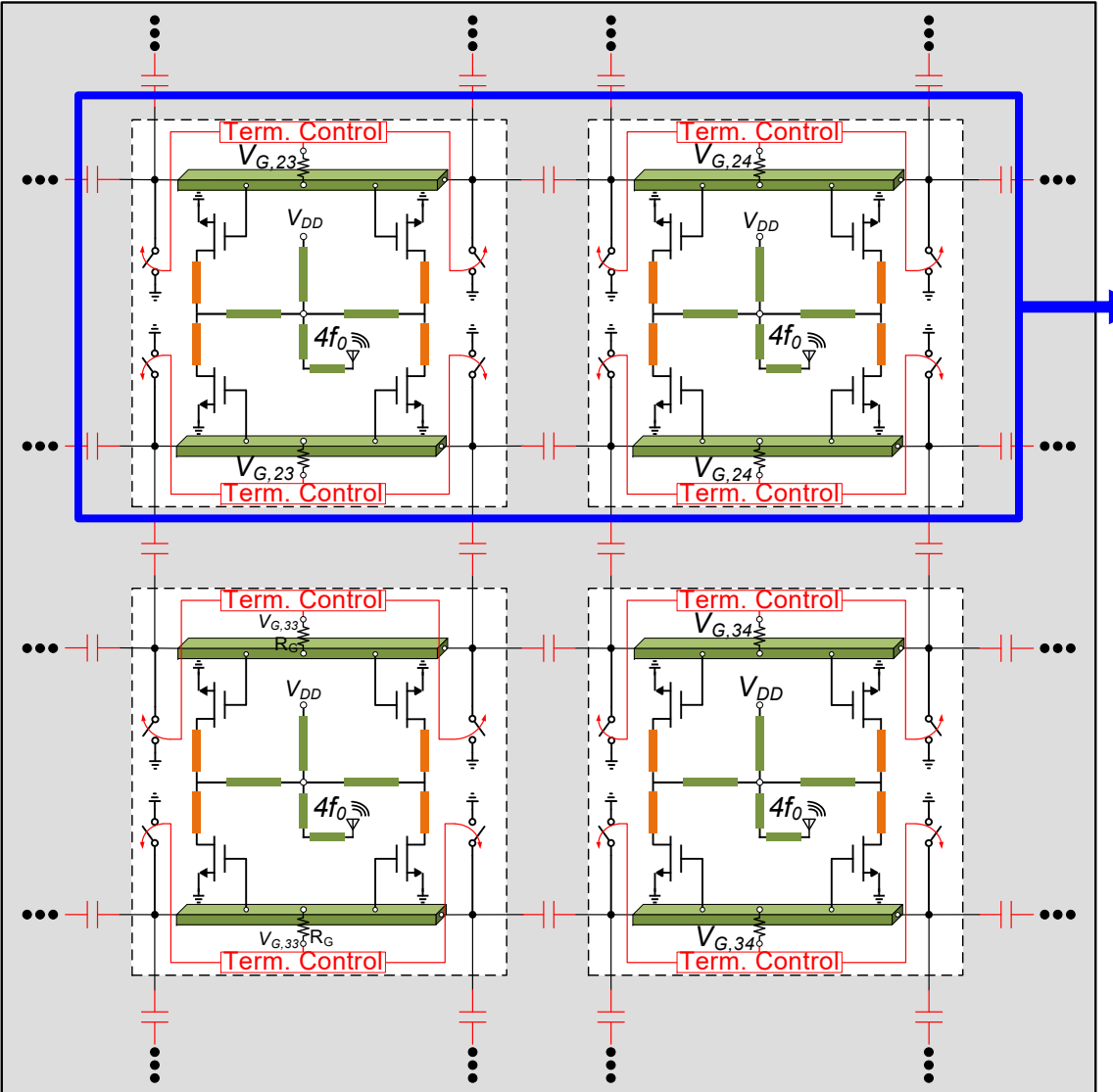
- C_c : **Injection**
- Inside activated segment
- Phase/frequency coupling
- Maintains operation (frequency & power)



Unit Cell Coupling: 1-Cell ON

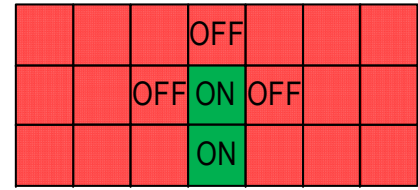
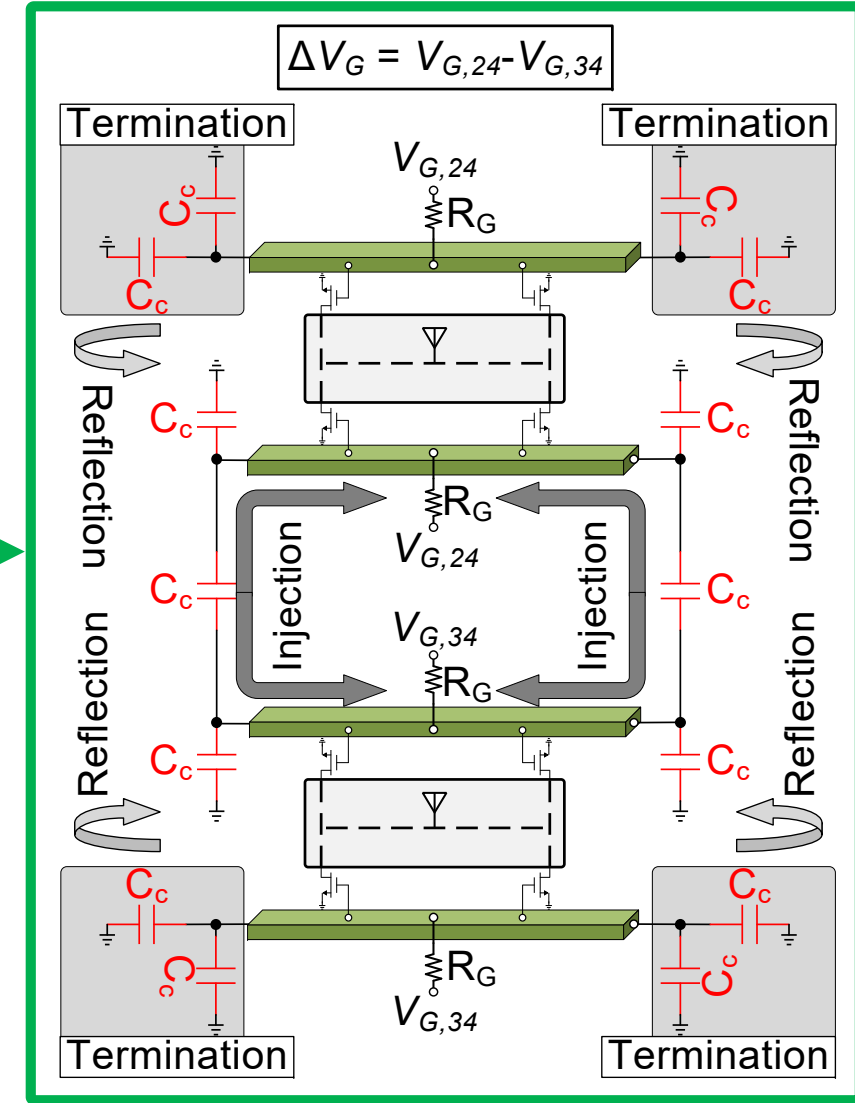
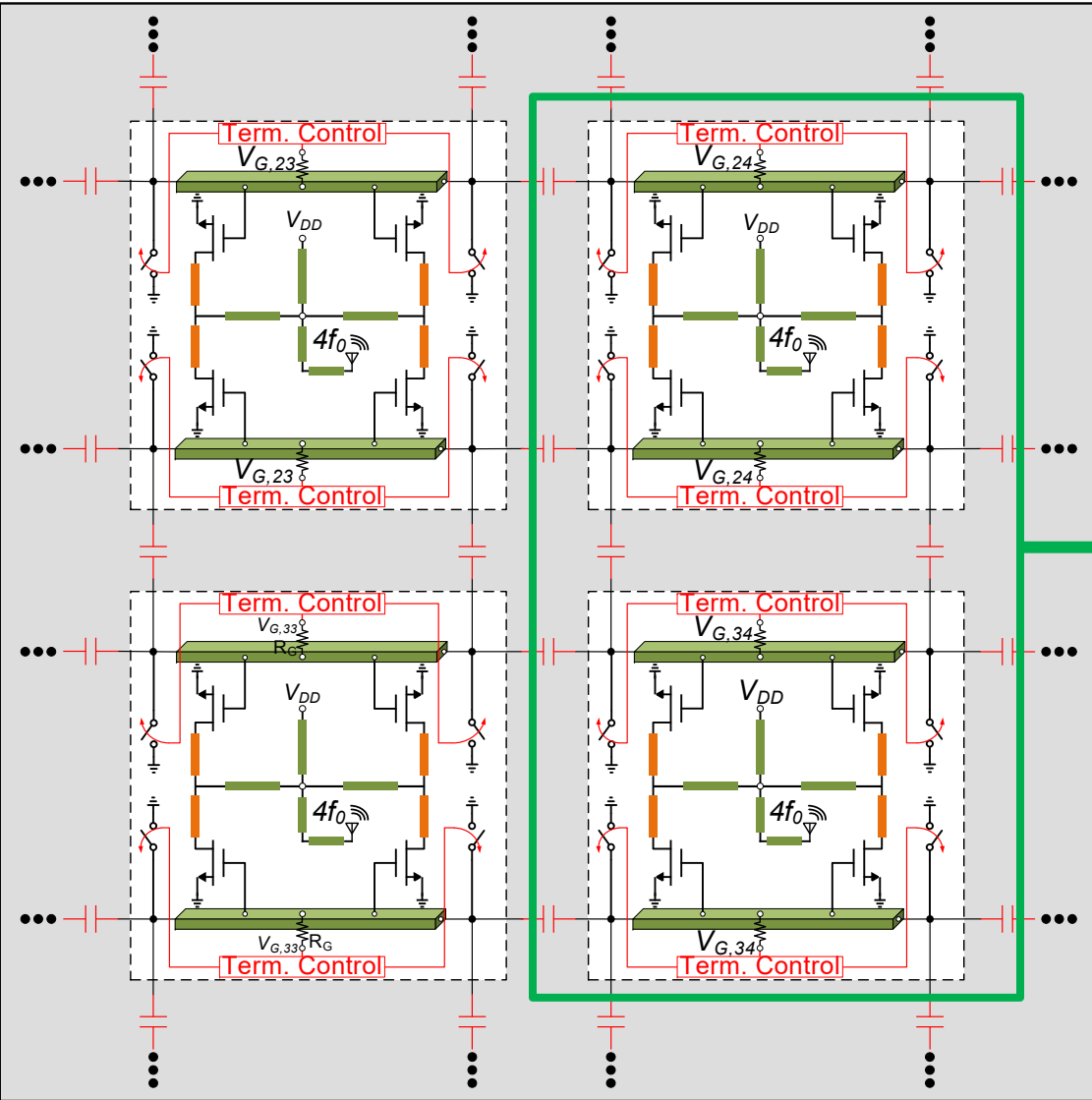


Unit Cell Coupling: 1×2 ON



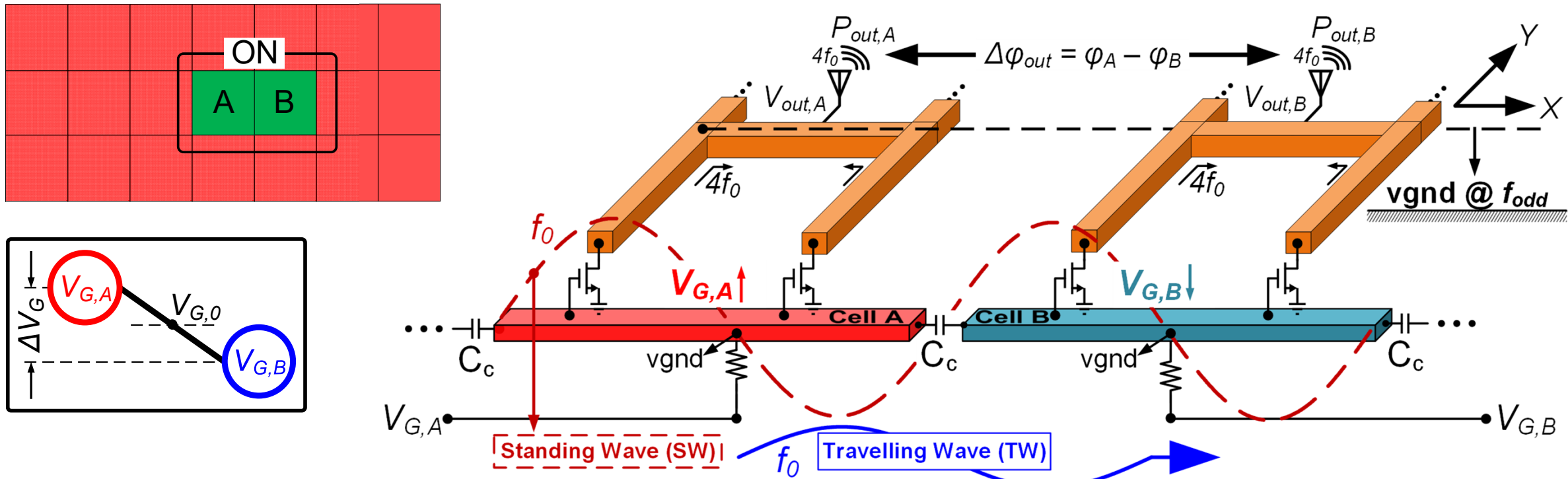
Horizontal coupling in a row within the array

Unit Cell Coupling: 2×1 ON



Vertical
column
coupling

Phase Shifting



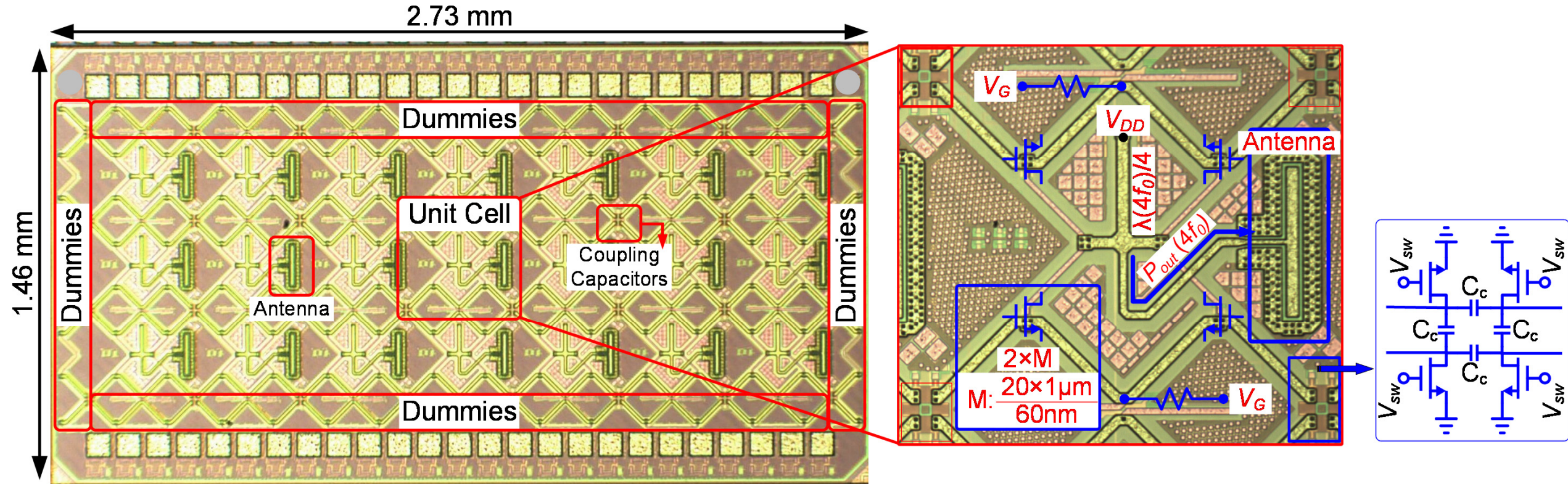
- Phase difference created by combining *standing* (SW) and *traveling* waves (TW)
 - $\Delta V_G = 0 \rightarrow$ Only SW $\rightarrow \Delta\varphi_{out} = 0$
 - $\Delta V_G \neq 0 \rightarrow$ SW+TW $\rightarrow \Delta\varphi_{out} \neq 0$

[H. Jalili, ISSCC 2017] [H. Jalili, JSSC 2019]

Outline

- Introduction
- Lens-integrated beam steering
- Reconfigurable array architecture
 - Array's unit cell: core oscillator + on-chip antenna
 - Reconfigurable coupling
- Experimental Results
- Conclusion

Die Photograph

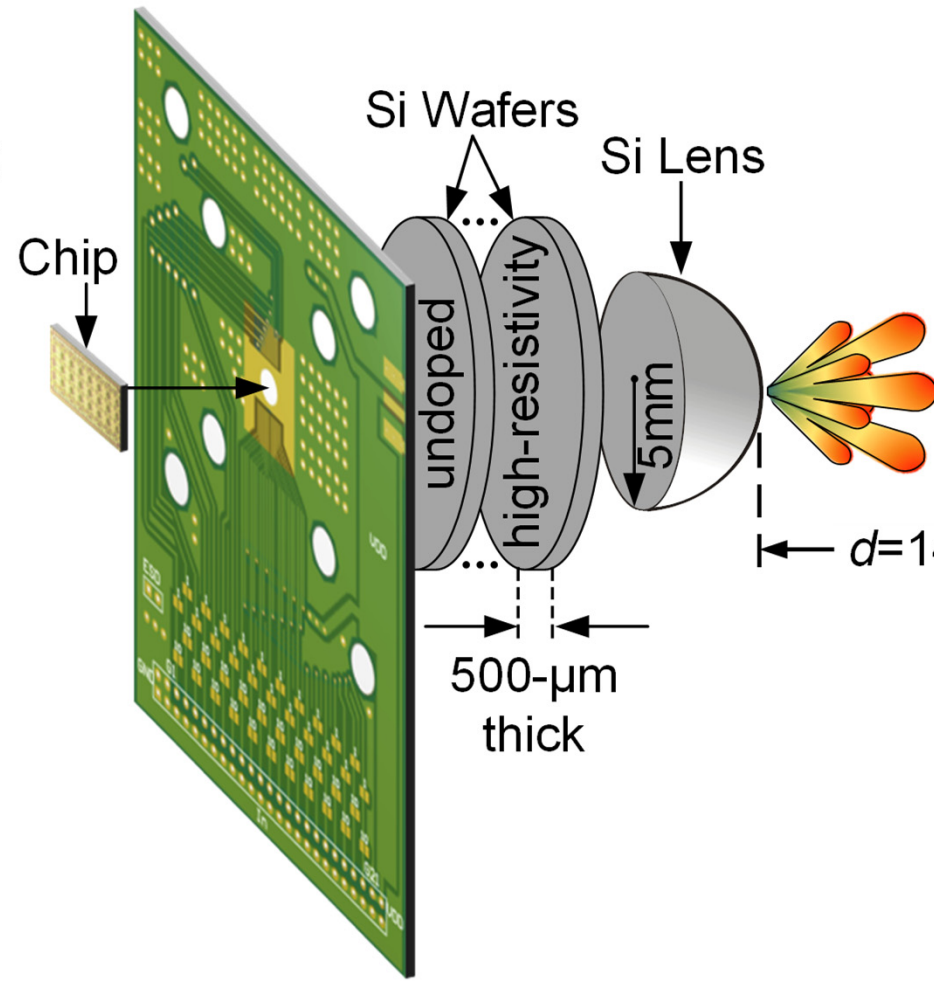


□ Technology: 65-nm CMOS

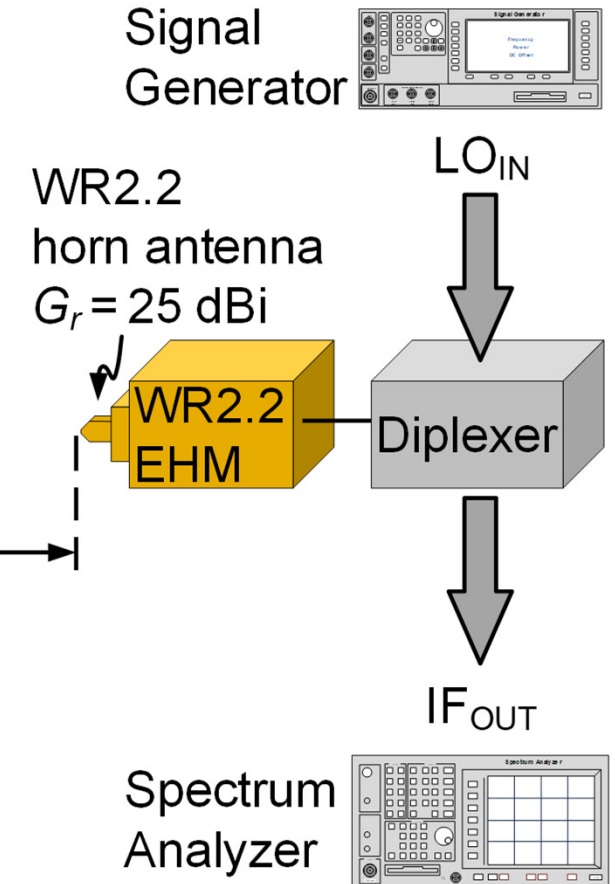
□ Area: 4-mm²

Prototype Assembly & Measurement

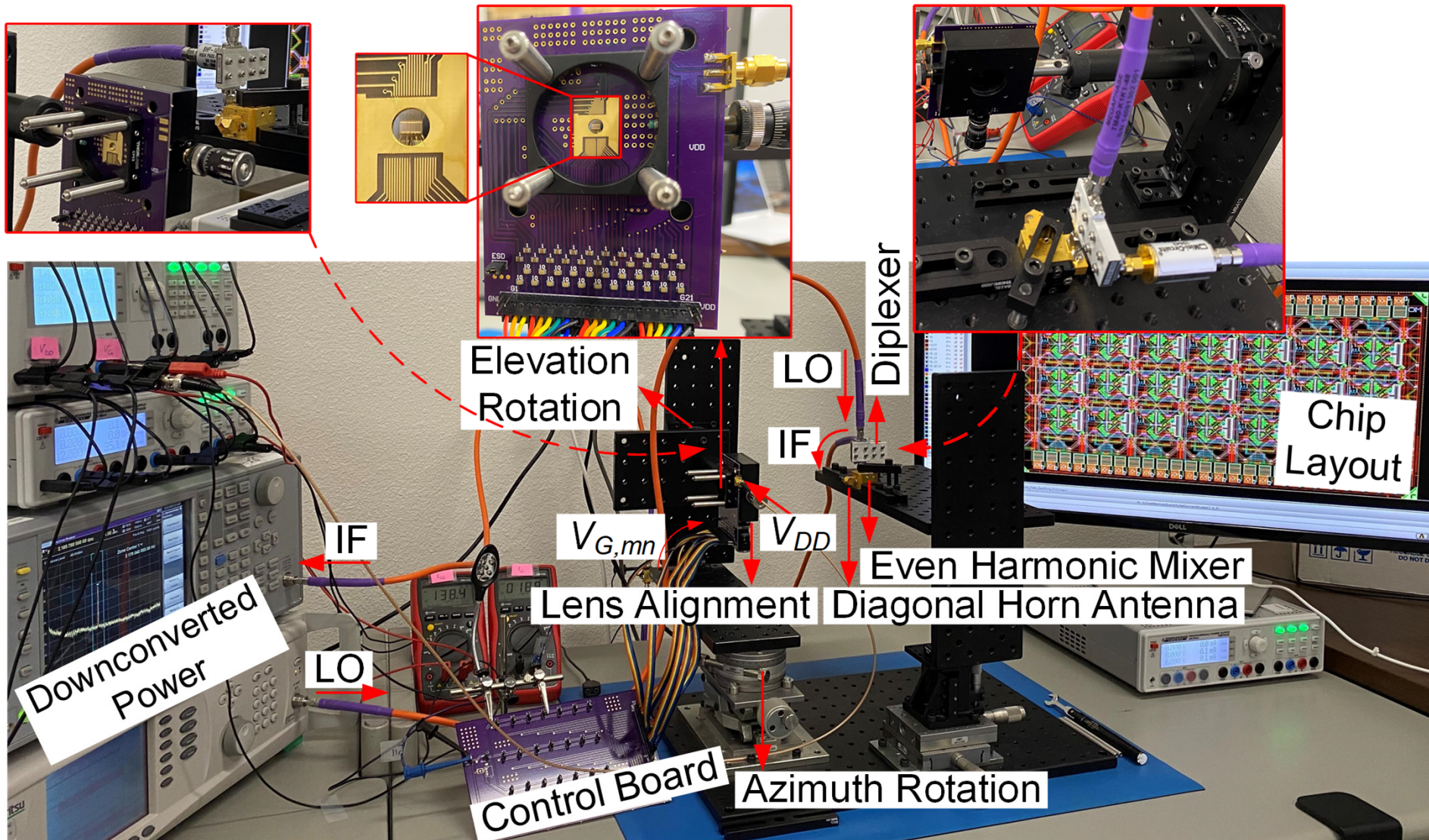
- Tx Backside radiation:
 $n \times 500\text{-}\mu\text{m}$ thick Si wafers
+ 5-mm radius Si lens



- Rx detection:
WR2.2 even harmonic mixer (EHM)

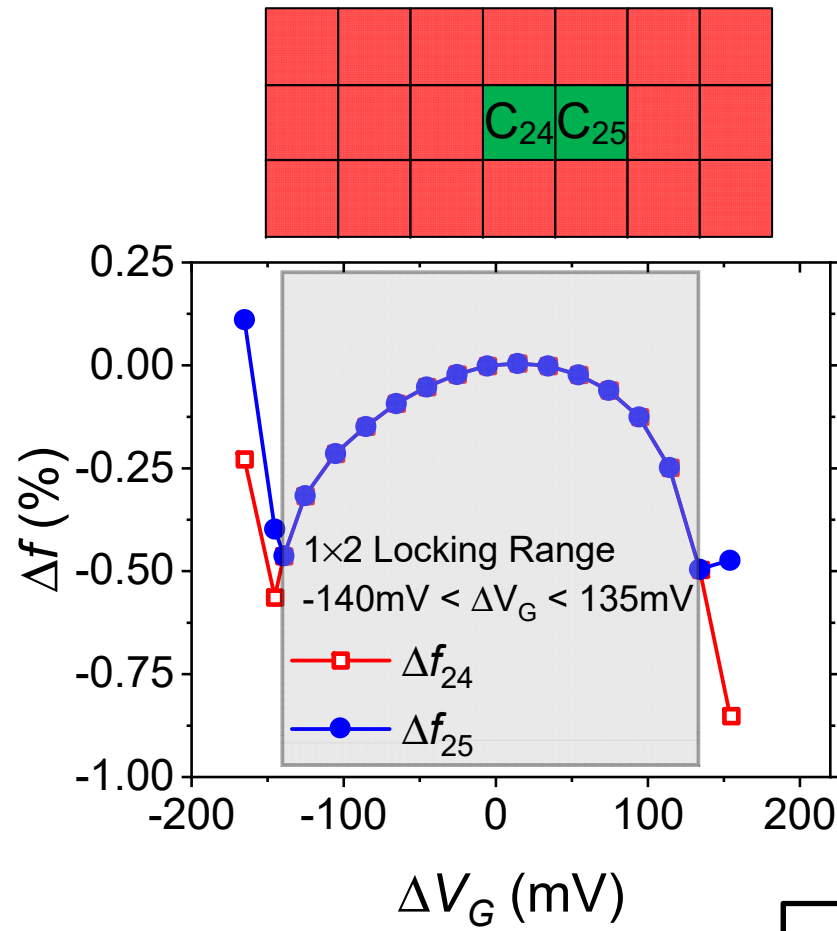


Measurement Setup



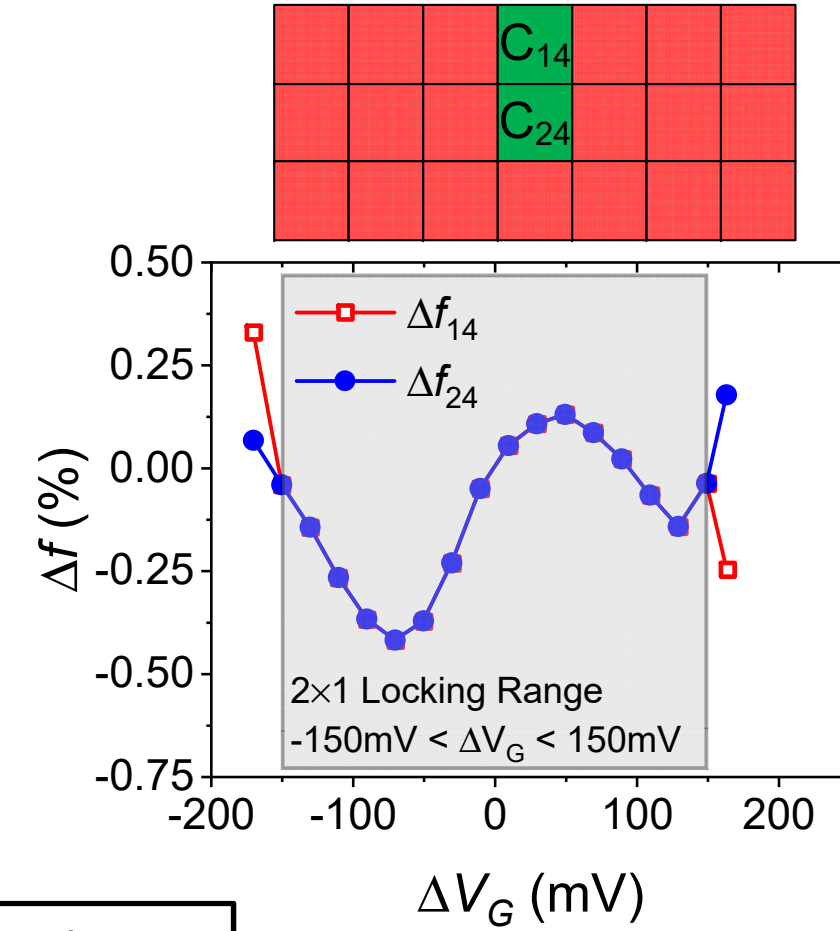
23.2: A 436-to-467GHz Lens-Integrated Reconfigurable Radiating Source with Continuous 2D Steering and Multi-Beam Operations in 65nm CMOS

Robust Locking Range



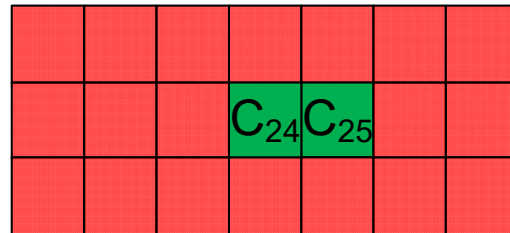
$$\Delta V_G = V_{G,24} - V_{G,25}$$

$$\Delta f = \frac{f(\Delta V_G) - f(\Delta V_G=0)}{f(\Delta V_G=0)} \times 100$$

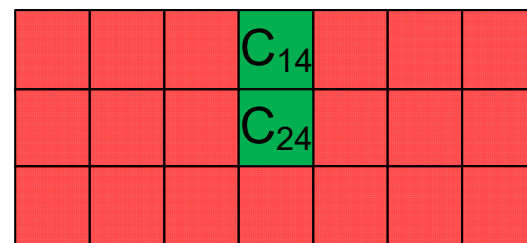
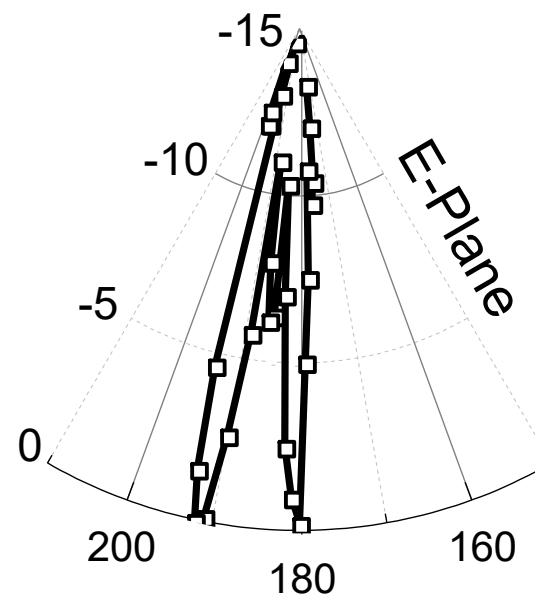


$$\Delta V_G = V_{G,14} - V_{G,24}$$

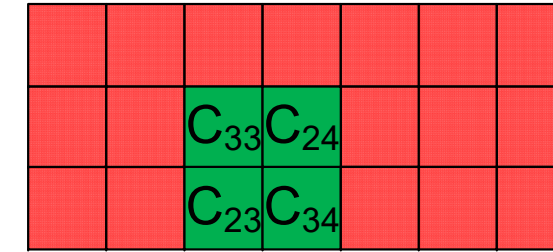
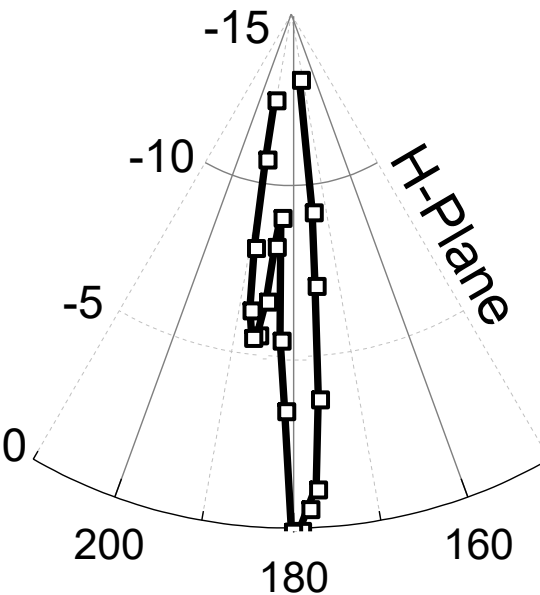
Radiation Patterns



$$L_{ext} = 1.5\text{mm}$$

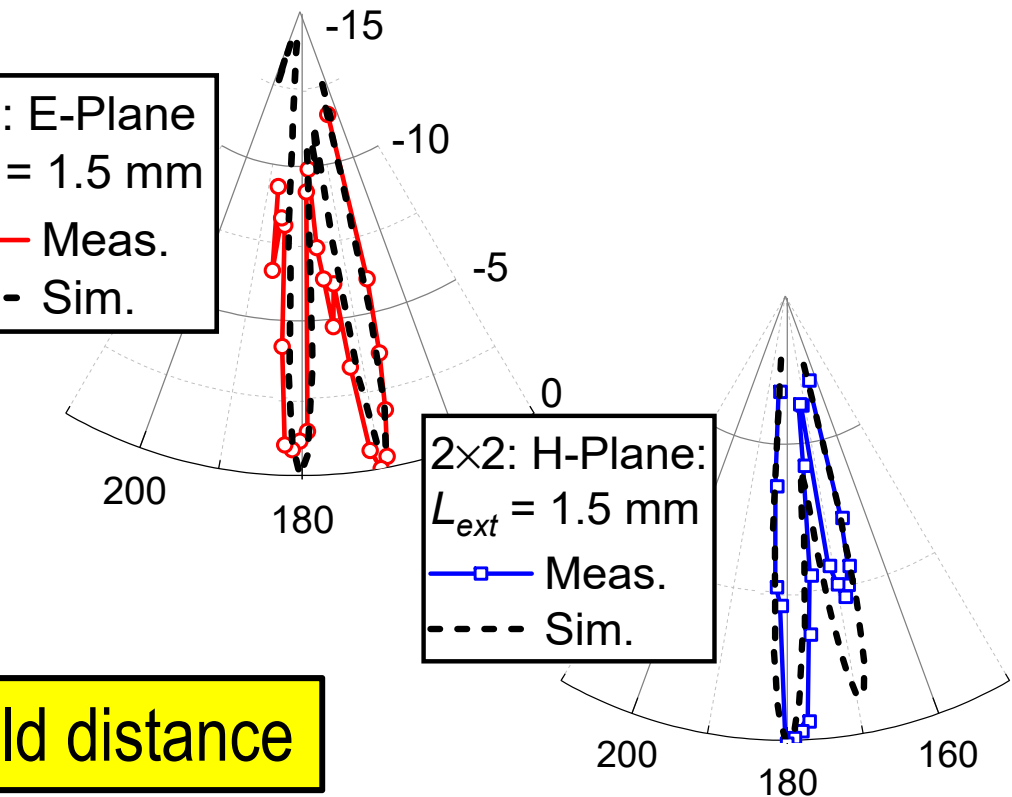


$$L_{ext} = 1.5\text{mm}$$



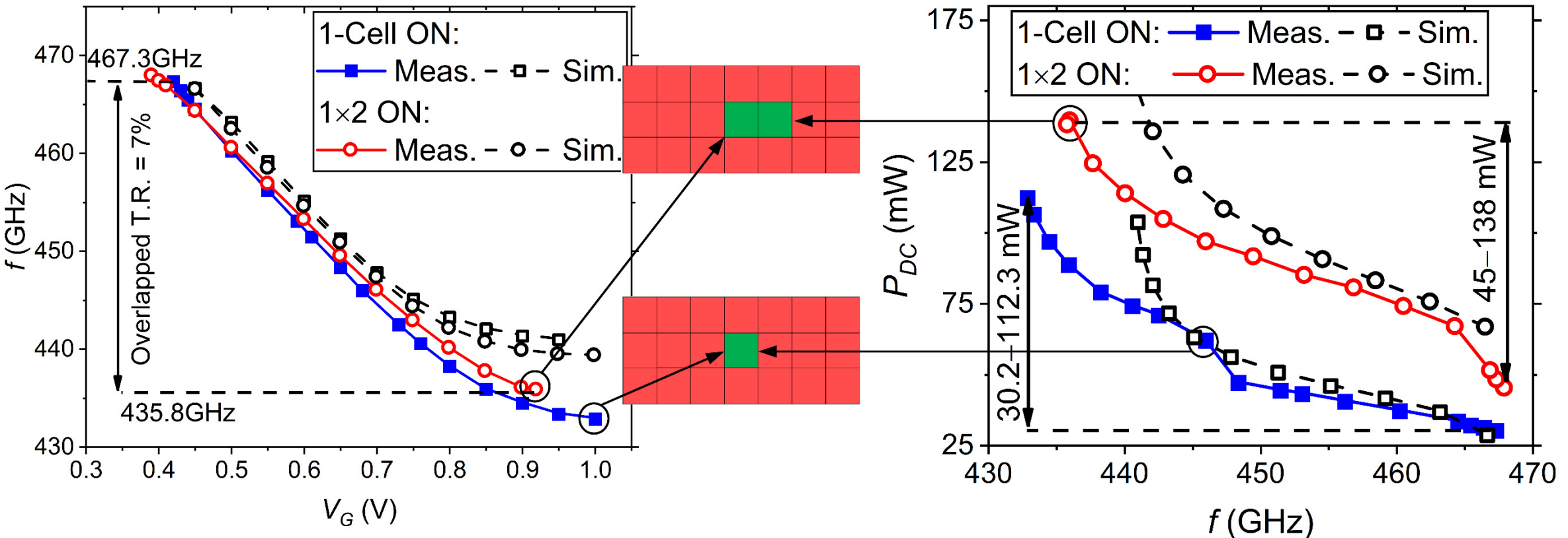
2x2: E-Plane
 $L_{ext} = 1.5\text{ mm}$
—○— Meas.
- - - Sim.

2x2: H-Plane:
 $L_{ext} = 1.5\text{ mm}$
—□— Meas.
- - - Sim.



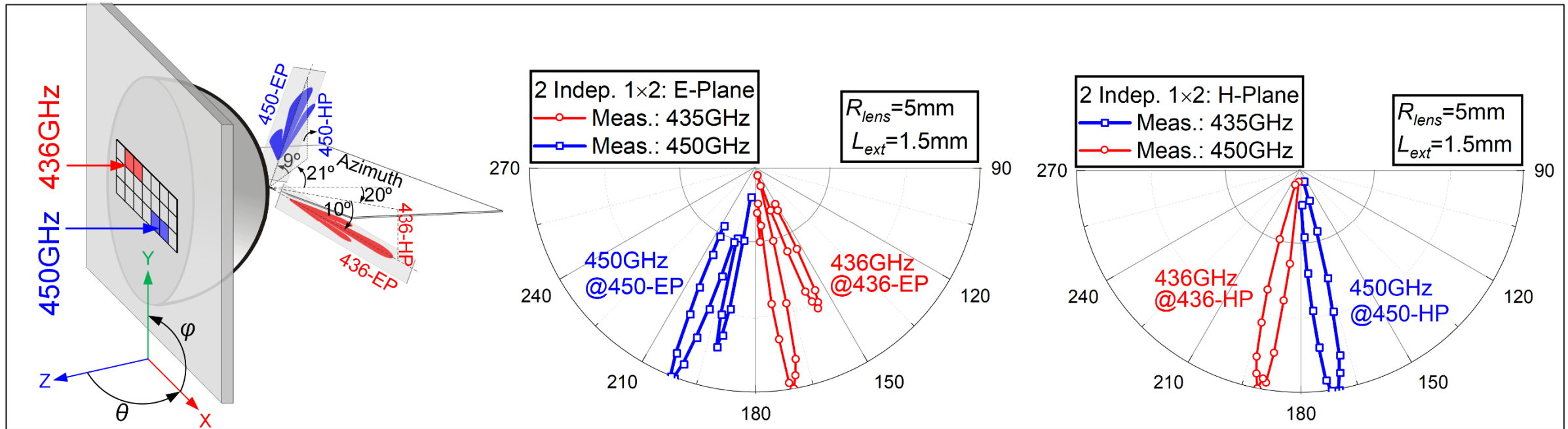
Measured at 14cm far field distance

Frequency & Power Consumption



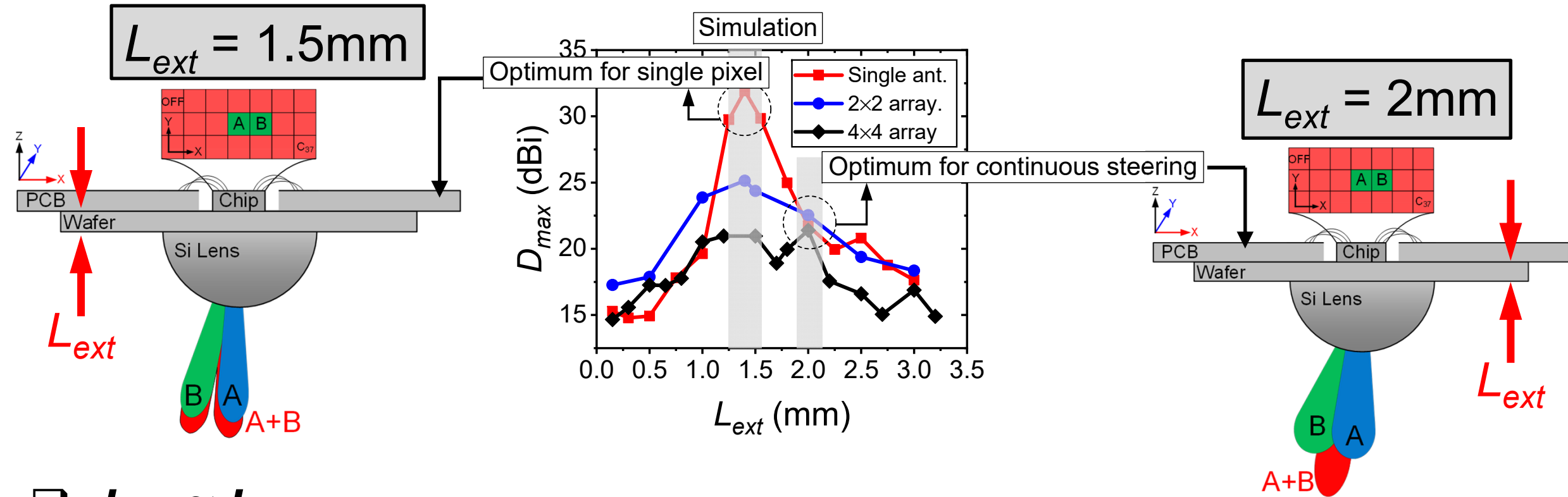
- Frequency ~unchanged when switching between 1-cell & 1x2
- 7% overlapping frequency tuning range

Multi-Beam Operation + 2D Beam Steering



- Arbitrary set of non-intersecting sub-arrays can be turned ON at the same time
- Example: 2 simultaneous beams at 436 & 450 GHz with E- & H-plane beam steering

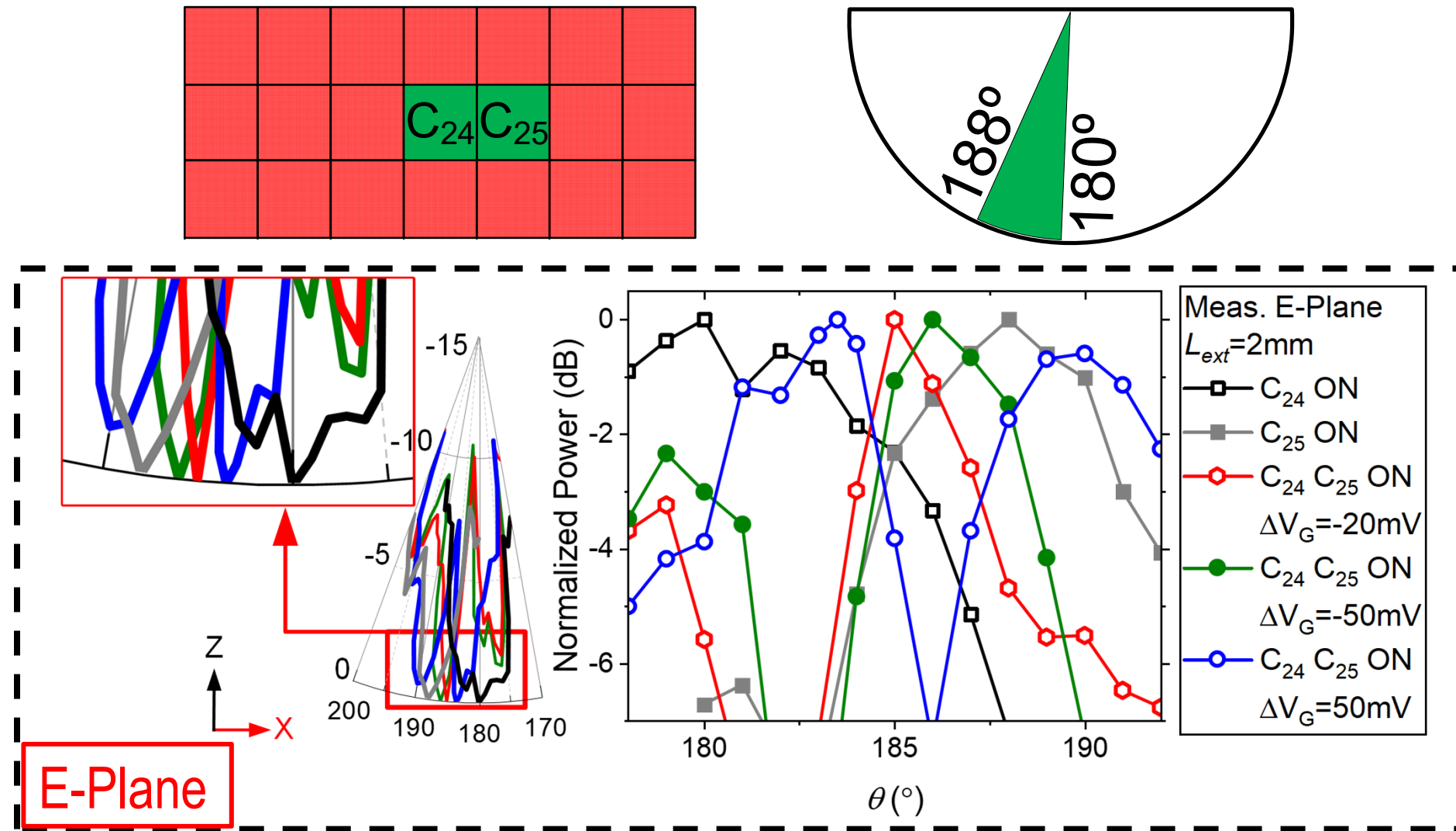
Directivity vs. Beam Steering trade off



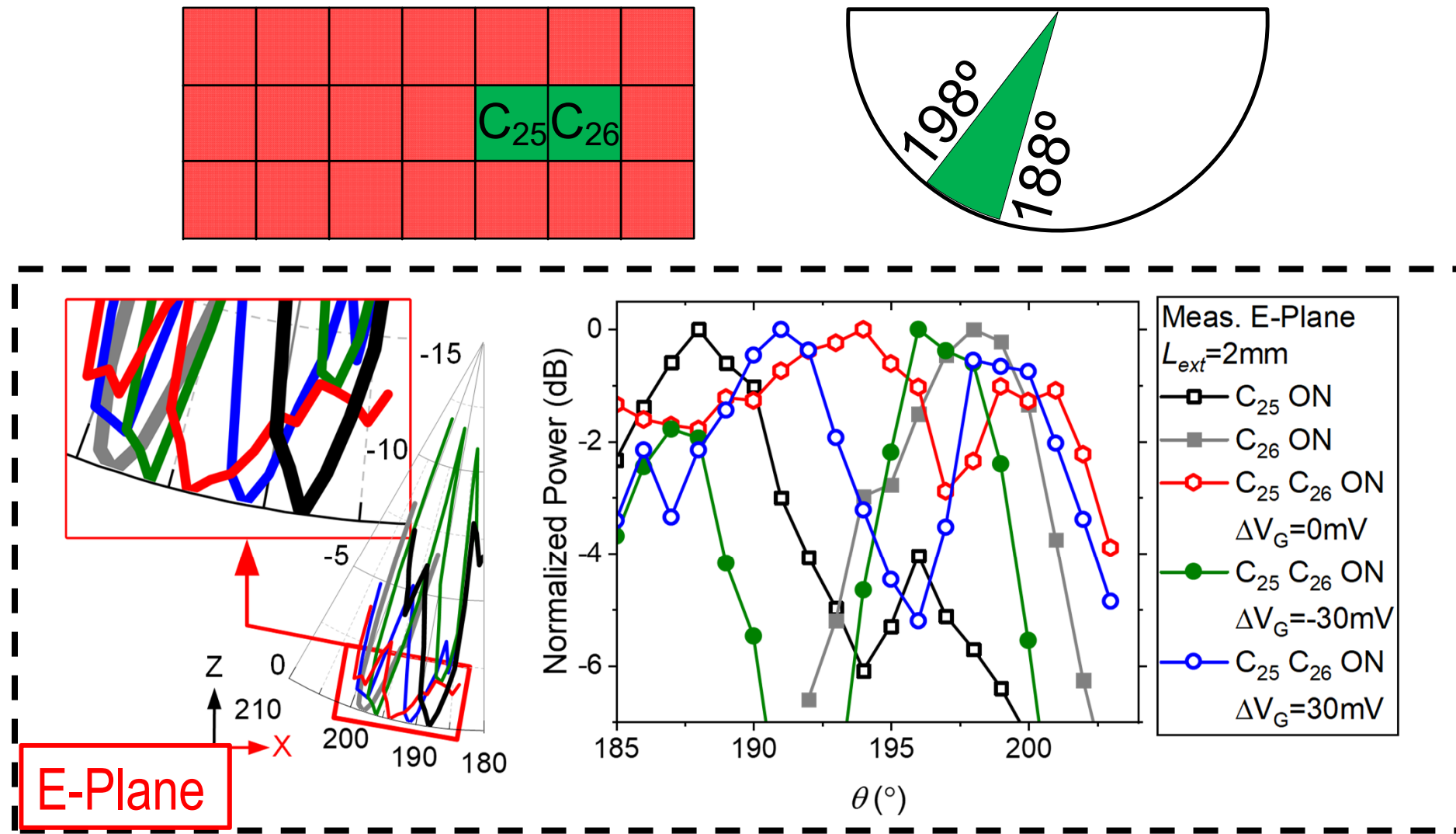
- $L_{ext} \approx L_{ext,opt}$:
 - Individual beams too narrow
 - No interaction/superposition between beams
 - ☹ No beam steering

- $L_{ext} > L_{ext,opt}$:
 - Individual beams overlap
 - ☺ beam steering

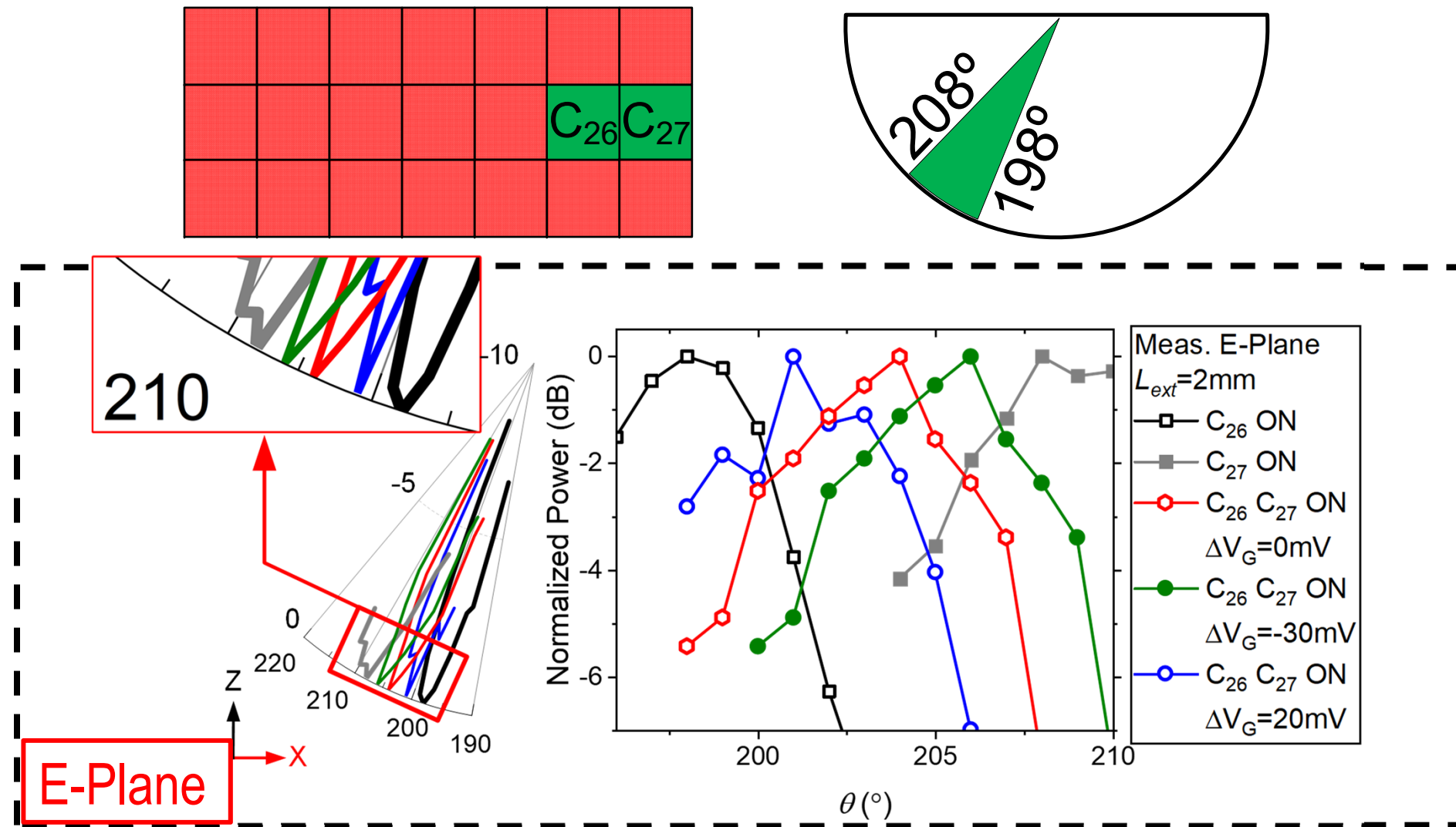
Measurement: X-direction Beam Steering



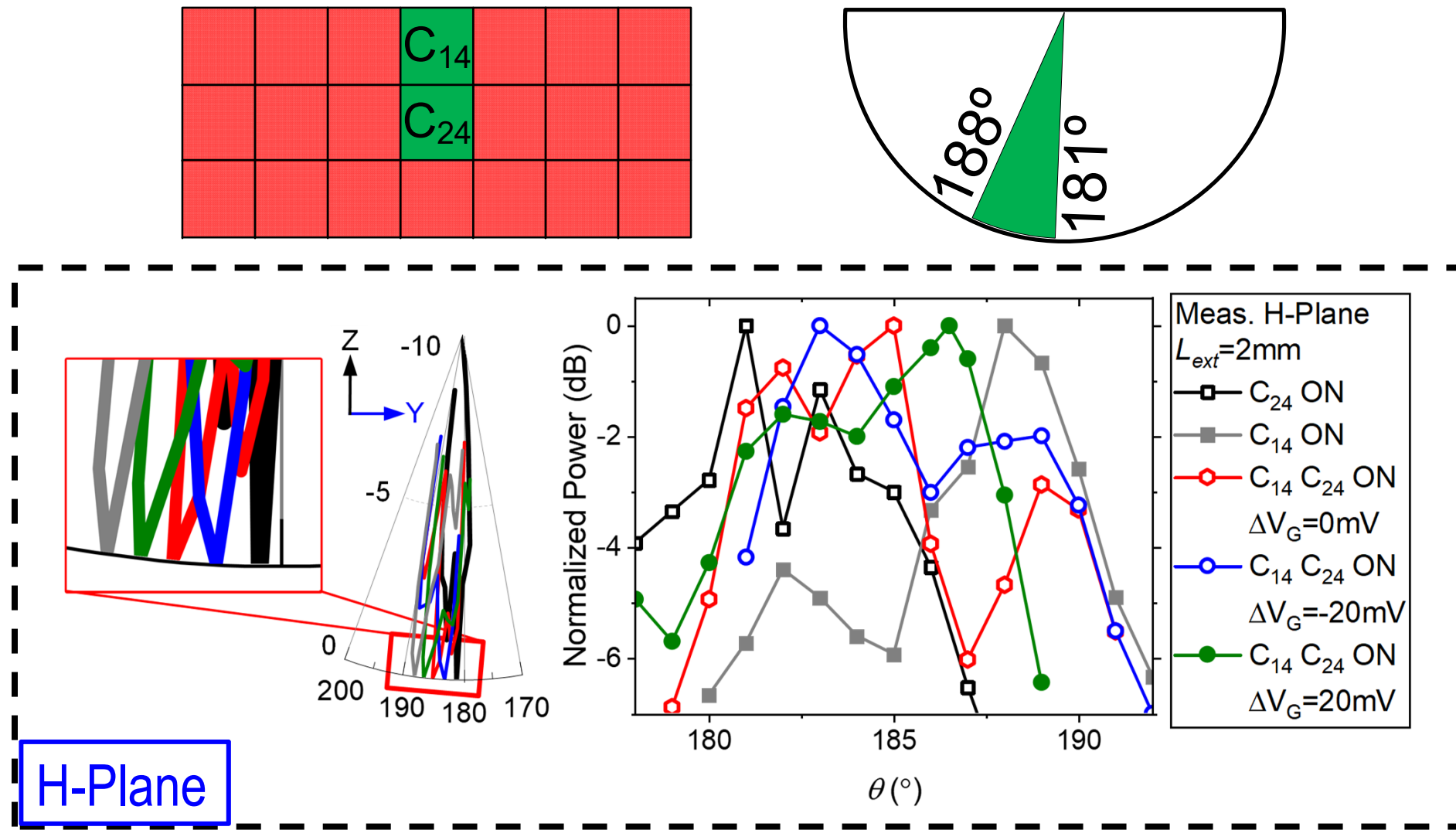
Measurement: X-direction Beam Steering



Measurement: X-direction Beam Steering



Measurement: Y-direction Beam Steering

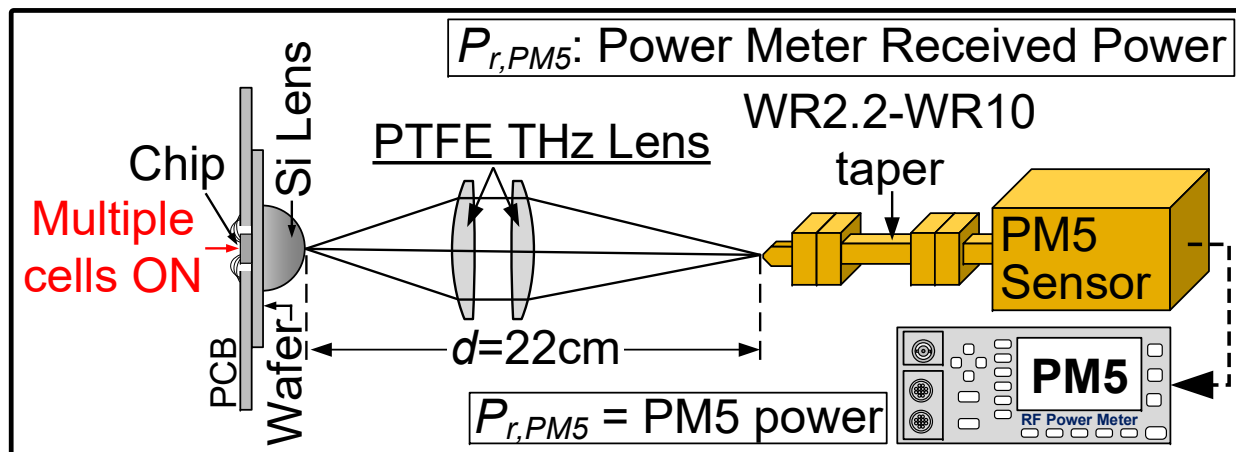
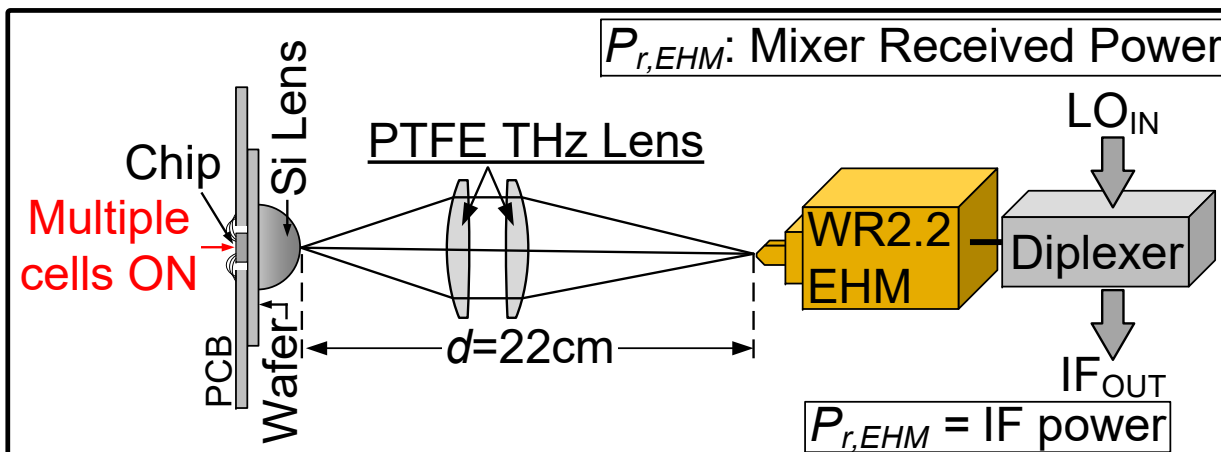
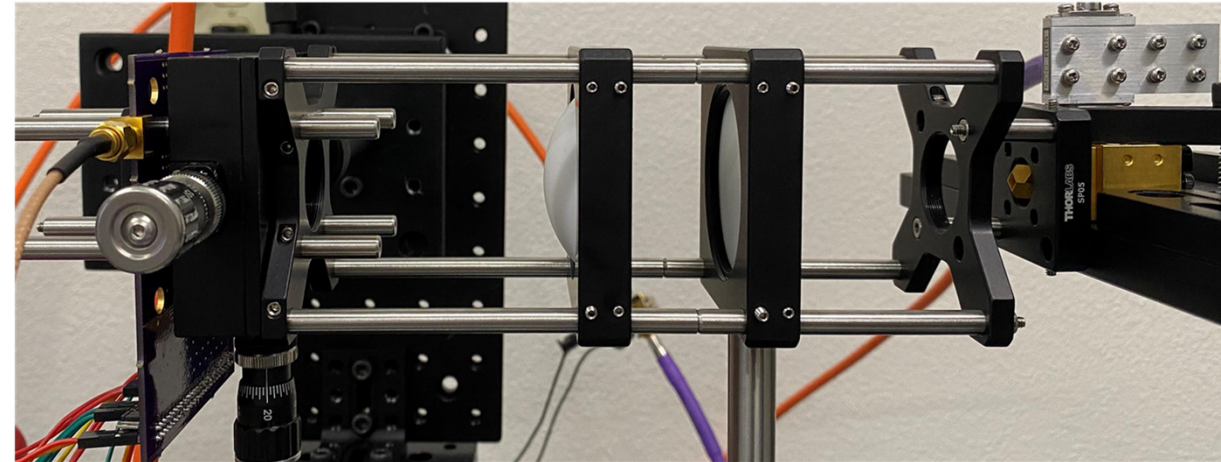


EIRP Measurement

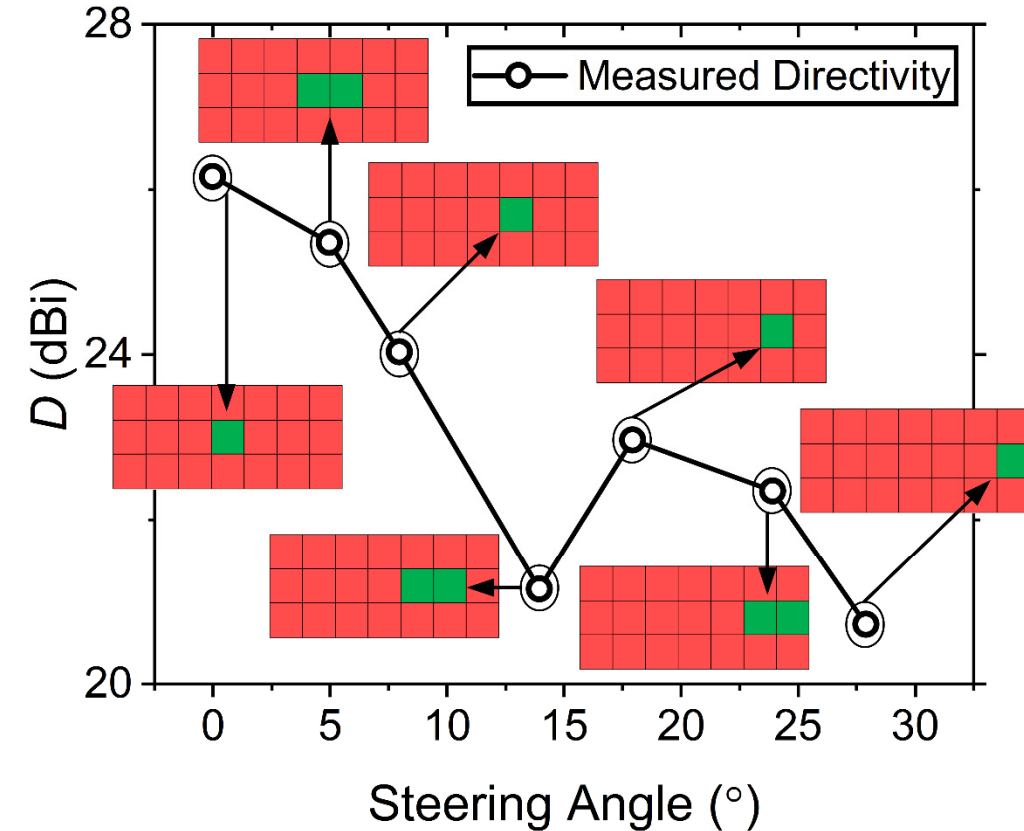
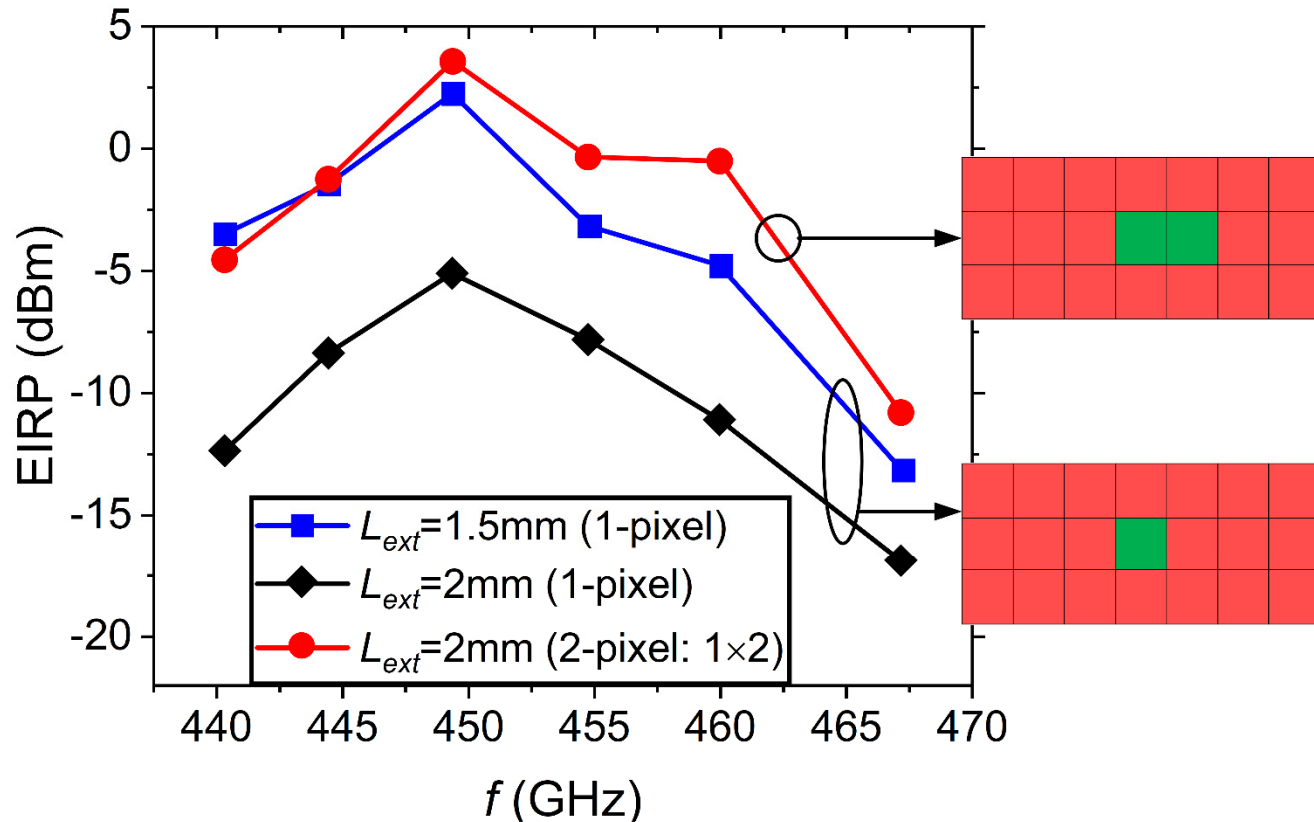
Mixer Loss Characterization for EIRP measurements

$$L_{\text{mixer}}(f: \text{LO, IF}) = P_{r,PM5} + L_{\text{taper-wg}} - P_{r,\text{mixer}}$$

PM5 received power Mixer received power
↓ ↑
Mixer loss at frequency f Taper & waveguide loss



EIRP & Directivity



- Directivity $> 20\text{dBi}$ for all steering angles
- EIRP ($L_{ext}=2\text{mm}$, 1×2) \sim EIRP ($L_{ext}=1.5\text{mm}$, 1-cell)

Comparison with Prior Art

	Array Size	Radiation	Tech.	f_{max} (GHz)	f_c (GHz)	Scan Range (°)	T.R. (%)	Peak Directivity (dBi)	Peak EIRP (dBm)	P_{DC} (W)	Area (mm²)
This Work	3×7^1	Folded Slot Ant. + Si Lens ($R_{lens}=5\text{mm}$)	65nm CMOS	340	450	56/16 (2D)	7	25.35 ²	3.6 ²	0.095 ²	4
								26.15 ³	-5.1 ³	0.051 ³	
ISSCC 2014 [2]	4×4	Patch Ant.	65nm CMOS	N/A	338	45/50 (2D)	2.1	18 ⁴	17	1.54	3.9
ISSCC 2020 [3]	4×4	Patch Ant.	65nm CMOS	250	416	60/60 (2D)	1.7	17 ⁴	14	1.45	4.1
JSSC 2019 [4]	2×2	Patch Ant.	0.13μm SiGe	215	344	128/53 (2D)	15.1	11.7	4.9	0.45	1.2
ISSCC 2020 [5]	6×6	Folded Monopole + Si Lens ($R_{lens}=5\text{mm}$)	40nm CMOS	300	586.7	30 (1D)	0.7	24	24.1	1.278	0.68
ISSCC 2020 [6]	8×8	Circular Slot Ant. + Si Lens ($R_{lens}=7.5\text{mm}$)	0.13μm SiGe	500	420	68 ⁵ (2D) (discrete)	0.7	36.4 ⁶	32.8 ⁶	6.9 ⁷	12.6
JSSC 2020 [1]	25	Folded Slot Ant. + Si Lens	R _{lens} = 12.5mm R _{lens} = 5mm	65nm CMOS	340	459	0	21.1	19.3	1.18	3.94
								16.8	14.7		

¹Reconfigurable

²Two-cell (1×2) activation

³Single cell activation

⁴Based on EIRP – P_{rad}

⁵7.5° beam spacing

⁶Estimated: Single pixel

⁷All pixels ON

Comparison

- Wideband operation
- Simultaneous multi-beam/-frequency radiation
- Compared to lens-less implementations:
 - Larger directivity → higher scanning resolution
 - Lower power consumption
- Among lens-coupled works:
 - Wide-angle 2D continuous & uninterrupted scanning

Outline

- Introduction
- Lens-integrated beam steering
- Reconfigurable array architecture
 - Array's unit cell: core oscillator + on-chip antenna
 - Reconfigurable coupling
- Experimental Results
- Conclusion

Conclusion

- This work presents a 450-GHz reconfigurable array source for fast high-resolution THz imaging/sensing that is capable of:
 - Wideband operation (7% bandwidth)
 - Multi-beam/-frequency radiation
 - Wide-angle ($56^\circ/16^\circ$), scalable, 2D, and continuous beam steering with Si lens
 - Large directivity (>20dBi) with low power (<100mW at center frequency)
consumption

Acknowledgements

- The National Science Foundation (NSF) for supporting this work

Thank you for your attention.